DI-2020-01-R0

Spent Nuclear Fuel Disposal in a Deep Horizontal Drillhole Repository Sited in Shale:

Numerical Simulations in Support of a Generic Post-Closure Safety Analysis

Revision 00
May 5, 2020

Deep Isolation, Inc.

2120 University Ave., Suite 623
Berkeley, California 94704
USA

This work was supported by Deep Isolation, Inc., Berkeley, California, USA

DISCLAIMER

This report may concern work in progress that may have had limited review. While this document is believed to contain correct information, neither Deep Isolation Inc. nor any Sponsor of this work make any warranty of any kind, either expressed, implied, or statutory, or assumes any legal responsibility for the accuracy, completeness, or usefulness of this information, or represents that its use would not infringe privately owned rights. Any use which a third party makes of the information presented in this work, or any reliance on or decisions to be made based on it, are the responsibility of such third parties.

REVISION HISTORY

Revision	Date	Description
00A	12/20/2019	Initial draft, for internal review
00B	01/06/2020	Internal review comments addressed; concurrence copy
00C	01/24/2020	Final draft
00D	01/28/2020	Added instant waste mobilization scenario; addressed additional review comments
00	05/05/2020	Sensitivity to repository depth added; editorial changes and other minor additions

IMPORTANT NOTE

This document describes post-closure safety calculations for a generic deep horizontal drillhole repository. The calculations are preliminary and do not derive from a specific geographic location or geological site. The layout and design of the repository represent only the general disposal concept as no site-specific characterization data or detailed technical designs are available. The conceptual and numerical models, as well as assumptions and parameters and their uncertainties, are reflective of this context. Generic calculations are a necessary step toward developing a comprehensive, site-specific safety analysis that eventually supports the safety case of a deep horizontal drillhole repository in compliance with all applicable regulations.

EXECUTIVE SUMMARY

This report presents generic post-closure radiological safety calculations of a horizontal drillhole repository for spent nuclear fuel (SNF) sited in an argillaceous host rock. The disposal concept consists of an array of deep horizontal drillholes bored into suitable host rocks using directional drilling technology. Individual spent fuel assemblies are contained in canisters, which are then placed end-to-end into the sub-horizontal disposal section of a cased drillhole with a diameter of 0.48 m.

A system of multiple engineered and natural barriers is relied upon to provide safety from radiological exposure. The performance of this barrier system with respect to waste isolation from the accessible environment has been quantitatively evaluated using a physics-based numerical model that accounts for coupled thermal-hydrological fluid flow and radionuclide transport processes. The model incorporates most subcomponents of the repository system, spanning spatial scales from that of an individual waste canister to the regional scale of the geosphere. Moreover, the time scale covered by the model starts with repository closure, contains the thermal period, and extends to ten million years, a period long enough to capture the time of peak dose. Including these relevant spatial and temporal scales in a single model helps maintain a consistent and transparent treatment of features and processes, and avoids artificial interfaces between submodels of disparate levels of complexity.

The main performance measure evaluated by the post-closure model and used for judging adequate safety is the maximum annual dose to a person at the surface who drinks potentially contaminated water from a well located directly above the center of the repository.

This and other safety metrics have been evaluated for a wide range of conditions and alternative system evolutions, using deterministic simulations of a nominal scenario, sensitivity analyses to examine assumptions and bounding cases, and a probabilistic analysis to evaluate the impact of uncertainties and spatial variability.

The results of these post-closure radiological consequences—calculated using a simplified representation of a generic deep horizontal drillhole repository located in shale— show for both the nominal case and disruptive-event scenarios that (a) the estimated maximum annual dose is low, and (b) the dose estimate is robust to changes in key assumptions as well as uncertainties inherent in the analysis. Furthermore, the calculations suggest that the key safety function of long-term isolation from the accessible environment is provided by the depth of the repository and the attributes of its configuration (i.e., linear arrangement of waste canisters in a drillhole with small cross-sectional area, small perturbation of the host formation). Long-term confinement of radionuclides in the stable waste matrix and long migration times allow for radioactive decay to occur within the repository system, considerably reducing the activity of radionuclides potentially being released to the accessible environment. Retardation and spreading of radionuclides in the geosphere, dilution in the near-surface aquifer and attenuation in the biosphere lead to low annual doses that are calculated to be significantly below a dose standard of 10 mrem per year.

The main objectives of this report are to:

- Assemble a preliminary list of relevant safety aspects that need to be analyzed and assessed when seeking a regulatory license for a deep horizontal drillhole repository.
- Demonstrate that long-term safety from the hazards presented by SNF can be evaluated for a deep horizontal drillhole repository sited in a sedimentary host formation, using established simulation tools and analysis methods.
- Provide arguments in support of a generic post-closure safety analysis as a basis for a subsequent, site-specific safety assessment and license application for such a repository.
- Establish a template for reports describing a site-specific safety analysis.
- Develop a technical basis for discussions with the public, stakeholders, regulators, and collaborators regarding the performance and safety of a horizontal drillhole repository for spent nuclear fuel.
- Determine the suitability of argillaceous formations (specifically shale) as a host rock for a horizontal drillhole repository containing heat-generating nuclear waste.
- Improve the understanding of the safety functions performed by each component of the multi-barrier system of the deep horizontal drillhole repository.
- Assess the robustness of the analyzed disposal system to inherent uncertainties as well as adverse events.
- Determine which elements of a future site-specific safety analysis cannot be supported by a generic analysis because of the lack of relevant characterization data, system understanding, or analysis capabilities.

It is understood that repository performance will have to be reassessed as new information becomes available, and reevaluated for each potential disposal site, accounting for the final repository design and site-specific conditions. Nevertheless, these generic calculations are considered a useful if not necessary step toward developing a comprehensive, site-specific safety analysis which will support the safety case of a deep horizontal drillhole repository in compliance with all applicable regulations.

TABLE OF CONTENTS

LIST OF FIGURES

LIST OF TABLES

1 Introduction

1.1 Background

The fundamental safety objective for a nuclear waste repository is to protect people and the environment from harmful effects of ionizing radiation (IAEA, 2006). The preferred strategy for the management of radioactive waste is to contain and isolate it from the accessible biosphere by disposal in deep geological formations (NAS, 2001; DOE, 2008; Blue Ribbon Commission on America's Nuclear Future, 2012).

According to IAEA (2012), a safety analysis provides the scientific and technical arguments and the evidence needed for the subsequent safety assessment, in which radiation hazards are systematically evaluated for comparison with radiation dose and risk criteria. The safety assessment is an important component of the safety case,* which in turn provides the basis for demonstrating the safety of the repository. The safety analyses and associated assessments evolve with the development of the repository concept, its design, and eventually the as-built facility and its operation. The safety case also facilitates the dialog with all interested parties and supports the license application.

The safety requirements for radioactive waste disposal demand that a safety case be developed together with a supporting safety assessment (IAEA, 2011a,b; 2012), which in turn requires that a safety analysis be performed and documented. An overview of previous repository safety assessments can be found in SNL (2013, Appendix C).

In accordance with Requirement 3 of IAEA (2011a), Deep Isolation Inc. assumes responsibility for carrying out the safety analysis for a deep horizontal drillhole repository. This report documents technical work performed to examine safety-relevant aspects of the proposed drillhole repository.

1.2 Purpose and Role

This document presents generic post-closure radiological safety calculations for the disposal of spent nuclear fuel (SNF) assemblies in a deep horizontal drillhole repository sited in a suitable, argillaceous† host formation, with the purpose of (1) identifying the disposal concept's key safety features and the main factors affecting them, (2) examining

---

* According to Nagra (2002a), "(t)he safety case is the set of arguments and analyses used to justify the conclusion that a specific repository system will be safe. It includes, in particular, a presentation of evidence that all relevant regulatory safety criteria can be met. It includes also a series of documents that describe the system design and safety functions, illustrate the performance, present the evidence that supports the arguments and analyses, and that discuss the significance of any uncertainties or open questions in the context of decision making for further repository development."

† Argillaceous formations consist of sedimentary rocks that contain substantial amounts of silt- or clay-sized particles or clay minerals (hydrous aluminum silicates, such as illite, montmorillonite, kaolinite, gibbsite, and diaspora). Argillaceous rocks include shales, argillites, silt- and claystones, and mudstones. The term shale has been used to denote all of these rock types.

the general behavior of individual repository components, (3) evaluating the overall, long-term system performance, and (4) assessing the robustness of the assessment to alternative scenarios or conceptualizations, changed conditions, and uncertainties in model assumptions, data and parameters. Where possible, evidence is presented to substantiate specific claims regarding the understanding of post-closure safety of the drillhole repository. The arguments and analyses documented here are intended to support the conceptual design, safety case, and licensing process, and help facilitate its site-specific implementation once the geological environment at a given site is sufficiently characterized.*

The role of this technical documentation is to integrate relevant information in a transparent way to demonstrate our understanding of the behavior and long-term performance of a generic deep horizontal drillhole disposal system in the post-closure period. Key uncertainties and their significance for post-closure performance are identified. Finally, this document and its subsequent revisions will support the iterative development of the safety case and facilitate communication between interested parties on safety issues related to a drillhole repository.

1.3 Scope

This generic analysis is concerned with the post-closure radiological safety of the disposal of SNF in a deep horizontal drillhole repository, focusing on argillaceous sedimentary host rocks. The study emphasizes the fate and transport of radionuclides in the engineered barrier system and through the geosphere; a simplified biosphere model is used to convert radionuclide activities in groundwater to annual exposure dose.

At the current stage of development, no disposal site has been selected or identified, and no data have been collected that characterize a specific repository host rock. Nevertheless, initial screening of the geology at prospective repository sites indicates that potentially suitable host formations exist.† Some of these formations have been extensively characterized (mainly by the oil and gas industry), so that a generic, but representative property set can be compiled for the post-closure safety calculations. Uncertainty and spatial variability in safety-relevant formation properties, source-term and biosphere parameters, as well as initial and boundary conditions are accounted for in a probabilistic analysis.

* This generic safety analysis focuses on an argillaceous host formation (see Section 3.4). However, the disposal concept does not preclude the consideration of other geologic environments, including volcanic rocks, granites, or evaporates.

† Deep Isolation Inc. is in the process of establishing criteria that need to be met for a candidate site to be considered suitable. The criteria include stability, the age of the water in the disposal horizon, the isolation of the water at the disposal horizon from water above and below (determined, for example, by isotopic age dating methods), and geochemical conditions that favor the preservation of engineered barriers and promote geochemical immobilization or retardation of radionuclides along their migration path towards the receptor. Candidate host formations are not limited to shales (as chosen here for the generic safety analysis) and other sedimentary rocks, but the concept and related technologies are evaluated also for drillhole disposal in crystalline basement rocks and other suitable formations.

In addition to the nominal scenario, in which the performance of the repository is assessed assuming the system evolves as expected, disruptive events of low probability must be considered. These initial safety calculations examine the consequences of select disruptive events (fault activation by a seismic event and early canister failure). However, no attempt was made to quantify the (low) probability with which such events occur, as such an assessment requires detailed site-characterization data and a final design of the engineered repository components.

In these generic safety calculations, we only consider clay-containing sedimentary host formations (referred to as argillites) to constrain the number of geologic features and the range of material properties that need to be evaluated.

Work on the design of the facility is in its early stages. It should be noted, however, that the subsurface components of a drillhole repository are expected to be relatively simple, reducing the amount of detailed subcomponent analyses and assumptions that need to be made. Some parameterized design options are included in the probabilistic analysis by sampling properties over wide ranges.

While a drillhole disposal is potentially a viable disposal solution for a wide variety of waste types, we only analyze the disposal of SNF assemblies from a pressurized water reactor (PWR). Disposal of this relevant waste type raises issues (e.g., regarding canister size, activity and half-life of inventory and associated heat generation rates) that are more challenging to address than those of most other waste types. The decision to limit the analysis to SNF affects waste acceptance criteria and constrains the range of design options to be examined.

The calculations are limited to evaluating the post-closure period, i.e., safety issues related to surface facilities, repository construction, waste handling and transportation, waste emplacement, and repository closure will be discussed in a separate report and integrated in later iterations of the safety analysis.

A list of features, events, and processes (FEPs) is developed. However, only a subset of these FEPs is analyzed with variable levels of detail. The FEPs are selected to illustrate different aspects of the repository and how they can be addressed.

Finally, the legal environment and regulatory requirements have to be considered when undertaking a safety assessment and preparing the safety case. Regulations for a borehole repository have not yet been issued. This precludes a formal assessment of the repository's performance against regulatory requirements for compliance determination. Nevertheless, statements about the adequacy of safety measures and overall radiological impact of the horizontal drillhole repository can be made.

In summary, the analysis presented here is generic in that it considers realistic and relevant system properties that are, however, not related to a specific site. The evaluation of potential sites and of their suitability as a location of a drillhole repository for nuclear waste is not part of this analysis. The analysis is based on a reference repository concept and reference design that will likely be revised and adapted to site-specific conditions as part of the safety case development.

An iterative, graded approach is followed to demonstrate the post-closure safety of a horizontal drillhole repository. This implies that the scope and level of detail of the analysis reflects the development stage of the repository concept, the complexity of the evaluated disposal system, the amount of information available at the time of the analysis, and the magnitude of the potential hazard as estimated in previous assessments; the context of these safety calculations is further discussed in Section 2.1.

Future revisions of this document will (a) address concerns, feedback and review comments by the scientific community, regulators, stakeholders, and decision-makers, (b) incorporate improved scientific understanding, (c) adopt expertise, experience and lessons learned from the international community, (d) take advantage of technological advances, (e) include available site characterization data, (f) evaluate design modifications, (g) focus on key areas of concern identified in previous analyses or raised by newly available information, (h) respond to changes in the regulatory environment, and (i) comply with regulatory and managerial decisions.

1.4 Document Outline and Conventions

The outline of this document follows the guidance and templates provided by the International Atomic Energy Agency (IAEA, 1981; 1983; 1985; 2012; 2017), the examples provided by published SARs (e.g., Nagra, 2002a–c; Posiva, 2007; DOE, 2008; GRS, 2008; NDA, 2010; NWMO, 2012, 2013; SKB, 2015), and other related publications (e.g., SNL, 2009; 2013; Freeze et al., 2019a,b).

Footnotes are used to provide definitions, short explanations, cross references and some technical details that support the reproducibility of the modeling work; they are considered useful but are not necessary to fully understand the general approach, results and interpretation of these generic safety calculations.

2 Safety Strategy

2.1 Context

This report documents numerical calculations for a deep horizontal drillhole repository. The analyses and findings are therefore preliminary and will be revised as the disposal concept, technology, and other conditions evolve (see Section 1.3).

While the horizontal drillhole concept is novel, the safety of nuclear waste disposal in deep (nominally vertical) boreholes has been discussed for several decades. An early evaluation was done by the U.S. National Academy of Sciences (NAS, 1957). In 1979, a study commissioned by the U.S. Atomic Energy Commission (O'Brian et al., 1979) outlined the possibility of waste disposal in deep vertical boreholes. The report evaluates geotechnical, geophysical, environmental and safety issues, discusses data adequacy and identifies research and development needs. Technical feasibility was further examined in a report commissioned by the Office of Nuclear Waste Isolation (ONWI) (Woodward-Clyde, 1981). In 1989, Juhlin and Sandstedt (1989) concluded that waste disposal in very deep vertical boreholes drilled into the crystalline basement rock in Sweden is feasible. In 2003, the interdisciplinary MIT study on the future of nuclear power (Ansolabehere et al., 2003) recommended that deep vertical borehole disposal be investigated as an alternative to mined repositories. Starting in 2009, the vertical borehole disposal concept was further examined by Sandia National Laboratories (Brady et al., 2009; Bates et al. 2014) and a reference design was developed Arnold et al. (2011). Performance assessment modeling capabilities were developed (Freeze and Vaughn, 2012) and applied to the deep vertical borehole concept (Freeze et al., 2013; 2016; 2019a,b). The project was expanded by the U.S. Department of Energy (DOE) in 2012, when an experimental program and demonstration project was initiated (SNL, 2016). The Blue Ribbon Commission on America's Nuclear Future considered deep vertical borehole disposal a potentially promising technology that should be pursued (BRC, 2012). In 2015, the Nuclear Waste Technical Review Board (NWTRB) dedicated one of its board meetings to technical presentations and discussions of the deep vertical borehole disposal concept (NWTRB, 2015). Finally, summary descriptions of European deep vertical borehole disposal programs can be found in Sapiie and Sapiie and Driscoll (2009), Nirex (2004), and Bracke et al. (2017).

The deep horizontal drillhole disposal concept is described in Muller et al. (2019) and summarized below in Section 3. Technical aspects regarding heat dissipation and corrosion have previously been reported, respectively, in Finsterle et al. (2019) and Payer et al. (2019).

Given this context, the present document expands on the previous analyses, adds results of new investigations, and integrates relevant information to document the current understanding of the post-closure behavior and long-term performance of a generic deep horizontal drillhole repository.

2.2 Safety Analysis Process and Approach

The documentation of calculations described here generally follows the applicable IAEA guidance for preparing and documenting analyses that support the safety case for a radioactive waste disposal facility after closure (IAEA, 2012). The following tasks are performed:

- The process begins with a high-level description of the disposal concept and repository design.
- The engineered and natural barrier systems are described and requirements for each component defined.
- Based on this description, safety-relevant FEPs are identified and classified sufficiently that the subsequent safety analysis will eventually attain adequate coverage of the relevant phenomena.
- The FEPs are screened using criteria of probability, consequence, or regulation to determine which FEPs must be included in the safety assessment model, and which may be excluded. FEPs may also be omitted from the model in an initial safety analysis if their effects are readily identified as being positive for repository performance (referred to as "reserve FEPs").
- Based on the list of included FEPs, multiple scenarios are constructed that describe possible initial states and subsequent evolutions of the repository system, specifically regarding the pathways of radionuclide release and migration to the accessible environment.
- A nominal scenario (also referred to as reference scenario or baseline scenario) may be identified, which describes the expected behavior of the repository system. Specifically, the near field is assumed to evolve according to the design functions of the engineered barrier system, the geosphere behaves as inferred from knowledge gained by site characterization, and the biosphere responds based on current conditions making conservative, but reasonable assumptions.
- Alternative scenarios address uncertainty in system evolution as well as "what-if" scenarios to illustrate robustness of the repository system. These scenarios typically deal with disruptive events, such as seismicity, volcanism and human intrusion.
- The scenarios may be screened either in or out using criteria similar to those applied during the FEPs screening process.
- The screened-in scenarios are conceptualized to a suitable level of abstraction in preparation for the development of a corresponding mathematical and numerical safety assessment model.
- Deterministic simulations of the nominal and alternative scenarios are performed and analyzed.
- Epistemic and aleatory uncertainties can be examined by simulating select sensitivity cases, or by performing linear uncertainty propagation analyses or sampling-based probabilistic analyses.

- Alternative repository designs may be simulated to examine the flexibility of the disposal concept and for optimizing the components of the engineered barrier system or the disposal concept as a whole.
- Simulation results are examined for their compliance with postulated regulations and alternative safety indicators.
- Qualitative credit may be taken for reserve FEPs and conservative assumptions or omissions.
- Outstanding issues are identified.

The process outlined above describes a rather comprehensive safety analysis that feeds into a safety assessment and eventually the safety case. In summary, a safety analysis is based on a general understanding of the roles of each of the components of the engineered and natural barriers. Their long-term performance is quantified through numerical analyses, and their robustness to uncertainties and irreducible variabilities is examined through scenario development, sensitivity analyses and probabilistic assessments. These analyses aim at demonstrating that the barrier requirements are met. A series of tests and arguments is presented that justify the confidence in the approach and the results.

Scenarios and models are formulated based on currently available knowledge. If this knowledge is insufficient to justify a particular conceptualization of a FEP, assumptions have to be made that are considered reasonable but generally cautious. Furthermore, if sufficient information is available, realistic parameter values are selected; if such information is highly uncertain or absent, values that are reasonably conservative with respect to the relevant performance measures (defined in Section 4.4) are chosen.

This cautious approach is pursued to make the analysis relevant to a wide range of sites that may be considered for hosting a deep horizontal drillhole repository, and to keep the conclusions regarding safety justifiable. For example, the permeability of the host rock is not expected to be extremely low; it is chosen significantly higher than those of argillaceous formations that have been specifically targeted as host rocks because of their low permeability (see, e.g., Nagra, 2002a; Andra, 2005; Bock et al., 2010; SNL, 2010). Instead of choosing and referencing a site-specific value, properties are selected that serve the purpose of a generic analysis, with the added condition that they are consistent with property values reported in review articles for the corresponding material (see, e.g., Neuzil (2019) for permeabilities and porosities of shales and clays, Babadagli and Al-Salmi (2004) for reservoir properties, and Heath (1983) for thermal properties).

Parameter combinations are examined over a wide range (see Section 4.6) to keep the analysis generic and broadly applicable; moreover, the impact of spatial variability is included. Parameters, their values, ranges and uncertainty distributions are discussed in Section 4.5.11 and listed in Appendix B.

As mentioned in Section 1.3, the level of detail of the analysis should reflect the development stage of the repository concept. For example, the initial, preliminary safety calculations (as the one documented here) may not incorporate all included FEPs into the safety model. Instead of developing complex submodels that are difficult to defend in the absence of sufficient knowledge or characterization data, conservative, simplifying assumptions can be made as appropriate, and the detailed treatment can be deferred to a future iteration of the analysis. In the absence of site-specific characterization data and a finalized repository design, the modeling should be based on reasonable, generic descriptions and parameter values, with the uncertainty in these parameters being reflected by a correspondingly broad sampling distribution.

The analysis described below addresses most of the items listed above to demonstrate the overall process and to obtain feedback on its suitability for future safety assessments and the development of the final safety case.

3 System Description

3.1 General Description of Geologic Disposal Facility

A geologic disposal facility is usually described as consisting of three subsystems or spheres (see, e.g., SNL, 2013): (1) the engineered barrier system, (2) the geosphere, and (3) the biosphere. For a horizontal drillhole repository, these three spheres can be summarized as follows:

(1) The engineered barrier system (EBS), which includes (a) the ceramic UO_2 fuel pellets, (b) the zirconium alloy cladding of the assemblies, (c) any material that fills the spaces within the canisters (if any), (d) the canisters, which are made of corrosion-resistant alloy, (e) the buffer material between the canister and the casing (if any), (f) the carbon steel casing, (g) the cement or other filling between the casing and the drillhole wall, as well as (h) plugs, seals and backfill materials that seal potential flow paths along the horizontal disposal section and the curved and vertical sections of the access hole.

(2) The natural barrier system (NBS) or geosphere, which consists of the host rock containing the geologic disposal facility, and the other geologic units above and below the repository horizon. These geologic formations provide mechanical protection of the repository as well as hydrological and geochemical barriers for radionuclide migration towards the accessible environment.

(3) The biosphere, which is at or near the land surface, defining the accessible environment through which the receptor may be exposed to ionizing radiation.*

A comprehensive safety analysis considers all relevant thermal, hydrologic, geochemical, geomechanical, biological, and radiological processes occurring within these three subsystems. It examines scenarios that include features and events that exist or occur during the expected, nominal evolution of the repository system, or if the system is perturbed by disruptive events.

The following subsections contain a general description of the engineered and natural components of the horizontal drillhole repository system. The features and events of the nominal and disruptive scenarios are summarized in Sections 4.2 and 4.3. Key processes are discussed as part of the model description in Section 4.5.4.

* The calculations documented in this report only consider post-closure radiological hazards; if required, demonstration that the disposal system provides adequate protection also against non-radiological hazards will be documented elsewhere.

3.2 Overall Description of Horizontal Drillhole Repository Configuration

These calculations are concerned with a repository concept for the disposal of spent nuclear fuel from commercial reactors. The concept consists of a single or an array of deep horizontal drillholes bored into suitable host rocks (specifically argillites) using off-the-shelf directional drilling technology. Individual PWR assemblies are encapsulated in customized, corrosion-resistant canisters, which are placed end-to-end into the relatively small-diameter, cased and potentially backfilled horizontal disposal sections of the drillholes.

The overall configuration of a horizontal drillhole repository is schematically presented in Figure 1. A vertical access hole is drilled and cased from the surface through confining geologic units to a kickoff point a few hundred meters above the target repository depth. The purposes of the conductor and surface casings are, respectively, to guide the drilling and to protect freshwater aquifers, schematically shown in Figure 1b. Below the kickoff point, a smaller-diameter hole is drilled that gradually curves until it is nominally horizontal. The radius of curvature is large enough to avoid any impedance during casing installation and waste canister emplacement. After the casing in the curved section is cemented in place, a final smaller-diameter drillhole continues near-horizontally for a few hundred meters to several kilometers. For larger-diameter canisters, the horizontal[*] section may be drilled in two stages: a first small-diameter stage for characterization and testing of the disposal section followed by a reaming operation to create a diameter large enough to house the canisters. The near-horizontal part of the drillhole is the waste disposal section of the repository, having a minimal diameter needed to accommodate the canister size designated for a given drillhole. The final casing runs continuous from the surface through the vertical, curved, and horizontal sections of the drillhole; it facilitates the emplacement (and potential retrieval) of the canisters and supports backfilling operations. This casing is also cemented in place, potentially with monitoring systems embedded or attached to it,[†] which communicate real-time data about the repository condition to the surface during the pre-closure and evaluation periods.[‡] None or only minimal safety functions are ascribed to the casing.

As the hole is being drilled, rock cores, fluid samples and well logs are collected to aid in site characterization and emplacement decisions. Drilling technology has advanced to the

[*] From here on, the orientation of the "near-horizontal" disposal section will be referred to as "horizontal," even though small deviations from true horizontal will occur, either due to drilling imprecisions or by design to (a) better follow the stratigraphic inclination of the formation, or (b) to keep fluids and dissolved radionuclides from migrating towards the vertical access hole by inducing density- or buoyancy-driven fluid gradients pointing towards the dead-end of the drillhole.

[†] Careful sealing of the access hole and plugs at or along the disposal section minimize the risk that preferential pathways develop along monitoring lines.

[‡] The performance confirmation period is used "to confirm that subsurface conditions are within licensing limits and that natural and engineered barriers are functioning as intended" (NWTRB, 2018). The evaluation period is on the order of 100 years and may include time during either or both of the pre- and post-closure periods.

point where rotary steerable systems have high precision, and drilling, completion, and monitoring operations are performed routinely in the oil, gas, and geothermal industries.

Several drillholes may be completed from the same or multiple surface pads, either using separate vertical access holes or possibly by drilling multiple laterals (potentially at different depths) from a single access hole. Modular drillhole repositories could be constructed at or near the sites where the waste was generated and is currently stored, minimizing or even avoiding the need for waste transportation outside the boundaries of the nuclear facility. Alternatively, larger, regional repositories could be built if considered appropriate for social or technical reasons or if otherwise preferred. These safety calculations consider disposal holes that are drilled individually from the land surface.

As an example, Figure 1 shows a configuration with 10 parallel drillholes that are separated by 100 m. Each disposal section is 1 km long and at a depth of 1 km. Such an array of drillholes represents the configuration for which the safety calculations are performed, assuming that drinking water wells extract water from the aquifer directly above the center of the repository. While the number of parallel drillholes depends on the amount of waste being disposed of,* the actual number is of little relevance for the analysis, as the calculations can be done for a single symmetry cell (see Section 4.5.2 and Appendix C).

* About 10 drillholes are required to dispose of the waste from a 1 GWe PWR generated over a period of 30 years.

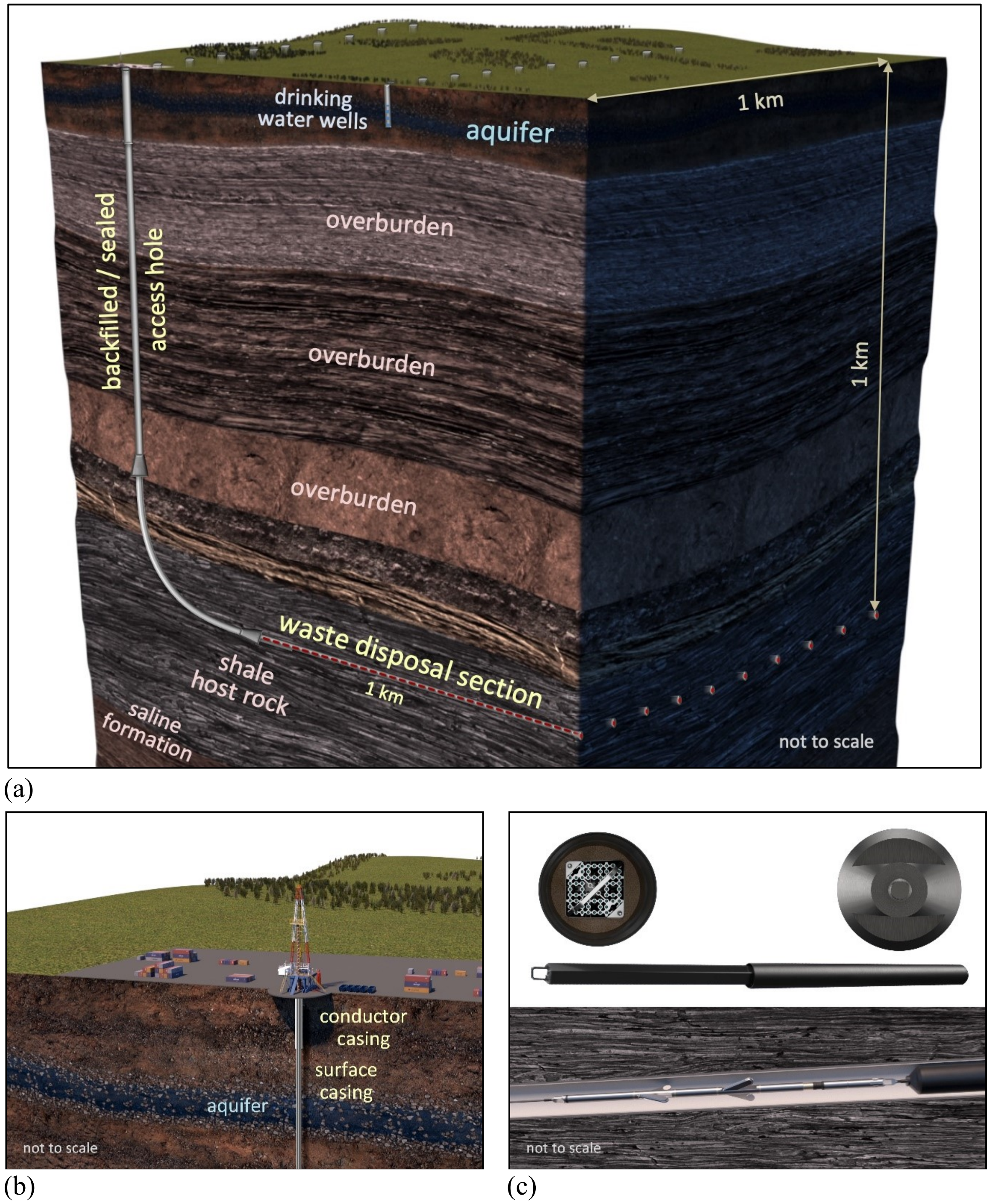

Figure 1. Schematic of a deep horizontal drillhole repository (not to scale); (a) a vertical access hole is drilled to the kickoff point below confining layers, where the hole is gradually curved until it is horizontal, which is the waste disposal section holding the canisters. A repository may consist of multiple drillholes; (b) during pre-closure operations, casings provide stability, protect aquifers and guide waste canister emplacement; (c) individual spent fuel assemblies are placed into canisters which are capped; a tractor, coiled tubing or drill pipe is used to push the canister into the horizontal disposal section of the drillhole.

3.3 Engineered Barrier System

The EBS includes the waste form, canister, buffer, casing, cement behind the casing, as well as backfills and plugs used to seal the drillhole. The EBS is represented by the source-term model and the near-field model.*

In general, the release of radionuclides from the repository to the geosphere is constrained by a system of multiple engineered barriers. The radionuclides are encapsulated in the waste form matrix, which is enclosed in corrosion-resistant canisters. Radionuclides may leach out of the matrix and be released from the canisters only after the canisters are breached and the waste form slowly degrades. The waste-degradation and source-term models are described in Section 4.5.5.

The canisters are embedded in a suitable buffer material† that can (a) reduce or prevent ingress of formation water and advective transport of leached radionuclides, (b) reduce or prevent axial radionuclide migration, (c) protect the canisters from high, localized mechanical stresses, (d) buffer the environment to keep it chemically benign, (e) retard radionuclide transport by adsorbing them to the surfaces of buffer particles or through precipitation, (f) suppress biological and microbial activities, and (g) facilitate the conductive dissipation of the decay heat emanated by the decaying waste.

The buffer is kept in place by the casing, whose main purpose is to enable the smooth and controlled emplacement (and potential retrieval‡) of the canisters during the operational phase of the repository. The casing is not specifically designed to resist corrosion, and no long-term barrier functions are assigned to it. While the casing in the disposal section will remain in place, the casings (and potentially the surrounding concrete) in the vertical and potentially the curved sections of the access hole will be removed prior to backfilling and sealing (e.g., Vrålstada et al., 2019).

Cement (or other suitable grouting materials) will be placed into the annulus between the casing and the drillhole wall, stabilizing the casing during waste emplacement operations. The cement also changes the chemical environment so as to reduce corrosion of the casing during and after the operational phase. Moreover, the cement mitigates the uninhibited axial flow of water, which could carry radionuclides towards the vertical access hole or a water-conducting feature that may have intersected the repository during a disruptive event.

Plugs, which can substantially reduce axial flow, can be installed at certain intervals within the horizontal disposal section and at the beginning or end of the curved hole, or along the

---

* The near-field model also includes the excavation disturbed zone (EDZ), which is the transition zone affected by the repository, but typically assigned to the natural barrier system (see SNL, 2013; Figure 2-1).

† For these generic safety calculations, no specific buffer material has been selected; instead, generic buffer properties (see Appendix B) have been assigned to the space between the canister and casing.

‡ See NEA (2011, 2012) and NWTRB (2018) for a discussion of the retrievability requirements during the pre- and post-closure periods.

vertical access hole. All open spaces within the access hole will be backfilled using suitable materials, effectively sealing and thus isolating the disposal section from axial flow and transport.*

The representation of the engineered barrier system in the near-field model is described in Section 4.5.7.

3.4 Natural Barrier System

The NBS extends from the drillhole wall to the biosphere and includes the disturbed rock zone around the drillhole, the host rock, and other units of the geosphere. The NBS is mainly represented by the far-field model.

The key safety function of the natural barrier system is the effectiveness of the host rock to improve repository performance, in part by mechanically protecting the repository from near-surface impacts and disturbances, and in part by inhibiting radionuclide migration. The transport of radionuclides is slow due to the host rock's low permeability and porosity, and is further retarded by adsorption of the solutes onto the solid phase (see Section 4.5.4.3 for details).

Different types of geological formations have been considered as host rocks for nuclear waste repositories, including salt, granites, tuffs, as well as sedimentary rocks such as shales, unconsolidated muds or mudstones, and claystones.

These safety calculations focus on shale as the host formation. Shales are fine-grained, laminated sedimentary rocks with a fissile texture that are formed by compacting silt and clay-size mineral particles. Despite a relatively large total volume of the shale's pore space (Neuzil, 2019), the individual pores are very small; consequently, shale permeability is typically very low. The clay minerals present in shale have the ability to take up and adsorb considerable amounts of water and ions, including radionuclides. Shale mechanically perturbed by the repository may gradually self-seal (Bock et al., 2010; Sone and Zoback, 2013; Geng et al., 2018).

Shale has been selected for this generic analysis because shales and other argillaceous formations are considered viable host rocks for a high-level waste repository (Nagra, 2002a; Andra, 2005; SNL, 2010; NWTRB, 2016),† and because the ability to complete

* The performance of multiple sealing materials has been analyzed in detail, for example, by Blümling (2005), Blümling and Adams (2008), Arnold et al. (2011), AMEC (2014), SKB (2018), Vrålstada et al. (2019), and Freeze et al. (2019b). For these generic safety calculations, no particular sealing material has been chosen; instead, generic properties (see Appendix B) are assigned to the portions of the drillhole that are backfilled.

† It is recognized that other potential host formations, especially salts and igneous rocks, have particular features (such as creep flow or extensive fracturing, respectively) that are not adequately addressed in a safety analysis that focuses on argillites. Nonetheless, it is necessary to choose a host-rock type even in a generic safety analysis to be able to present a self-consistent discussion of the repository system. The final safety analysis in support of a site-specific safety case and a license application will be based on all available information and address a particular

extended horizontal drillholes in such formations has been amply demonstrated by the oil and gas industry. However, shale properties, including their self-sealing capability*, vary considerably. For the purposes of hosting a repository, shales that are clay-rich and more plastic, less indurated and less fissile are preferable (Gonzales and Johnson, 1984). However, to remain generic, safety-relevant shale properties are examined over a rather wide range.

The natural barrier system also involves formations above and below the host rock, as these adjacent units may affect the conditions in the repository, its evolution, and its ultimate safety. Units overlying the host formation are also encountered by radionuclides as they migrate towards the accessible environment. For these numerical simulations, the formation between the host rock and the aquifer is conceptualized as a generic formation with properties that do not unduly contribute to the overall safety of the system.†

Similarly, the formation underlying the host rock is conservatively assumed to be relatively permeable, i.e., it can respond to and transmit changes in the regional hydrogeologic conditions that may affect the repository. It may represent a deep saline formation, which might be used for wastewater injection or geologic carbon sequestration, human activities that may occur at a considerable distance from a nuclear waste repository.

A near-surface aquifer used to provide potable water is represented in the model as it defines the interface to the biosphere. Groundwater is pumped from the aquifer at a high enough rate so that almost all contamination from the repository reaches the drinking water well and enters the local water supply.

In general, the geochemical conditions in a deep, saturated host rock and surrounding formations are reducing. Such conditions decrease or inhibit the dissolution of spent fuel pellets, offset potential deleterious effects of radiolysis, and favor the immobilization of several long-lived transuranic and fission product radionuclides in the waste form. The latter occurs through formation of relatively insoluble secondary phases, and through

---

set of features, events, and processes using site characterization data.

* The swelling and self-sealing capacities of argillites are considered a desirable property of a host rock. However, the behavior of a clay-rich host rock strongly depends on its mineralogy and the local geochemical conditions. For example, smectite can absorb significant quantities of water, but only in the presence of dilute groundwater; at high ionic strength, it is likely to lose water and shrink. Other clay minerals, e.g., illite, do not have this capacity to gain or lose water. Furthermore, although smectites can adsorb a variety of ions, other clays are more limited, much depending on charge and ionic radius of the ion in question. Some clay minerals do not adsorb ions at all. It should be noted that swelling and shrinking of clays are processes that mainly occur during hydration and dehydration of the material. This is important to consider in mined repositories, which are ventilated and require resaturation of the initially unsaturated backfill and buffer materials. A drillhole repository is always fully saturated, i.e., these processes are of less significance.

† The overburden is not ascribed specific barrier properties (such a low permeability of a typical sealing layer); it simply separates the repository from the aquifer (thus prolonging radionuclide transport distance and time) and generically protects the repository from surface processes.

preferential adsorption on reducing minerals, thereby enhancing their retardation during transport through the engineered and natural barrier system. Reducing conditions also afford the opportunity to design long-lasting engineered barriers that could isolate the waste from chemical attack by saline waters until most fission-product radionuclides have decayed to insignificant levels.

Details about the implementation of the natural barrier system in the far-field model can be found in Section 4.5.8.

3.5 Biosphere

The biosphere consists of the accessible environment where the receptor resides. These near- and above-surface environments as well as the receptor's lifestyle are described in the biosphere model (see Section 4.5.9). A detailed description and representation of the biosphere requires site-specific information. For these generic safety calculations, the biosphere is highly simplified and consists of a well extracting drinking water from the aquifer located immediately above the horizontal disposal section of the drillhole repository, capturing all radionuclides that potentially enter the aquifer from underlying formations or along the vertical access hole. The receptor is exposed to ionizing radiation by the ingestion of contaminated groundwater, which is assumed to be the exclusive source of drinking water. This abstraction of the biosphere is further described in Section 4.5.9.

4 Generic Post-Closure Safety Calculations

4.1 Overview

As discussed in Section 2.2, the post-closure safety analysis method includes multiple steps, leading to a quantitative evaluation of repository performance and related arguments that assess the safety of the repository system. Because the time frame of concern is far beyond that of social and technical experience or planning, safety cannot be demonstrated by direct observation. Instead, long-term performance of the engineered and natural barrier components—or of the total repository system—must be illustrated by developing defensible conceptual and numerical models, and by accounting for the impact of assumptions, uncertainties, and variabilities.

Given the generic nature of these initial safety calculations of the deep horizontal drillhole disposal concept, only a subset of FEPs is analyzed. Furthermore, the analysis is limited to a preliminary repository design and a generic hydrogeologic environment. Some of the subsystems and processes are represented by simplified models or are replaced by conservative assumptions. Transport calculations include only four radionuclides: ^{129}I, ^{36}Cl, ^{79}Se, and ^{99}Tc. As described in Section 4.5.5.2, these radionuclides are selected because of their respective inventory, half-life, adsorption potential, and toxicity, each illustrating a characteristic group of radionuclides.

Relevant features, events and processes were identified by a FEPs analysis (see Section 4.2), which is based on existing FEPs lists. These generic and site-specific FEPs lists are adapted and amended to account for the specifics of the horizontal drillhole disposal concept. Based on an initial FEPs disposition, multiple scenarios are developed (see Section 4.3), describing the nominal case as well as select disruptive events. Scenarios for select deterministic sensitivity analyses are also described.

Section 4.4 introduces the metrics to be calculated by the numerical model as a basis for the evaluation of repository performance and its sensitivity and robustness to uncertainties in input parameters and modeling assumptions.

Section 4.5 is dedicated to a description of the conceptual and numerical model developed to assess repository performance under the various scenario classes. The methods used to account for uncertainty and variability are discussed in Section 4.6.

Model results are presented in Section 4.7, starting with a discussion of the simulated system evolution and performance metrics for the nominal case. The results of the sensitivity analyses and probabilistic uncertainty propagation analyses are described next, as they are all based on the nominal scenario. Finally, the results obtained for disruptive-event scenarios are discussed.

4.2 FEP Analysis

A list of safety-relevant FEPs[*] has been compiled to eventually approach phenomenological completeness of the safety analysis. The FEPs list is specific to a horizontal drillhole repository and was developed based on the international FEP (IFEP) list, which is a comprehensive and structured generic list of factors relevant to the assessment of the long-term safety of geologic repositories, developed by the OECD/NEA (NEA, 2000; 2006). The IFEP list was then supplemented with various project-specific FEPs lists, specifically those related to the deep borehole disposal concept (Brady et al., 2009) and projects involving argillaceous host rocks (Nagra, 2002c; SNL, 2010). The FEPs of these lists were adopted if appropriate or modified as needed. Furthermore, FEPs that are specific to the horizontal drillhole disposal concept were added. Only FEPs concerned with the post-closure period are relevant for the current analysis.

The FEPs were categorized according to the numbering scheme of the IFEP list. In an initial screening, FEPs were then designated as included, excluded, or deferred, where the last designation was used to indicate FEPs that depend on specific design decisions or site characteristics that have not yet been made at this stage of the repository development. Short rationales are provided for excluded FEPs, whereas included (or retained) FEPs are subject to further analysis by the model described here.[†]

Sections that discuss the various scenarios (Section 4.3), the conceptual model (Section 4.5.2) and the corresponding mathematical models (Sections 4.5.4–4.5.9) contain descriptions of the FEPs that are included for these generic analyses.

4.3 Scenarios

4.3.1 Scenario Development

A scenario (also referred to as an assessment case) is a specific set of assumptions regarding (a) the broad evolution of the repository and its environment, (b) the conceptualization of individual FEPs relevant to the fate of radionuclides within the disposal system, and (c)

---

[*] FEPs is a list of aspects (categorized as features, events, and processes) that potentially impact the performance of the repository system. An exhaustive list of such FEPs typically consists of many hundreds of items. The number of FEPs retained for inclusion in a safety analysis is smaller, as FEPs with low probability or low consequence can be excluded without undue impact on repository safety. Examples of *features* include waste forms (e.g., inventory of different radionuclides), waste packaging (spent fuel pellets, cladding, canisters), buffers, seals and plugs, the disturbed rock zone, the host formation and other geological units, and elements of the biosphere. Examples of *events* include early corrosion failure, seismic or volcanic events, a criticality accident, or human intrusion. Examples of *processes* include advective and diffusive transport, thermal effects, geochemical reactions, geomechanical deformations, and climate change.

[†] Retained FEPs can also be examined by means other than numerical modeling, such as natural analog studies; such studies are summarized, for example, in Miller et al., (2000), Nagra (2002a; Section 5.7.1), NWMO (2013, Section 10), SNL (2013; Appendix B), and (Milodowski et al., 2015).

the parameters used to describe these FEPs (Nagra, 2002a). Different scenarios can thus be viewed as alternative lists of retained FEPs, where each list describes a reasonable, potential evolution of the repository system (Swift et al., 1999; DOE, 2008). Similar to the development of the FEPs list, scenarios are identified, classified and screened before they are used as a basis for conceptualizing the corresponding systems and implementing them into safety analysis models.

In the present calculations, several assessment cases are defined and analyzed, specifically the nominal scenario, but also disruptive scenarios that illustrate the impact of detrimental FEPs and related uncertainties on the level of safety provided by the disposal system. Given that neither a finalized design nor site-specific data are available in this early stage of repository development, the range of assessment cases is incomplete and, therefore, does not include all realistically conceivable possibilities affecting the post-closure evolution of the repository system.

4.3.2 Nominal Scenario

The nominal scenario considers several conceivable pathways for radionuclide migration from the waste form to the recipient of contaminated groundwater under undisturbed conditions (disturbed conditions resulting from disruptive events are analyzed separately; see Section 4.3.3). These potential pathways include diffusive releases from the degrading waste form through breached canisters to the backfilled drillhole. After mobilization of radionuclides from the solid waste matrix and their release from the canister, they are transported by advection and diffusion (a) in axial direction (i.e., along the backfilled drillhole as well as the excavation-disturbed zone of the horizontal disposal section to the curved and eventually the vertical access hole towards the near-surface aquifer), and (b) outwards into the host rock and through the overburden to the near surface aquifer. Radionuclides enter the aquifer either vertically from the underlying formation or radially from the access hole penetrating the aquifer. They are then transported (predominantly by advection) through the aquifer towards a well, which feeds into a water supply system that distributes the untreated water to the recipient (see Section 4.5.9).

Diffusive radionuclide transport is driven by concentration gradients. Water flow leading to advective radionuclide transport is driven by head gradients, which in turn are affected by ambient hydrologic conditions, pressurization due to thermal expansion of the fluid, and buoyancy effects due to differences in temperature and salinity. Transport of certain radionuclides may be retarded by adsorption. The total mass of radionuclides within the modeled repository system diminishes with time due to radioactive decay.

The nominal scenario considers the timeframe that starts immediately after repository closure. It includes the thermal period and extends to a final simulation time of 10 million years, ensuring that the time of peak dose is captured.

The nominal scenario can be adapted to site-specific conditions once characterization data and other relevant information about a potential repository site become available.

4.3.3 Disruptive Scenarios

4.3.3.1 Introduction

Disruptive events are low-probability events with potentially high impact. As such, they are outside the envelope of repository evolutions described by the nominal scenario, i.e., they are possible deviations from the expected evolution. Long-term safety of a repository system is significantly improved in a setting that is less prone to disruptive events. In these generic calculations, we examine the impact of a few disruptive events on the performance measures without evaluating their occurrence probabilities, which are site-specific.*

4.3.3.2 Seismic Scenario

A disruptive seismic event is defined here as the effect of a natural† earthquake large enough to activate a new fault or reactivate an undetected, existing fault‡. While vibratory ground motions have no detrimental impact on waste canisters emplaced in a disposal drillhole,§ waste canisters may be sheared during the activation of faults or fractures that directly intersect the repository** and exhibit a sufficiently large displacement.†† Moreover, faults activated during an earthquake and the associated fracture zone may generate preferential flowpaths for fluid flow and radionuclide transport, potentially creating a new,

---

* For example, for the disruptive seismic event scenario, the annual probability with which different levels of vibratory ground motion and fault displacement are exceeded is typically determined by a probabilistic seismic hazard analysis (PSHA), which takes into account the site-specific tectonic and geological settings.

† Drilling and operation of the repository will not induce earthquakes, as no fluids are injected at high pressures; microseismic events may be induced by the repository heat during the thermal period, but the energy released during such events is far below that needed to cause a disruptive event comparable to the large, natural earthquakes discussed here.

‡ Existing faults detected during the logging of the drillhole or characterization of the host rock should be avoided, i.e., no canisters should be emplaced at or near such fault intersections, reducing the probability that fault reactivation causes the breaching of one or multiple canisters.

§ In a mined repository without backfill (such as at Yucca Mountain), vibratory ground motions during an earthquake need to be considered because they may cause rock fall or drift collapse, potentially damaging the canisters or making them susceptible to localized corrosion. No such hazards are possible in a backfilled drillhole, i.e., the waste canister's internal structure and the waste form are not affected by vibratory ground motion and remain intact during an earthquake.

** The probability that an activated fault intersects the horizontal disposal section of the repository can be reduced by orienting the drillhole axis perpendicular to the direction of the minimum horizontal stress.

†† During fault displacement, waste canisters may slightly rotate if embedded in a sufficiently soft backfill material. However, even moderately large earthquakes generate offsets that exceed the maximum available rotation angle, which is restricted by the small diameter of the disposal drillhole. It is assumed that canisters intersected by a fault activated during an earthquake will be breached.

direct connection between a pressurized compartment of the deep subsurface and the repository, or between breached waste canisters and the near-surface aquifer. Finally, deformations caused by large earthquakes may induce fluid-pressure changes and thus driving forces, specifically across the fault line. However, such gradients tend to dissipate within time frames that are short compared to the time scale relevant for repository performance.

A disruptive scenario is formulated to capture the effects of a seismic event. This seismic scenario is based on the nominal scenario described in Section 4.3.2, but includes a sub-vertical high-permeability feature, which represents an activated fault and associated fracture zone.[*] Note that faults are not necessarily highly permeable. Brecciation of the rock during displacement or sealing of the fault aperture with fine-grained gouge material or precipitates may create a sealing fault with low permeability. Furthermore, the fault offset leads to the juxtaposition of strata with different properties, which may make the fault sealing (or leaking) in fault-perpendicular direction. In the current simulations, a non-sealing fault is postulated. The fault zone intersects the repository and extends to the land surface (Wang et al., 2016); it exists from the beginning of the simulation, i.e., the earthquake is assumed to strike shortly after repository closure.[†] The fault remains conductive throughout the simulation period, i.e., no fault closure or sealing is expected to occur.

4.3.3.3 Early Canister Failure Scenario

The engineered barrier system may fail prematurely by the through-wall perforation of the waste canisters and casing[‡] due to manufacturing- or handling-induced defects or damage. This penetration would occur considerably earlier than predicted by the corrosion model used in the nominal scenario. Early failure of a defective canister or casing is pessimistically assumed to occur at the time of repository closure.

Canister performance may be detrimentally affected by improper base material selection, improper fabrication or treatment of the outer shell and lid, improper application of the corrosion-resistant alloy layer, improper welding, improper burnishing, surface contamination, or mishandling of the canister during operations in the power plant, re-packaging, transportation and emplacement in the drillhole. The consequence common to these types of defects is an increased susceptibility to stress corrosion cracking. The probability of a canister defect depends on the fabrication and handling processes and associated quality control procedures as well as human error probability data.

---

[*] In the numerical model, the fault zone is represented by a subvertical, flat ellipsoid, with permeabilities that increase from the background value at its edge to the fault value at the axes of the ellipsoid according to a spherical distance function.

[†] The probability of an earthquake of a certain magnitude to occur is typically analyzed as part of a probabilistic seismic risk analysis, and may be supported by a site-specific baseline micro-seismic monitoring program.

[‡] The main purpose of the casing is to facilitate emplacement (and potential retrieval) of waste canisters in the horizontal disposal section of the drillhole. No specific barrier function is assigned to the casing, which is expected to degrade relatively quickly.

4.3.4 Sensitivity Analyses

Sensitivity analyses are used to examine the impact of certain FEPs on repository performance. The corresponding conceptual models are not scenarios in the sense defined above, as they may not necessarily represent an expected or even possible evolution of the repository system.* The sensitivity analyses presented below typically examine the influence of a single parameter on a single performance metric (specifically annual dose) by perturbing this parameter by its expected uncertainty, or by setting it to bounds that are considered reasonable, or my removing it altogether.

All sensitivity analyses are based on the nominal scenario; they are therefore local.† The perturbed parameters or tested assumptions are described along with the corresponding modeling results in Section 4.7.3.

4.4 Performance Metrics

The safety of a long-term repository system is evaluated based on whether pre-defined protection objectives are met. The safety principles and protection objectives will be defined by regulations. For this generic analysis, a number of performance metrics‡ are calculated, assuming they are meaningful indicators and will be useful for eventual comparison with regulatory protection objectives.

The main metric used to assess the performance of the deep horizontal drillhole repository is the maximum effective dose received by an individual who obtains drinking water exclusively from a well drilled into an aquifer above the disposal section of the repository.§ Because properties (such as half-life and adsorption coefficients) are radionuclide-specific, the time at which the radionuclide concentration in drinking water reaches its maximum is different for each radionuclide. Moreover, properties of the engineered barrier system and

---

* For example, diffusion may be entirely removed from the numerical model to examine its importance for radionuclide migration relative to that of advective transport. Such a sensitivity analysis is meaningful, even though the assumption of a vanishing diffusion coefficient is not.

† A local sensitivity analysis evaluates parameter influence and model output sensitivity at (or around) a single point in the n-dimensional parameter space, where n is the number of uncertain or adjustable model input parameters. A global sensitivity analysis calculates composite sensitive measures over the entire parameter space, accounting for non-linearities and parameter interactions. See Saltelli et al. (2008) for a detailed discussion of various sensitivity analysis methods.

‡ Performance metrics are also termed performance indicators, which can be defined as follows (Becker et al., 2009): "*A performance indicator is a quantity, calculable by means of appropriate models, that provides a measure for the performance of a system component, several components or the whole system in comparison with each other.*" If the performance indicator is compared with a reference value, a safety indicator is obtained: *"A safety indicator is a quantity, calculable by means of suitable models, that provides a measure for the total system performance with respect to a specific safety aspect, in comparison with a reference value quantifying a global or local level that can be proven, or is at least commonly considered, to be safe.*"

§ Details about the dose calculation can be found in Section 4.5.5.

geosphere (which are evaluated for various different values in a probabilistic safety analysis) also affect timing and magnitude of concentrations and thus exposure rates. To properly account for this variability, the peak dose is calculated based on the sum of the dose contributions of all relevant* radionuclides, and is evaluated for each realization generated by probabilistic sampling of property sets and scenarios. This results in a distribution of maximum dose exposures at the realization-specific time when the peak dose arrives at the water supply system. The overall performance measure is the maximum peak dose—independent of the time it occurs. Peak dose is calculated as a single value for select, deterministic simulation cases, or is reported as the probabilistically evaluated peak-dose distribution (the distribution is either visualized or described by statistical parameters such as mean, median, mode, and select percentiles).

While peak dose is considered the main performance measure, other metrics are calculated to gain insight into the behavior and robustness of the repository system. Table 1 is a list of performance measures evaluated as part of these generic safety calculations. These performance measures will be consistently evaluated for each scenario and realization, enabling a comparative analysis. In addition, all state variables calculated by the simulator (i.e., pressures, temperatures, brine mass fractions, radionuclide concentrations, fluid and component flow rates, and property fields at each computational point in the three-dimensional model domain and over the simulated performance period) are available for inspection.

No time cut-off is imposed on the analysis, i.e., the performance metrics are evaluated at least up to the time when maximum potential consequences have passed. Finally, long-term repository safety must be achieved without the need for further safety measures or mitigation after repository closure; no such mitigation measures are represented in the model.

* See Section 4.5.5.2 for a discussion of how relevant radionuclides are selected from the total inventory of isotopes in the waste form.

Table 1: Performance metrics

#	Performance Metrics	Comments
1	Peak dose [a)]	Deterministic peak dose value or quantile of peak dose distribution; peak dose is the maximum of the sum of the dose contributions of all considered radionuclides over the entire performance period.
2	Maximum radionuclide concentration in ground-water [b)]	Maximum radionuclide concentration (or corresponding activity) in groundwater over the entire performance period.
3	Radionuclide flux into host rock	Flux into host rock indicates effectiveness of engineered barrier system.
4	Radionuclide flux into aquifer	Flux from underlying formation into aquifer indicates effectiveness of host rock and overlying formations.
5	Radionuclide flux along drillhole	Flux along drillhole indicates effectiveness of backfill, seals, and plugs.
6	Maximum temperature [c)]	Maximum temperatures at select points (waste form, canister, backfill, casing, host rock) indicates heat dissipation effectiveness.
7	Maximum repository-induced pressure change [d)]	Overpressures generated by thermal expansion.

[a)] Peak dose is the main performance measure used to assess the long-term safety of a nuclear waste repository by comparison to an individual dose-based standard. 10 mrem per year (0.1 mSv yr^{-1}) is a typical individual dose not to be exceeded by the release of radionuclides from a sealed repository given processes and events reasonably expected as described by the nominal scenario.

[b)] Maximum radionuclide concentrations in groundwater (expressed as activity in units of pCi per liter) can be used to assess compliance with 40 CFR 141.66, *Maximum Contaminant Levels for Radionuclides*.

[c)] High temperatures may lead to vaporization and high thermal stresses, and may affect component properties in the near field.

[d)] Thermally induced overpressures may affect the integrity of the engineered barrier components and the effective stress in the near field.

4.5 Model Development

4.5.1 General Approach

The general modeling approach is guided by the purpose of the model, which is to evaluate the system-level performance of the deep horizontal drillhole disposal system. This means that the safety analysis must address all potentially relevant features, events and processes (i.e., those not having been excluded during the FEPs screening process), so their effects on repository performance can be examined. It is not feasible to incorporate all retained FEPs in a single model. The FEPs structure itself (see Section 4.2) suggests that certain features, events and processes refer to a specific subsystem only (e.g., the engineered barrier system, far field, or biosphere) and may thus be studied in separate submodels. Moreover, the effect of some FEPs may be independent or only weakly correlated to the impact of other FEPs. Finally, the fact that the repository system involves complex coupled processes, spans many orders of magnitude in both spatial and temporal scales, and is highly heterogeneous makes its evaluation by numerical modeling computationally very demanding and imposes other practical limitations.

Nevertheless, it is important to realize that the various repository subsystems as well as many FEPs are interlinked to each other, i.e., they are not independent, requiring that information must be properly propagated from one subsystem (or one spatial region, or one time frame) to the next. This challenge is typically addressed by developing a single system-level model that is based on highly abstracted versions of the various submodels. Model abstraction has the advantage that the behavior of a subsystem is reduced to its key features and its most influential parameters, and that the computational cost to evaluate the model is considerably reduced, which is important specifically for probabilistic safety analyses.

However, the simplifications inherent in model abstraction require defensible justification, and the interfaces between abstracted submodels in the system-level model introduce additional issues. Specifically, consistency of scenarios, assumptions, parameters, as well as the impact of discrete effects must be assured across the many interfaces.

As mentioned above, this approach to system-level modeling is often driven by the need for computational efficiency, as the model must be evaluated many times as part of a sampling-based probabilistic safety analyses. However, this approach may lead to a lack of transparency, because the necessary abstractions lead to a compartmentalization of the system with many interfaces between submodels, making it difficult to track the flow of information. Furthermore, it is clear that sacrificing the fidelity of the process model—whose role is to accurately capture the first-order, systematic component of the disposal-system behavior—for the sake of a more accurate probabilistic analysis—which captures the random component and calculates higher-order moments—is a trade-off that requires careful consideration and justification. That consideration and justification, if done well, characterize an acceptable analysis, and their absence would be unacceptable.

A horizontal drillhole repository is considered relatively simple compared to other disposal concepts. This simplicity is believed to innately contribute to a much better ability to understand the repository's safety and robustness (Muller et al., 2019). Moreover, it offers a unique opportunity to develop a transparent system-level model for safety analysis that does not compromise its fidelity in representing features, events, and processes and their interactions. This can be accomplished by creating a single numerical model that includes all subsystems encountered along the radionuclide transport pathway from the heat-generating waste to the receptor. Such an approach avoids the need for multiple abstraction models that must be connected across difficult-to-define interfaces. To the extent possible, the model shall also include most of the key processes in a fully coupled manner, and describe as many multi-scale features as possible using a common set of parameters that are conceptually and numerically consistent throughout the model.

The following sections describe the development of a comprehensive high-fidelity numerical process model for preliminary calculations and eventual use in a safety analysis for a horizontal drillhole repository. The goal of completeness of the model regarding its ability to represent all relevant FEPs is not fully achieved. Specifically, it appears prudent to develop separate models for some of the disruptive scenarios. The model also focuses on coupled thermal-hydrological processes, with geochemical and geomechanical effects only approximately accounted for through the use of effective parameters. This approach is considered acceptable at this stage of repository development, specifically since during the probabilistic analysis (see Section 4.7.4), considerable uncertainties are assigned to effective parameters (such as the k_d value, which represents geochemical processes, or pore compressibility, which represents poroelastic effects).

The code used for the analysis is an extended version of the TOUGH2 numerical simulator for modeling non-isothermal, multiphase flow and transport in fractured porous media (Pruess et al., 2012). The extensions to TOUGH2's basic simulation capabilities are described in Finsterle (1998; 2017; 2019), Finsterle and Kowalsky (2007), and Wainwright and Finsterle (2016). The simulator is integrated in the iTOUGH2 framework, which is used here for formal sensitivity and uncertainty propagation analyses (Wainwright et al., 2014; Finsterle, 2015; Finsterle et al., 2017).

4.5.2 Conceptual Model

Long-term repository performance is assessed by modeling the evolution of the engineered and natural barrier systems from their initial, undisturbed states, and by calculating the transport of radionuclides through this system to the accessible environment. The conceptual model describes which system aspects and processes are included in the model, and how they are simplified and translated into a mathematical form for numerical treatment.

As the goal is to represent all subsystems in a single model, the description of the conceptual model starts with the geometry of each component of the disposal system.

- *Model Domain*: The model domain is determined by (a) the extent of the repository, (b) the location of well-defined natural boundaries or symmetry boundaries, and (c) the distance needed to make unwanted boundary effects insignificant.
- *Dimensionality*: The actual disposal system is inherently three-dimensional. This aspect is preserved in the part of the model that represents the geosphere. Geometry and processes in and around the drillhole are not fully three-dimensional, but can be well represented by a local, radial-axial coordinate system. Specifically, heat conduction and diffusive radionuclide migration from the canisters to the near field

and into the host rock occur almost exclusively in a radial direction, whereas potential advective flow and transport in the drillhole and excavation disturbed zone occur predominantly in axial direction. Note that the axial coordinate follows the trajectory of the drillhole, i.e., from the surface along the vertical access hole through the curved segment to the near-horizontal disposal section of the drillhole. Changes in the gravitational component along the entire length of the drillhole axis are accurately represented, which is relevant for the calculation of hydrostatic pressure conditions and buoyancy-driven flow. In the radial direction within and in the immediate vicinity of the drillhole, gravity can be ignored for the sake of a more accurate representation of the radially symmetric geometry of the waste form, canister, backfill, casing, drillhole, and excavation disturbed zone, as well as for a more accurate and efficient calculation of diffusion-dominated processes radially away from the central string of waste canisters. Section 4.5.3 describes in detail how this axial-radial subsystem is integrated into the three-dimensional Cartesian geosphere model.

- *Waste*: The waste is conceptualized as a heat-generating, degrading, radionuclide-releasing amorphous porous medium placed within 153 individually represented, initially impermeable canisters. Waste degradation processes are not explicitly simulated, but are abstracted by a fractional waste degradation rate. The source-term model for radionuclides is described in Section 4.5.5; the heat source generated by radioactive decay in the waste is discussed in Section 4.5.6.
- *Engineered Barrier System*: The components of the engineered barrier system (i.e., the uranium dioxide spent fuel pellets, the waste canister, buffer material, casing, cement in the annulus, as wells as plugs, seals, and backfills between the waste canisters and along the access hole) are explicitly represented in the model (see Section 4.5.3). Their properties are represented by effective porous-medium parameters. Construction of the repository is assumed to have created an excavation disturbed zone around the drillhole. Corrosion processes are not explicitly simulated; however, the corrosion and eventual perforation of the canisters and casing is represented by a time-dependent increase in permeability based on the corrosion model described in Payer et al. (2019). Gas generation due to corrosion is neglected.*

* Preliminary simulations of hydrogen generation due to general corrosion of the canisters and the casing indicate that most of the hydrogen remains dissolved in the brine (mainly due to the relatively high-pressure environment) and readily diffuses away from the repository. When the solubility limit is exceeded, a free gas phase (consisting of hydrogen and water vapor) exsolves. However, the maximum gas saturation value remains small and declines shortly after the corrosion of the casing is complete. Pressure increases due to the evolution of a free gas phase are moderate and readily dissipate into the geologic formation. The entire repository system reverts back to single-phase liquid conditions due to redissolution of the hydrogen and its radial diffusion away from the repository. While gas generation and its temporary impact on the conditions within the engineered barrier system may be analyzed in specialized submodels, the assumption of fully saturated conditions throughout the long performance period appears justified. See also Section

- *Geosphere*: The geosphere is conceptualized as consisting of four horizontally layered hydrostratigraphic units, representing (1) the near-surface aquifer, (2) the overburden (the set of formations below the aquifer and above the formation that hosts the repository*), (3) the host rock, and (4) an underlying, relatively permeable saline formation.† While each layer has reference properties typical for the corresponding formation, they have heterogeneous porosities, which exhibit a spatially correlated and anisotropic structure (see Section 4.6 and Figure 30). A steeply dipping fault and associated fracture zone may be present, cutting through the geosphere and the horizontal disposal section of the repository (see Figure 32).

- *Biosphere*: Processes in the biosphere are represented by a simple dose coefficient, which is a measure of the radiological impact due to the ingestion of water containing radionuclides. The exposed individual is assumed to obtain drinking water exclusively from a well that is centered above the disposal section of the drillhole repository. Contaminated groundwater withdrawal from the aquifer is explicitly simulated. The biosphere model is described in Section 4.5.9.

- *Processes*: Fluid flow is simulated throughout the model domain using consistent process descriptions, accounting for viscous flow based on Darcy's law driven by pressure gradients and gravity. Fluid properties (specifically density and viscosity) are functions of pressure, temperature and salinity, potentially giving rise to buoyancy effects. Conductive and convective heat transfer is considered. Radionuclide transport from the waste form to the drinking water well occurs by advection and diffusion. Radioactive decay is accounted for. Dispersion is not included because radionuclide transport is diffusion-dominated in the shale and most of the overburden (see Section 4.7.3.2).‡ Reactive geochemical processes are not explicitly simulated; however, the effect of porewater geochemistry is partly reflected by assumptions on degradation rates, adsorption coefficients, fluid properties, and the assumptions underlying the biosphere model. Similarly, geomechanical processes are not explicitly modeled, with the exception of pore compressibility, which

---

4.5.4.2 for a discussion of single-phase liquid conditions during the thermal period.

* The term "overburden" as used here is consistent with its general definition, with the host rock being the formation of interest.

† The hydrostratigraphic layers are not site-specific, but generic, i.e., they represent a variety of rock types. Typically, the near-surface aquifer consists of quaternary or tertiary sedimentary rocks; the overburden can be a carbonate (e.g., limestone, dolomite), marl, sandstone, siltstone, shale, mudstone or clay; as discussed in Section 3.4, the host rock is consider to be a shale; the saline formation can be a carbonate, sandstone, metamorphic rocks (e.g., schist, gneiss), composite rock, or igneous basement rock. All these generic formations are modeled using effective properties that vary over a relatively wide range (see Appendix B).

‡ Dispersion is a scale-dependent property that emerges due to averaging and upscaling. A dispersion term is needed if pore-scale phenomena and small-scale heterogeneities that affect advective transport are not explicitly incorporated in the model. Also note that artificial numerical dispersion is introduced by the spatial discretization of the governing equations.

reflects the coupling between poroelasticity and fluid pressures. The mathematical models describing these fluid and heat flow and radionuclide transport processes are discussed in Section 4.5.4.

- *Initial and Boundary Conditions*: The groundwater table is assumed to be close to the land surface. The initial temperature profile follows a natural geothermal gradient. The initial pressure profile is approximately hydrostatic, accounting for density effects due to changing temperatures and salinity, both increasing with depth. Moreover, a regional pressure gradient is applied in the saline formation below the host rock, slightly affecting the initial pressure and temperature distributions throughout the model domain. No-flow symmetry boundaries are specified in the vertical planes that go through the repository axis and parallel to it at a distance of 50 m, assuming that multiple drillholes are constructed with a separation distance of 100 m. No-flow boundaries are also specified at a sufficiently far distance to the left and right of the repository. A constant pumping rate is applied at the location of the drinking water well in the aquifer. The implementation of these initial and boundary conditions is further described in Section 4.5.4.1.

This conceptualization aims at yielding a single model with an accurate and consistent representation of key features, events, and processes, with a level of detail and sophistication that is appropriate for the limited scope and purpose of these initial generic model calculations.

4.5.3 Mesh Generation

Mesh generation is an essential step in model development, as it determines the level of geometrical details that can be represented, the accuracy with which gradients can be resolved, and computational efficiency. Specifically (as described in Section 4.5.2), the integration of the radial-axial near-field submodel (which follows the trajectory of the drillhole) into the three-dimensional Cartesian model of the geosphere yields a better reproduction of the geometry of the engineered barrier components, a more accurate resolution of radial and axial gradients, and higher computational efficiency. The steps required to develop the computational mesh are described in Appendix C.

Figure 2 shows the mesh in two-dimensional, vertical cross-sections, along with a sketch of the radial-axial model of the drillhole. Details about the near-field discretization can be found in Table 5 and Table 6 of Appendix C. The computational mesh consists of 34,424 elements and 91,765 connections between them.*

* Flow of each mass component and heat is calculated for each connection. The number of unknown variables to be solved for each element is equal to the number of mass and energy balance equations, i.e., one for water, brine, heat, and one for each of the included radionuclides. The resulting system of equations has in excess of 100,000 unknown variables. It needs to be solved many times, once for each Newton-Raphson iteration within each time step, up to a total simulation time of 10 million years. Nevertheless, these large systems can be solved efficiently enough to perform the required number of simulations, including those needed for a sampling-based probabilistic uncertainty analysis, which can be executed in parallel.

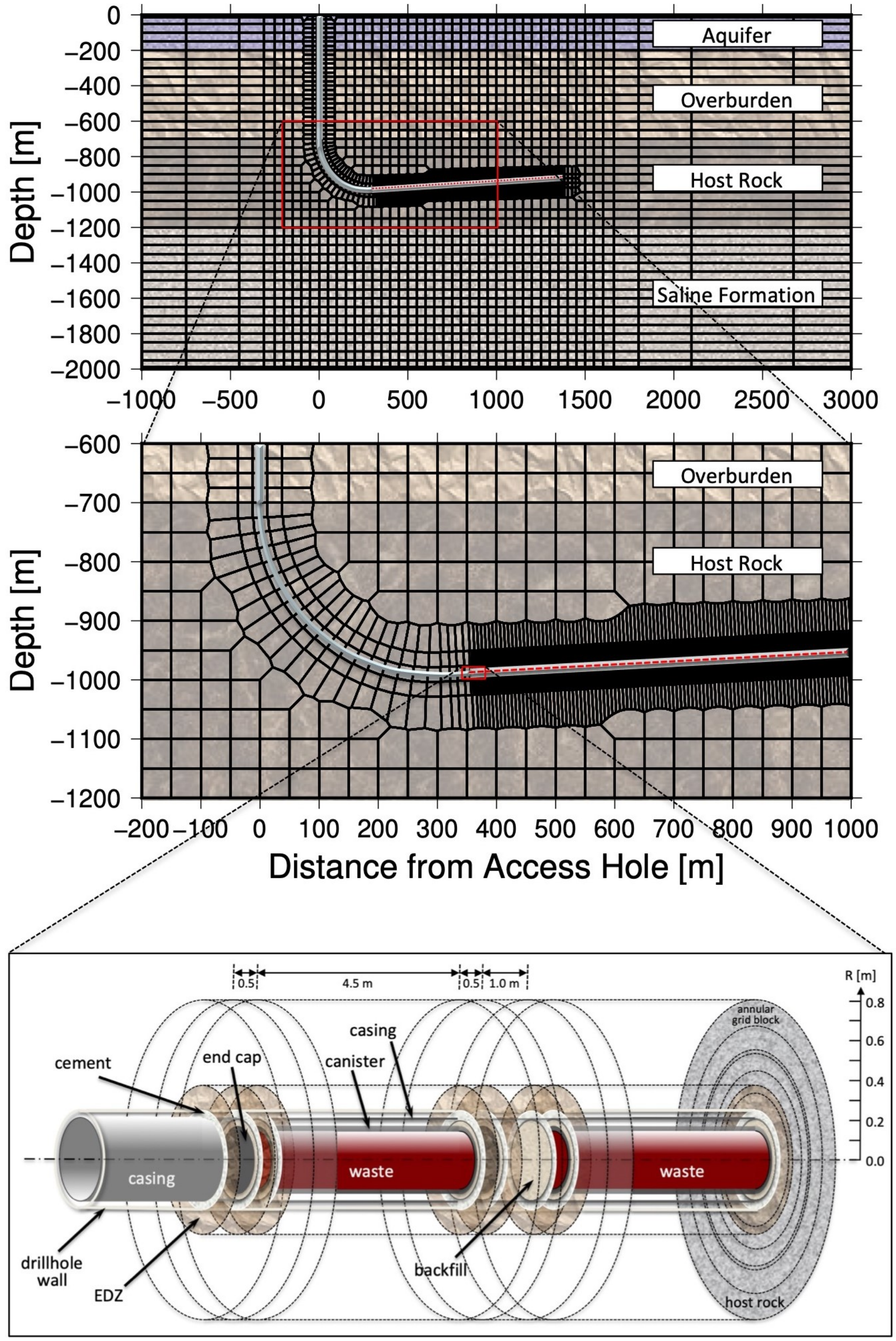

Figure 2. Computational grid: (top and middle) 2D vertical cross sections extracted from 3D Voronoi grid; (bottom) Radial-axial grid of near-field model following the trajectory of the drillhole, embedded in the Cartesian geosphere grid. All computational cells of the near-field model are ring-shaped annular grid blocks. The radial discretization is shown on the rightmost cross section; interface radii conform to material contacts. The axial discretization is indicated by the spacing of the circular cross sections. See Appendix C for details.

4.5.4 Mathematical Model

4.5.4.1 Introduction

The following subsections provide short discussions and mathematical formulations of the flow and transport processes that are considered in the model. The same mathematical equations are used throughout the model, with material-specific parameters (see Section 4.5.11) determining the behavior at any given point within the model domain. The key processes considered in this model include fluid and heat flow as well as radionuclide transport.

The TOUGH2* code (Pruess et al., 2012) used for the simulations is based on a finite volume formulation for space discretization and a first-order implicit scheme for time discretization. Time-dependent mass- and energy-balance equations are formulated for each fluid component κ (water, brine, radionuclides) or heat; they can be written in a general integral form for an arbitrary subdomain V_n delimited by the closed surface Γ_n:

$$\frac{d}{dt}\int_{V_n} M^{\kappa}\, dV_n = \int_{\Gamma_n} \mathbf{F}^{\kappa} \cdot \mathbf{n} d\Gamma_n + \int_{V_n} q^{\kappa} dV_n \tag{1}$$

The quantity M [kg m^{-3} or J m^{-3}] appearing in the accumulation term represents mass or energy per volume. $\mathbf{F}$ [kg s^{-1} m^{-2} or W m^{-2}] denotes mass or heat flux, and q [kg s^{-1} m^{-3} or W m^{-3}] indicates sinks and sources of mass or energy. The normal vector on the surface element $d\Gamma_n$, $\mathbf{n}$, points inward into dV_n. The specific accumulation and flux terms are detailed in the following subsections.

The resulting coupled nonlinear algebraic mass- and energy-balance equations (with pressure, temperature, and mass fractions of brine and radionuclides in each grid block as the unknown primary variables) are solved simultaneously using Newton–Raphson iterations. The elements of the Jacobian matrix are calculated numerically. The set of linear equations arising at each Newton-Raphson iteration are solved using an iterative sparse matrix solver. More details about the implementation of the governing equations into the numerical simulator can be found in Pruess et al. (2012).

4.5.4.2 Fluid Flow

Fluid flow through the repository system is appropriately described by the standard mass balance equations used for fluids in porous media. For assessing a deep drillhole repository, the fluid of interest is a multi-component mixture of water, brine, and radionuclides. It is assumed to be a liquid phase throughout the model domain and over the entire simulation period.

The assumption of single-phase liquid conditions throughout the repository system is considered justifiable for the following reasons. The repository is in the saturated zone. The

* TOUGH2 (Pruess et al., 2012), which is the precursor simulator integrated into the iTOUGH2 simulation-optimization framework (Finsterle et al., 2017), has been qualified for use in the Yucca Mountain Project (Wu et al., 1996).

drillhole is liquid filled, during drilling, completion, waste emplacement, and closure. Given the large depth of the disposal section and the fact that the drillhole and its immediate environment are not significantly depressurized* during construction and waste emplacement, no steam phase is expected to emerge due to evaporation or boiling, even if temperatures become significantly elevated around the heat-generating canisters. Figure 3 shows the boiling temperature as a function of pressure, which is correlated to depth assuming a hydrostatic pressure profile. For example, for a repository depth of 1 km, temperatures below 300°C will not lead to boiling.

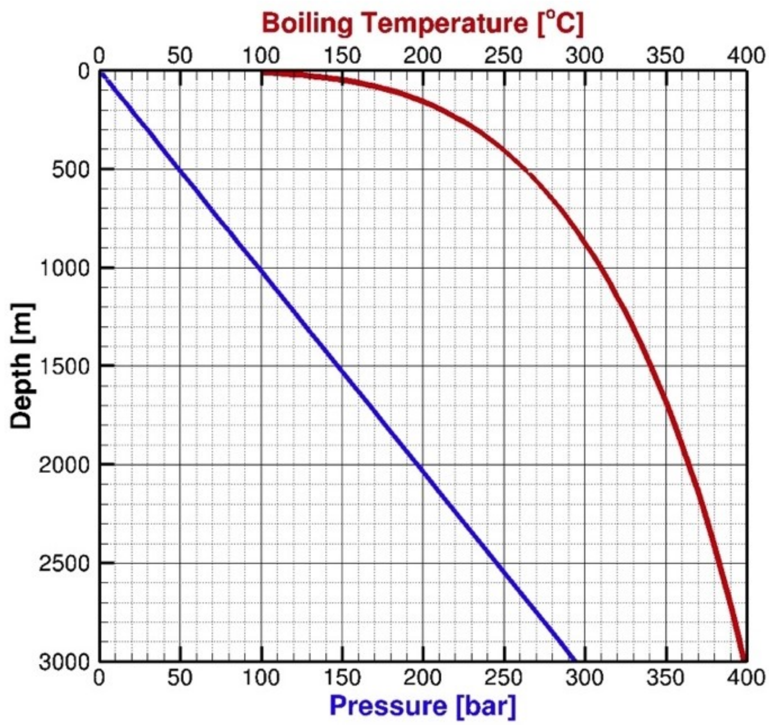

Figure 3. Boiling temperature as a function of pressure and approximate depth, assuming a hydrostatic pressure profile and fully liquid-saturated conditions in the disposal section of the horizontal drillhole.

* Small pressure perturbations may occur during over- or under-balanced drilling as well as casing installation, waste emplacement, and sealing operations. However, these perturbations are minor compared to the overall total fluid pressure at depth, and equilibrate fast compared to the period needed to reach very high temperatures. Also note that only negative pressure excursions are relevant in this context.

A free gas phase may also appear because hydrogen (and potentially other gases, such as CO_2 or CH_4)* are being generated by the degradation of the waste form† and corrosion of waste canisters and drillhole casing; microbial activity may also generate non-condensible gases. Preliminary simulations of hydrogen generation using conservative assumptions about corrosion rates (Payer et al., 2019) indicate that while most of the hydrogen is dissolved in the pore water and diffuses away from the corroding metal surfaces, a free gas phase might indeed emerge. However, because the pressure in the saturated zone at depth is very high, and gas is produced at a low rate and over an extended linear source, the volumetric gas content is very small and does not induce substantial pressure buildups and associated advective flow of potentially contaminated water. The period over which two-phase conditions might persist is very short in comparison to the performance period. Relatively shortly after its generation, the hydrogen re-dissolves into the aqueous phase, where it is diluted by radial outward diffusion, thus never exceeding the gas solubility limit. Detrimental impacts of gas generation on the engineered barrier system are unlikely, and no effects on the long-term performance of the repository are expected. The simplicity of single-phase liquid conditions throughout the near and far fields greatly simplifies the characterization and assessment of the repository system as well as the actual design of engineered barrier components.

The mass accumulation term M [kg m^{-3}] of component κ (water, brine, radionuclides) is written as:

$$M^\kappa = \phi \rho_w X_w^\kappa \tag{2}$$

where ϕ [m^3 m^{-3}] is porosity (which is a function of pore pressure and temperature), ρ_w [kg m^{-3}] is the density of liquid water (which is a function of pressure, temperature, and brine mass fraction), and X_w^κ [kg kg^{-1}] is the mass fraction of component κ in the liquid phase. Porosity ϕ changes with pore pressure according to the relation

$$\phi(P) = \phi_0 c_\phi \Delta P \tag{3}$$

where ϕ_0 [m^3 m^{-3}] is the initial porosity, and $c_\phi = (1/\phi)(\partial\phi/\partial P)|_T$ [Pa^{-1}] is the pore compressibility.‡

---

* In the unlikely event that significant amounts of CO_2 are generated, a cement grout would sequester CO_2 with production of secondary carbonates. CH_4 could be generated from the post-closure thermal pulse, especially if the host rock is a carbonaceous shale, or through hydrogen consumption by methanogenic bacteria, or through abiotic methanogenesis from H_2 at elevated temperatures.

† The formation of volatile radionuclides, however, is unlikely. ^{129}I is released to solution as iodide, a non-volatile form. $^{14}CO^2$ may form and exsolve under oxidizing conditions; it's chemical form under reducing conditions is not well known. Some of the ^3H inventory may be rapidly released from the fuel as a volatile species, a release that is insignificant because of the short half-life of tritium (12.5 years).

‡ Water compressibility is about $4{\cdot}10^{-10}$ Pa^{-1}; it is added to pore compressibility to yield the storativity term, which affects (with permeability) hydraulic diffusivity and thus pressure propagation.

The advective mass flux [kg s^{-1} m^{-2}] of component κ is given by

$$\mathbf{F}^{\kappa} = X_w^{\kappa}\mathbf{F} \tag{4}$$

where the flux of the liquid phase is described by Darcy's law (Darcy, 1856):

$$\mathbf{F} = \rho_w \mathbf{u} = -k\frac{\rho_w}{\mu_w}(\nabla P - \rho_w \mathbf{g}) \tag{5}$$

Here, $\mathbf{u}$ [m s^{-1}] is the Darcy velocity, k [m^2] is the absolute permeability, μ_w [Pa·s] is the dynamic viscosity of the liquid phase as a function of temperature and brine mass fraction, P [Pa] is fluid pressure, and $\mathbf{g}$ [m s^2] is the vector of gravitational acceleration.

All thermophysical properties of pure liquid water are a function of pressure and temperature, accurately calculated based on the IAPWS-95 formulation (Wagner and Pruß, 2002). The impact of salinity on liquid density is calculated based on the assumption that fluid volume is conserved when pure water and brine are mixed (Herbert et al., 1988). Salinity effects on liquid phase viscosity are modeled with a polynomial correction to the viscosity of pure water, following Herbert et al. (1988). A 5.06 molar NaCl solution is used as the reference brine. Dissolving radionuclides has no impact on the thermophysical properties of the aqueous phase, as they remain in trace concentrations.

4.5.4.3 Radionuclide Transport

The fate of radionuclides in the porous materials of the engineered barrier components and the geosphere are captured by mass-balance equations that are formulated for each radionuclide. The accumulation term includes the mass of radionuclide κ that is (a) dissolved in the pore fluid and (b) adsorbed on the solid grains of the porous medium:

$$M^{\kappa} = \phi\rho_w X_w^{\kappa} + (1-\phi)\rho_s\rho_w X_w^{\kappa} k_d f_R \tag{6}$$

Here, ρ_s [kg m^{-3}] is the density of the solid phase, k_d [m^3 kg^{-1}] is the aqueous phase distribution coefficient (de Marsily, 1986), and f_R is a rock-specific sorption scaling factor. Adsorption onto stationary grains reduces the mobility of the radionuclides, a beneficial effect that can be quantified by a retardation factor $R = 1 + (\rho_s k_d f_R/\phi)$ (Freeze and Cherry, 1979).*

While adsorption and desorption are complex kinetic geochemical processes, they are represented here as reversible instantaneous linear sorption. This simplified treatment—referred to as the k_d approach—is almost universally used in safety analyses for nuclear waste repositories, despite its recognized limitations (Davis and Kent, 1990; Betkhe and Brady, 2000). Detailed reactive geochemical transport models may be needed to properly capture kinetic surface complexation phenomena.

* For example, the retardation factor for a sorbing radionuclide with a k_d value of 10^{-3} m^3 kg^{-1} is about $R = 100$ for typical rock densities and porosities; such radionuclides travel with a velocity that is approximately 1% of that of a non-sorbing radionuclide.

Radionuclides may also adsorb onto colloids, which are small particles suspended in the pore fluid. The sorbed radionuclides migrate through the geosphere at the velocity of the colloids, which may be slower than the average pore water velocity due to filtration or straining effects, or higher if the colloids are negatively charged and thus preferentially travel in the central portion of large pore channels; unlike solutes, they are also likely excluded from entering small pore spaces (such the matrix in a fractured medium). Adsorption of radionuclides onto mobile colloids reduces the retardation effect; adsorption onto immobile colloids has no impact on retardation or is beneficial as the specific surface area and thus distribution coefficients are increased by the presence of colloids. Note that the stability of colloids in suspension depends on the geochemical conditions. In tight, low-porosity host rocks, filtration is very strong, essentially immobilizing radionuclide-bearing colloids. Colloid transport may occur along fast-flow pathways, such as faults, fracture zones, or gaps in the engineered barrier system. In the case of reversible radionuclide sorption on colloids and a preferred affinity of radionuclides for the accessible rock surfaces, one can neglect colloidal radionuclide transport. While potentially relevant in fractured rocks or a casing annulus, colloidal transport is not considered in the current calculations.

The flux of radionuclide κ has contributions from the advective phase flux and diffusion*:

$$\mathbf{F}^{\kappa} = X_w^{\kappa}\mathbf{F} - \phi\tau\rho_w d_w^{\kappa}\nabla X_w^{\kappa} \tag{7}$$

Here, τ [m m^{-1}] is tortuosity (which may also include a constriction factor) and d_w^{κ} [m^2 s^{-1}] is the diffusion coefficient of component κ in bulk water.† Tortuosity is assumed to be related to porosity as $\tau = \phi^{1/3}$ (Millington and Quirk, 1961). The diffusion coefficient is temperature dependent according to the Stokes-Einstein equation:

$$d_w^{\kappa}(T) = d_w^{\kappa}(T_0)\frac{T}{T_0}\cdot\frac{\mu_w(T_0)}{\mu_w(T)} \tag{8}$$

where T_0 [K] is the reference temperature (25°C). Diffusivity increases with temperature because of the higher kinetic energy of the molecules and reduced viscosity of the liquid.‡

In fractured media or media with a significant portion of the pore water being stagnant, i.e., trapped in dead-end pores, a phenomenon referred to as "matrix diffusion"§ may be

* The equations provided here do not only apply to radionuclides, but also to brine. Note that in this binary concept, diffusion of solutes is countered by an equal but opposite flux of water molecules.

† It is recognized that the Fickian diffusion model presented here is a simplified description of the processes occurring in intricate pore spaces, specifically in argillaceous rocks, where the exceedingly small pores make surface charge interactions a dominant factor. Models (typically based on electrical double-layer theory) have been developed to address this issue. Other, non-Fickian models for solute transport through disordered media have been proposed (see, for example, Berkowitz and Scher, 1995). Nevertheless, Fickian diffusion (often combined with matrix diffusion in fractured media) is almost universally used in nuclear-waste safety assessment models.

‡ For example, if the temperature increases from 40 to 80°C, diffusivity is approximately doubled.

§ The exchange of contaminants between the fractures and the matrix (or between mobile and immobile water in the pore network) occurs predominantly by diffusion. However, they may also relevant. If radionuclides enter the portion with stagnant or slow-flowing pore water, they will be retarded relative to the radionuclides that travel along the connected, higher-velocity flow paths. Retardation by matrix diffusion is an essential, beneficial process that is typically accounted for in safety analyses that involve fractured, granitic host rocks.* The shale is conceptualized as a single porous medium with an effective permeability that includes the effects of potential fractures.† Matrix diffusion is conservatively ignored in the current calculations. Moreover, the porosity accessible for ionic diffusion is assumed identical to bulk porosity.

A process referred to as hydrodynamic dispersion is not considered, because fluid flow velocities are very low‡.

4.5.4.4 Radioactive Decay

Radioactive isotopes decay with time *t* according to the equation

$$m(t) = m_0 \cdot e^{-\lambda t} \tag{9}$$

where m_0 [kg] is the initial mass, $\lambda = \ln(2)/t_{1/2}$ [s^{-1}] is the decay constant with $t_{1/2}$ [s] being the half-life. The decay equation applies to radionuclides that are encapsulated in the solid waste matrix (see Section 4.5.5.2), dissolved in the pore fluid within the canister, or migrating away from the repository through the geosphere. The calculation of activity or radionuclides reaching the biosphere is also directly related to radioactive decay (see Section 4.5.9).

While the decay of a parent radionuclide leads to a reduction in its activity with time, the activity of the daughter product (if it is also a decaying radioisotope) increases. This process applies to all daughter products in a decay chain, leading to a phenomenon referred to as ingrowth. The radioactivity of certain radionuclides and the total radioactivity at a given location may thus increase, until an equilibrium with the decay of the parent radionuclide is reached. The situation is further complicated by the fact that parent and daughter products may migrate through the geosphere at different velocities (due to different retardation behavior). The simulation of entire decay chains for proper representation of ingrowth is deferred to future safety analyses, if considered relevant.

---

be transported by advection, driven by pressure gradients or capillary suction; the term “matrix diffusion” is thus somewhat misleading.

* Matrix diffusion can be simulated on the continuum scale using double-porosity, dual-permeability, or multiple-interacting-continua (MINC) approaches, or by particle tracking and continuous-time-random-walk (CTRW) methods.

† See, for example, Bock et al. (2010). While the effective continuum approach reasonably accounts for the impact of fractures on global fluid flow, fracture-matrix interaction and associated radionuclide retardation effects are not included.

‡ Note that while dispersion may lead to earlier arrival times, it tends to reduce the peak dose, which is the relevant performance measure. Neglecting dispersion may thus be considered a conservative assumption.

4.5.4.5 Heat Flow

Heat and fluid flow are processes that affect each other and are thus fully coupled in the numerical model. Fluid properties (specifically density and viscosity) and porosity are affected by temperature, i.e., fluid and pore-volume expansions due to temperature changes lead to pressure changes, which in turn affect convective heat flow. In the near field, heat generated by the radioactive decay of the waste leads to significant, albeit temporally limited temperature changes. In the far field, the temperature profile is governed by the natural geothermal gradient, which is relatively stable unless perturbed by geothermal upflows, magmatic intrusions, or volcanic activity.

The heat accumulation term in the balance equation ($\kappa = h$ in Eq. (1)) is written as:

$$M^h = (1-\phi)\rho_s c_s T + \phi \rho_w u_w \tag{10}$$

where, ρ_s [kg m^{-3}] and c_s [J kg^{-1} °C^{-1}] are, respectively, the density and specific heat of the solid phase, T [°C] is temperature, and u_w [J kg^{-1}] is the specific internal energy in the liquid phase. Porosity ϕ changes with temperature according to the relation

$$\phi(T) = \phi_0 \varepsilon_\phi \Delta T \tag{11}$$

where ϕ_0 [m^3 m^{-3}] is the initial porosity, and $\varepsilon_\phi = (1/\phi)(\partial\phi/\partial T)|_P$ [°C^{-1}] is the thermal pore expansivity.

Heat flux [W m^{-2}] includes conductive and convective components:

$$\mathbf{F}^h = -K\nabla T + h\mathbf{F} \tag{12}$$

Here, K [W m^{-1} °C^{-1}] is the effective thermal conductivity, h [J kg^{-1}] is the specific enthalpy of the liquid phase, and **F** [kg s^{-1}] is the fluid flow rate as given by Eq. (4).

All thermal properties are material-dependent, but assumed to remain constant with time. In the nominal scenario, the near-field heat flows are conduction-dominated due to the small fluid flow rate.

4.5.5 Source-Term Model

4.5.5.1 Introduction

The source-term model describes the rate with which relevant radionuclides are released from the solid waste form into the pore fluids within the canister, from where they may be transported to the near field by diffusion and potentially advection.*

The relative simplicity of the disposal concept and the detailed representation of the engineered barrier system in the safety analysis model allow for the development of a relatively simple and well-defined source-term model, which consists of the following elements:

- Initial isotope inventory
- Radioactive decay within the waste form
- Waste form degradation
- Dissolution in pore fluid

Each of these elements of the source-term model is discussed in the subsequent subsections. The source-term model results in a time-dependent generation rate† of radionuclides that instantaneously dissolve in the aqueous phase present within the waste container. The migration of the radionuclides away from the waste form is not part of the source-term model, but is simulated explicitly based on the conditions in the near field. No credit is taken for the cladding or adsorption of radionuclides within the canister or its corrosion products.

4.5.5.2 Inventory

The isotopic composition (and thermal output) of spent uranium oxide fuel from commercial pressurized water reactors (PWRs) is determined by (1) the initial enrichment, (2) the fuel's fission energy yield (also referred to as "burn-up", measured in gigawatt days per metric ton of initial heavy metals, GWd/MTIHM), and (3) the age of the spent fuel after discharge from the reactor.‡

---

* The process described here (i.e., radionuclides that are initially encapsulated in the solid waste matrix are released due to waste degradation and become available for dissolution in potentially mobile liquids or gases) is sometimes also referred to as "waste mobilization". The terms "release" and "mobilization" may both be ambiguous, as "release" is also used to describe the escape of radionuclides from the canister or their migration from the engineered barrier system to the geosphere, and "mobilization" does not necessarily imply that the radionuclides start migrating immediately after they have been dissolved in fluids, specifically if the canisters are still intact, or if the released radionuclides exceed the solubility limit in the aqueous phase (see Section 4.5.5.4).

† This generation rate does not represent the rate with which radionuclides are created in the waste form, but the rate at which they are released from the solid waste matrix and become available for dissolution in the aqueous phase.

‡ Changes in reactor design and reactor operation as well as potential modifications of the nuclear

Carter et al. (2012) provide an estimate of potential waste inventory and waste form characteristics for spent nuclear fuel and for a variety of commercial once-through fuel cycle alternatives. For the current analysis, we select characteristics of commercial used fuel with an initial enrichment of 4.73%, a burn-up of 60 GWd/MTIHM, and a cooling time of 30 years, as presented in Table C-1 of Carter et al. (2012).

The list of radionuclides present in spent nuclear fuel assemblies is screened to select radionuclides that are potentially relevant for the long-term safety of a drillhole repository. This initial screening is based on the following four criteria:

(1) *Initial inventory*: Only radionuclides of relatively high abundance in the waste form (see Carter et al., 2012; Table C-1) are selected. A cut-off value 0.1 grams per assembly was selected for this generic analysis.

(2) *Half-life*: Relatively short-lived radionuclides are likely to decay before they reach the accessible environment and thus do not significantly contribute to dose. Migration times of radionuclides to the biosphere are expected to be long, on the order of a few hundred thousand years (this assumption is readily tested by the calculated migration times of a conservative tracer or long-lived radionuclide). Only radionuclides with a half-life longer than 25,000 years are considered for this generic analysis.

(3) *Adsorption coefficient and solubility limit*: Radionuclides that do not readily dissolve in pore water or that adsorb to the grains of the geologic formation are significantly retarded, leading to prolonged migration times. Only non- or weakly sorbing radionuclides with a high solubility limit need to be considered. For this screening, retardation is measured by the distribution coefficient (k_d value); only radionuclides with a minimum k_d value of less than 1 $m^3\ kg^{-1}$ are considered.

(4) *Toxicity*: For this screening, the toxicity of a radionuclide is reflected by the dose coefficient, *dcf* (see IAEA, 2003; Table C5). Only radionuclides with a *dcf* value greater than 10^{-10} Sv Bq^{-1} are included in this generic analysis. For more details about the dose calculation, see Section 4.5.9.

All criteria must be met for a radionuclide to be included in the model. For these generic calculations, ^{129}I, ^{36}Cl, ^{79}Se, and ^{99}Tc are initially selected for numerical evaluation.* While the amount and properties of the radionuclides in the repository are key measures, the initial inventory is not the sole or most important criterion used to make a selection of the most safety-relevant radionuclides. The main purpose of geological disposal of nuclear waste is to isolate the radionuclides from the accessible environment. This isolation has both a spatial and temporal component. The spatial separation protects the repository from external impacts, promotes dispersion of contaminants, and determines the length of the transport pathways. It also makes the natural barriers effective. The temporal component is

---

fuel cycle need to be accounted for when projecting the inventory of future waste forms.

* None of these radionuclides produce short-lived daughters that would need to be tracked (along with their progenies) for inclusion in the dose calculation.

controlled by the spatial component (specifically depth), the effectiveness of the engineered and natural barrier systems, and the properties of the radionuclides themselves (e.g., diffusion and sorption coefficients, decay mode and daughter products). The fact that considerable time elapses between disposal and the potential release of radionuclides to the biosphere is a dominant factor affecting the exposure dose. Consequently, the key factors to be used to rank the safety-relevance of radionuclides are mobility along the transport pathway and toxicity at the land surface, rather than initial activity in the canister.

Table 2 summarizes the initial inventory of radionuclides that are potentially relevant for the long-term safety of the drillhole repository system. This list of safety-relevant radionuclides is consistent with the radionuclides emerging in other, comprehensive safety analyses (DOE, 2008; Nagra, 2012b) as the main contributors to the annual individual effective dose.

Table 2: Initial inventory of select* radionuclides

Isotope	Half-life [a] [years]	Inventory [b] [g/MTIHM]	Inventory [c] [g/canister]	Activity [d] [Bq/canister]
^{129}I	1.57×10^{7}	313.	136.	8.88×10^{8}
^{36}Cl	3.01×10^{5}	0.501	0.218	2.66×10^{8}
^{79}Se	2.95×10^{5}	10.5	4.57	2.59×10^{9}
^{99}Tc	2.11×10^{5}	1280.	556.	3.52×10^{11}

a) Source: https://periodictable.com (accessed September 26, 2019)

b) Source: Carter et al. (2012; Table C-1)

c) For 0.435 MTU per PWR assembly (SNL, 2013, Appendix E-1). There is one PWR assembly per canister, and a total of 153 canisters in the 1 km long disposal section.

d) Activity A [Bq] is calculated as: $A = \lambda N = \frac{m}{MW} \cdot \frac{\ln(2)}{t_{1/2}} \cdot N_A$
where $\lambda = \ln(2)\,/t_{1/2}$ [s^{-1}] is the decay constant, N is the number of decaying particles, m [g] is inventory mass, MW [g mol^{-1}] is the molecular weight, $t_{1/2}$ [s] is the half-life, and $N_A = 6.022\times10^{23}$ [mol^{-1}] is the Avogadro number;

* The initial safety analysis only includes ^{129}I, ^{36}Cl, ^{79}Se, and ^{99}Tc. In a site-specific analysis, Deep Isolation will account for additional safety-relevant radionuclides and their daughter products, specifically those from the actinium and uranium series, but also others. Comprehensive safety assessments for repositories in argillaceous formations under reducing conditions done by other nuclear waste disposal organizations—(e.g., Nagra (2002a), Andra (2005), NWMO (2013)—confirm that the list of Table 2 is consistent with the radionuclides contributing most to peak dose and these assessments. As the chemical conditions in the host rock control the chemical form of the radionuclides and thus their sorption and retardation behavior, a careful characterization of site-specific hydrogeochemical conditions is needed, and a broad spectrum of radionuclides will be analyzed for their potential safety-relevance.

1 Ci = 3.7×10^{10} Bq.

4.5.5.3 Waste Form Degradation

The degradation of the waste form, which for commercial spent nuclear fuel predominantly consists of UO_2, determines the release and thus potential mobilization of radioisotopes. Waste form degradation is described by an annual fractional degradation rate, ω [yr^{-1}], which is the rate with which the remaining waste mass degrades per year.*

The rate with which the mass of radionuclides in the waste form is reduced due to decay and release is given by:

$$\frac{dm}{dt} = m(t) \cdot (\omega + \lambda) \tag{13}$$

The radionuclide mass present in the degrading waste matrix at time t is thus

$$m(t) = m_0 \cdot e^{-(\omega+\lambda)t} \tag{14}$$

where m_0 [kg] is the initial inventory at the time of repository closure. The time-dependent rate q_{RN} [kg yr^{-1}], with which some of the radionuclide mass remaining in the solid waste matrix is released to the pore fluid, is given by†

$$q_{RN}(\mathrm{t}) = m(t) \cdot \omega \tag{15}$$

For the nominal scenario, a fractional waste form degradation rate of 10^{-5} yr^{-1} is assumed based on SNL (2013, Section 4.3.2).‡

Figure 4 shows the source terms (i.e., the declining mass of radionuclides encapsulated in the solid waste matrix) for each for the four considered radionuclides.§ (To highlight the inventory and release curves at early times after repository closure, the source term is also

---

* A fraction of the inventory may be released instantaneously. The instant release fraction (IRF) depends on the assumed structure of the waste form, specifically the presence of gaps and fractures, which in turn is affected by the linear power rating of the fuel (Johnson and Tait, 1997; Nagra, 2002a; Lemmens et al., 2017). The IRF tends to be relatively high for high-burnup UO_2 fuel. A waste degradation model accounting for an instant release fraction is considered in the sensitivity analysis of Section 4.7.3.1.

† Note that the contribution of radioactive decay to the reduction in activity within the waste matrix is not added to the release rate.

‡ While this reference value for the fractional waste degradation rate is lower (by a factor of 2) than the value used by SNL (2013), it is consistent with the value reported by Clayton et al. (2011, Section 3.3.3.3.2.2). Considerably lower values have been reported by, for example, Nagra (2002a,b), Ollila (2011), and Lemmens et al. (2017). The sensitivity of peak dose to the fractional waste degradation form is analyzed in Section 4.7.3.1.

§ For ^{99}Tc, the release rate is not directly used in the model, because the amount of Tc released from the solid waste matrix leads to a radionuclide mass per liter in the aqueous phase that exceeds the solubility limit; see Section 4.5.5.4.

shown in a log-log plot.) The normalized degradation of the waste form is depicted as a black solid line. For a fractional degradation rate of 10^{-5} yr^{-1}, it takes approximately 300,000 years to degrade 95% of the waste. The exponential degradation leads to a straight line on a logarithmic plot. For a radionuclide with a very long half-life (such as ^{129}I), the mass present in the waste matrix and the release rates are nearly parallel to the waste degradation line. The decay of shorter-lived radionuclides leads to a faster reduction of the mass being present in the waste form, and a correspondingly smaller release rate; the lines are steeper than the line showing waste degradation.

The source-term model described here is parameterized and implemented into the simulator. This parameterization enables probabilistic analyses with varying fractional waste-form degradation rates and initial inventories.

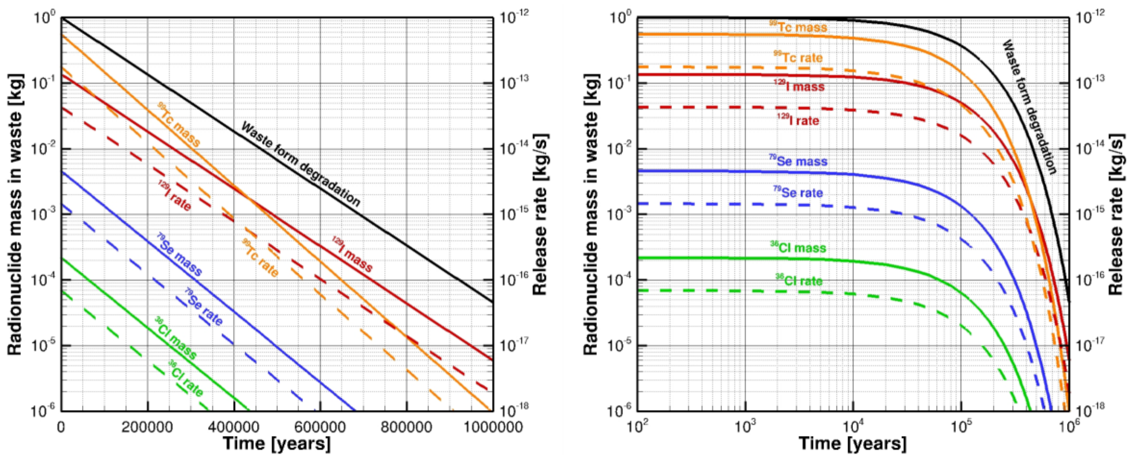

(a) (b)

Figure 4. Normalized waste-from degradation for a fractional waste degradation rate of 10^{-5} yr^{-1} (black line), radionuclide inventory in waste form (solid lines), and radionuclide release rates (dashed lines) as a function of (a) time, and (b) logarithmic time.

4.5.5.4 Radionuclide Dissolution in Pore Water

Radionuclides released from the degrading solid waste matrix dissolve in the aqueous fluid that is in contact with the assemblies. This assumes that water enters the canister at or shortly after the time of its failure. The large temporal scale combined with the small spatial scale justifies the assumption that equilibrium with the fluid is reached instantaneously.* The concentrations of ^{129}I, ^{36}Cl, and ^{79}Se released from the waste matrix for the given waste degradation rates are close to or below the solubility limit of these species in the aqueous phase under the prevailing hydro-geochemical conditions. The mobilization and subsequent release of these radionuclides to the near field is only limited by the efficiency with which

* Instantaneous dissolution is accounted for in the model by the local thermodynamic equilibrium assumption embedded in the TOUGH2 simulator.

they are transported away from the canister. As the main transport process is molecular diffusion, this radionuclide source is referred to as a diffusion-limited source-term model.

However, ^{99}Tc does not readily dissolve in water under reducing conditions.* ^{99}Tc released from the solid waste matrix reaches the solubility limit shortly after waste degradation begins.† The amount of dissolved ^{99}Tc that migrates away from the waste is immediately replaced by further dissolution of precipitate; as a result, the ^{99}Tc concentration within the canister remains constant at the solubility limit.

This conceptualization is referred to as a solubility-limited source-term model, which constrains radionuclide concentrations in the aqueous phase at the source and throughout the repository system. Rather than specifying a time-dependent waste dissolution rate combined by a local equilibrium assumption, the source term for ^{99}Tc is represented by a constant concentration boundary condition applied at each of the modeled canisters. At later times, the migration of the poorly soluble radionuclide away from the canister will exceed the release from the waste form, leading to a net reduction of precipitated mass within the canister. Eventually, the concentration drops below the solubility limit. At this point in time,‡ the constant concentration boundary condition is replaced by a time-dependent mobilization rate, i.e., the solubility-limited source-term model is substituted with a diffusion-limited source-term model, identical to that used for more soluble radionuclides.

Once dissolved in the aqueous phase, radionuclides become mobile and can be transported by diffusion or advection,§ processes that are explicitly implemented in the numerical model (see Section 4.5.4.3).

4.5.6 Heat Generation

The decay of radionuclides in the waste form generates heat as the emitted radiation is absorbed by the waste form and nearby materials. Radionuclides with very short half-lives decay quickly, mostly while the assemblies are still in cooling pools or dry casks at the surface. In contrast, radionuclides with very long half-lives (such as ^{129}I, ^{238}U and ^{235}U) decay so slowly that they have low radioactivity and low heat emission rates. However, radionuclides with intermediate half-lives (such as ^{137}Cs and ^{90}Sr) are the ones that contribute most to the heat generated in a repository. These fission fragments cause the high inten-

* Technetium oxide dissolves readily under oxidizing conditions, but has a low solubility limit under the reducing conditions prevailing in a deep horizontal drillhole repository. One of the dominant aqueous complexes of Tc is $TcO(OH)_2(aq)$, or $TcO_2 \cdot H_2O$ (e.g., Yalçıntaş et al., 2016).

† For the reference fractional waste degradation rate of 10^{-5} yr^{-1}, the Tc solubility limit of 10^{-8} mol L^{-1} is reached approximately two years after repository closure.

‡ For the reference parameter set, the ^{99}Tc concentration in the canister pore water drops below the solubility limit of 10^{-8} mol L^{-1} after approximately 800,000 years, at which point a diffusion-limited source-term model is engaged. This time is determined based on the initial inventory and accounting for radioactive decay, waste dissolution, and the cumulative amount of ^{99}Tc released from the canister.

§ Sorption of radionuclides on waste-form surfaces or canister corrosion products is neglected.

sity of the SNF's initial radioactivity; later, after the first few centuries, the transuranics contribute most to the long-lived radioactivity.

The decay heat generated by the radionuclides in a PWR spent nuclear fuel assembly is shown in Figure 5, reproduced from Ansolabehere et al. (2003). The curve is based on an initial enrichment of 4.5% and a burn-up of 50 GWd/MTIHM, i.e., conditions sufficiently close to those assumed for the radionuclide inventory described in Section 4.5.5.2. The total power output shown in Figure 5 is multiplied by 0.435, which is the average mass [10^3 kg] of heavy metals in a PWR assembly (SNL, 2013). The resulting power, which includes the decay heat from all is then supplied as a time-dependent heat source in to each of the 153 canisters represented in the near-field model, starting at 30 years, which is the assumed cooling time the fuel spends in surface facilities prior to disposal.

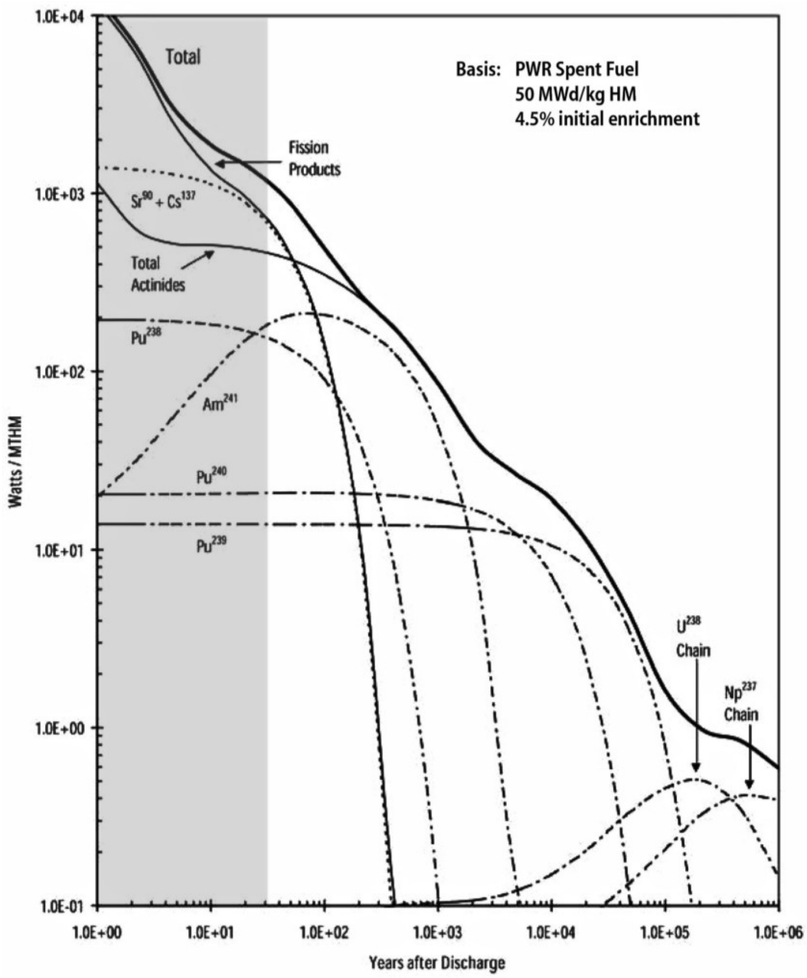

Figure 5. Decay heat profile of spent nuclear fuel (Ansolabehere et al., 2003; Figure 7-2). The shaded area indicates the assumed cooling time of 30 years.

4.5.7 Near-Field Model

The radionuclide-release rate (see Figure 4 and related discussion in Section 4.5.5) is specified as a time-dependent mass source term in the near-field model, applied to all volume elements that represent the waste form (see Table 5). In addition, heat is generated during the initial stage, referred to as the thermal period (see Section 4.5.6). The migration of radionuclides and dissipation of heat away from the waste depends on the properties of and processes in the engineered barrier system as represented in the near-field model.

The first barrier encountered by radionuclides leached from the waste form is the canister, which is initially intact but is eventually perforated due to corrosion. The conservative assumption is made that water is present in the interior of the canister immediately after waste emplacement. The overall permeability of the canister is very low. Approaching the time when corrosion starts perforating the canister, permeability increases from its low initial value to that of the backfill material. The canisters are assumed to have essentially lost their barrier function after 10,000 years, which is considerably shorter than the time frame calculated by Payer et al. (2019) for general corrosion of Ni-Cr-Mo alloys under comparable repository conditions of high temperature and high salinity. (An early canister failure scenario is also examined; see Section 4.3.3.3.) The corrosion of the steel casing is treated in a similar manner, but is assumed to pose no flow resistance after 100 years. The hydrological, mechanical, or geochemical effects of the corrosion (mainly the generation of hydrogen gas and the products of the corrosion of the canisters and casing) are not considered in this analysis. Accounting for such processes requires detailed, site- and design-specific knowledge about the geochemical environment and stress conditions, information that is not available at the current stage of repository development*.

The flow and transport processes in the immediate vicinity of the waste are initially affected by the temperature increase due to the decay heat. Radionuclides migrate into and through the buffer material mainly by diffusion, which is increased due to the temperature dependence of the diffusion coefficient (see Eq. 8). Sorbing radionuclides are retarded (see Eq. 6), specifically in clay-containing buffer materials.

Thermal expansion and contraction of the pore fluid (partly modulated by the expansion and contraction of the pore space; see Eqs. 3 and 11) affect the local pressure distribution. Other processes perturbing the local pressure field may also occur, either driven by local or regional changes in hydrological and mechanical stress conditions, or triggered by disruptive events. If sufficiently strong, these pressure gradients induce fluid flow and associated advective radionuclide transport, preferentially in axial direction along annuli that may exist or develop between interfaces,† within the buffer and other backfill materials, and potentially along the excavation disturbed zone.

---

* In addition, the coupled simulation of thermal-hydrological-geochemical-mechanical processes is complex and computationally very expensive. Such specialized simulations are feasible only for select submodels of the system, with its results justifying the conceptualization of a total system performance assessment model.

† Such gaps may preferentially develop between the canister (or its corrosion products) and the

While radionuclide transport in the engineered barrier system is expected to be diffusion-dominated, the near-field model properly accounts for fluid flow and advective transport should they be favored by local conditions. Similarly, heat dissipation is most likely dominated by conduction, but convective heat transfer is inherently accounted for should it occur. Heat and fluid flow are fully coupled.

As discussed in Section 4.5.3, the near-field model extends axially from the disposal section of the drillhole repository along the curved and vertical segments of the access hole to the land surface. Moreover, it is fully integrated in the far-field model. This means that no submodel abstractions or other simplifying assumptions about process couplings and feedback mechanisms across the interface between these two subsystems need to be made.

4.5.8 Far-Field Model

The seamless transition between the near field and far field in reality is well represented in the integrated model, both conceptually and numerically (see Sections 4.5.1 and 4.5.3). The assumed layering of the geosphere is described in Section 4.5.2. A spatially correlated field of porosity modifiers is generated using geostatistical methods and superimposed on the reference porosities of each hydrostratigraphic unit. Porosity is chosen as the heterogeneous parameter as it impacts diffusion, which is considered the main radionuclide transport mechanism; porosity also affects advective transport velocities. By changing the seed of the random-number generator for each realization during the probabilistic analysis (see Section 4.7.4), the impact of irreducible variability in geosphere properties on dose can be examined. Discrete structures, such as an exploration hole (or other openings related to inadvertent human intrusion activities), or an existing or activated fault or fracture zone that intersects the repository and provides a potential fast-flow pathway to the aquifer, can also be included in the model to examine consequences of disruptive events.

The far-field model accounts for all the flow and transport processes described in Section 4.5.4, including fluid flow driven by viscous and gravitational forces, conductive and convective heat transfer, as well as advective and diffusive radionuclide transport with retardation of sorbing isotopes.

The far-field model is linked to the biosphere model in that it simulates the production of groundwater from the drinking water well, which is potentially contaminated by radionuclides entering the aquifer through the geological formations or directly through the access hole.

4.5.9 Biosphere Model

One of the key metrics used to evaluate repository performance is the radiation exposure—expressed as an annual individual effective dose. The dose is calculated by the biosphere

buffer, the buffer and the casing (or its corrosion products), the casing and the concrete, or the concrete and the drillhole wall. If no buffer is installed, the open space within the drillhole could act as a fast-flow pathway for fluid flow and radionuclide transport, provided that horizontal gradients in axial direction exist.

model, which includes processes of different exposure pathways as well as the toxicity of the radionuclides. For this generic analysis, we adopt IAEA's Example Reference Biosphere 1A dose model, referred to as ERB1A (IAEA, 2003; Section C2). ERB1A is a simple dose model; it considers a limited set of processes and exposure pathways,* and makes the following assumptions:

- The repository is sited in an inland area with temperate climate and an aquifer at accessible depth.
- The individual consumes contaminated groundwater taken from a near-surface well penetrating an aquifer above the disposal section of the repository.
- The geosphere-biosphere interface is the water produced from a shallow well, which draws water for domestic use; drinking water is not monitored or treated.
- The exposure group consists of individuals who obtain all their drinking water from the well; no age group for the exposed individual is specified.
- The annual individual water consumption rate is 1.2 m^3 yr^{-1}.
- The radionuclide concentrations at the well are provided by the far-field model, i.e., no additional assumptions about processes occurring within the aquifer are made.
- No biosphere dynamics are considered, i.e., the total concentration of radionuclides does not change as it passes through the water supply system.
- The biosphere does not evolve over time; present-day conditions prevail over the entire performance period.

Each radionuclide is associated with distinct radiological hazards per unit activity. Because of the simplicity of the ERB1A biosphere model, the mathematical model produces simple conversion factors between the radionuclide concentration in water delivered at the well head and the annual individual effective dose (IAEA, 2003; Section C2.5.3):

$$H_{E,i} = C_{w,i} \cdot I \cdot dcf_i \tag{16}$$

Here, $H_{E,i}$ [Sv yr^{-1} or mrem yr^{-1}] is the annual individual dose from radionuclide i, $C_{w,i}$ [Bq m^{-3}] is the activity concentration of radionuclide i in water at the well head, I [m^3 yr^{-1}] is the consumption rate, and dcf_i [Sv Bq^{-1}] is the ingestion dose coefficient, which is a measure of the radiological impact associated with the ingestion of radionuclide i. Values

* In a comprehensive, site-specific safety analysis, all relevant exposure pathways will be considered when calculating the radiological dose. The relevance of many of these pathways depends on the local geographical, topological, climatological conditions and other factors. A detailed inclusion of all exposure pathways is thus not warranted in a generic analysis that is not based on site-specific characterization data. IAEA's simple ERB1A model, which accounts for one of the main exposure pathways directly linked to groundwater contamination by radionuclides, is considered appropriate for the objectives of a generic safety calculation.

for ERB1A are provided in IAEA (2003; Table C5) and are reproduced in Table 3 for the radionuclides considered in this analysis.

The far-field model calculates the mass fraction $c_{w,i}$ [kg kg^{-1}] of a radionuclide in the liquid phase at the well, which is converted to the activity concentration $C_{w,i}$ [Bq m^{-3}] by

$$C_{w,i} = c_{w,i} \cdot a_i \cdot \rho_w \tag{17}$$

where a_i [Bq kg^{-1}] is the specific activity of radionuclide i (see Table 3), and ρ_w [kg m^{-3}] is the density of liquid water.

It is important to realize that the mass fraction in the well is affected by the pumping rate, which controls (a) the size of the capture zone of the well, (b) the advective transport of radionuclides in the overburden and aquifer, and (c) dilution of the contaminated deep groundwater by clean surface water. Effects (a) and (b), which tend to increase the radionuclide mass fraction, are countered by effect (c), which decreases the mass fraction. This trade-off needs to be examined in detail for site-specific conditions in a refined biosphere model.

Table 3: Specific activity and ingestion dose coefficient of select radionuclides

Isotope	**Half-life** [a] **[years]**	**Specific activity** [b] **[Bq kg^{-1}]**	**Dose coefficient** [c] **[Sv Bq^{-1}]**	**Dose coefficient** [d] **[mrem Bq^{-1}]**
^{129}I	1.57×10^{7}	6.53×10^{9}	1.10×10^{-7}	1.10×10^{-2}
^{36}Cl	3.01×10^{5}	1.22×10^{12}	9.30×10^{-10}	9.30×10^{-5}
^{79}Se	2.95×10^{5}	5.68×10^{11}	2.90×10^{-9}	2.90×10^{-4}
^{99}Tc	2.11×10^{5}	6.33×10^{11}	6.40×10^{-10}	6.40×10^{-5}

a) Source: https://periodictable.com (accessed September 26, 2019)

b) Specific activity a [Bq kg^{-1}] is calculated as: $a = \frac{\lambda N}{m} = \frac{1}{MW} \cdot \frac{\ln(2)}{t_{1/2}} \cdot N_A$

where $\lambda = \ln(2)/t_{1/2}$ [1/s] is the decay constant, N is the number of decaying particles, m [g] is mass, MW [g/mol] is the molecular weight, $t_{1/2}$ [s] is the half-life, and $N_A = 6.022\times10^{23}$ [1/mol] is the Avogadro number; 1 Ci = 3.7×10^{10} Bq.

c) Source: IAEA (2003; Table C5; Example Reference Biosphere 1A (ERB1A))

d) Unit conversion factor: 1 mrem = 10^{-5} Sv

4.5.10 Model Initialization and Boundary Conditions

The simulated post-closure system behavior depends on the imposed boundary conditions, sink and source terms, and the initial conditions within the model domain. The initial state of the post-closure simulation model is itself the result of a simulation. The purpose of the initialization run is to calculate the flow field that is in equilibrium with the regional hydrological and geothermal boundary conditions (but without heat and radionuclide releases from the repository).

The initial temperature distribution (Figure 6a) is calculated by assuming an average surface temperature of 13°C and a geothermal gradient of 30°C km^{-1}, which yields a temperature of 73°C at the bottom of the model domain. This boundary temperature at a depth of -2 km is kept constant throughout the simulation period. Note that the temperature profile is affected by the thermal properties of the various geologic units; moreover, it affects fluid densities and thus the pressure profile.

The initial pressure distribution (Figure 6b) is calculated by running a model to steady state with atmospheric pressures at the land surface and no-flow boundary conditions on all other faces of the model, with the exception of a segment over the lower right quarter of the model boundary, where slight overpressures (with respect to the assumed hydrostatic pressure) are specified. This overpressure (of approximately 2 bars) is introduced to represent a regional pressure gradient in the underlying saline formation; it also induces a slight upward flow through the geosphere.* In summary, the pressure distribution used as initial conditions for the subsequent simulation of repository evolution is nearly static, but supports a small, steady-state flow through the geosphere. It accounts for the combined density effects from the imposed geothermal gradient and salinity (Figure 6c), which is introduced by specifying an average brine mass fraction of 0.2 in the saline formation (corresponding to a salinity of 50,000 ppm or a NaCl concentration of 0.86 mol L^{-1}, classifying the deep groundwater as a brine), and an initial mass fraction of 0.05 in the shale. In approaching the steady-state solution, thermal expansion of the brine reduces density with depth; however, this general trend is countered by salinity effects, which dominate and lead to an increase in the density gradient up to a depth of approximately -1,300 m. Fluid with constant salinity is supplied from the right-hand side of the model, reversing the density gradient in the lower part of the domain, where the temperature is kept high across the bottom (Figure 6d). At steady state, sufficient high-density brine is supplied from the bottom to equilibrate the pressure profile.

Construction and operation of the repository are activities that are assumed not to significantly affect the pressure and temperature distributions in the near field. This assumption is justified by the fact that slightly over- or underbalanced drilling, waste emplacement, and sealing of the repository lead to only small perturbations in pressure and temperature, which are equilibrated within a time frame that is very short compared to the thermal-pulse and repository performance periods.†

---

* See Section 4.7.3.3 for a sensitivity analysis of this assumption.

† It is acknowledged that repository construction will perturb the near field. However, they are expected to be much less pronounced and of shorter duration than the corresponding effects of a mined repository. The openings of a mined repositories are considerably larger (leading to larger stress changes and related excavation damage), and are drilled and operated under atmospheric conditions, inducing a strong pressure drawdown, drying out of the near field, and introducing oxygen. These conditions prevail for a longer period compared to that of a drillhole repository, which remains fully saturated under near-static pressure conditions throughout the (shorter)

Starting after repository closure, groundwater is continuously pumped at a constant rate of 2.0 kg s^{-1} from a well that is centered above the disposal section of the repository and perforated immediately above the interface between the overburden and the aquifer. The rate is consistent with pumping rates of a well used to supply residential drinking water; it is large enough to ensure that the well collects all the contamination stemming from the nuclear waste repository.

These initial and boundary conditions are chosen to generate a configuration that is not unduly optimistic regarding the potential for upward flow and related upward transport of radionuclides. While continuous pumping leads to a sustained increase of the gradient from the repository towards the well, intermittent pumping may lead to temporally higher concentrations immediately after restarting of the pump. Such scenarios may be evaluated as the biosphere model is refined in a site-specific safety analysis. A sensitivity analysis on the impact of the large-scale head gradient can be found in Section 4.7.3.3.

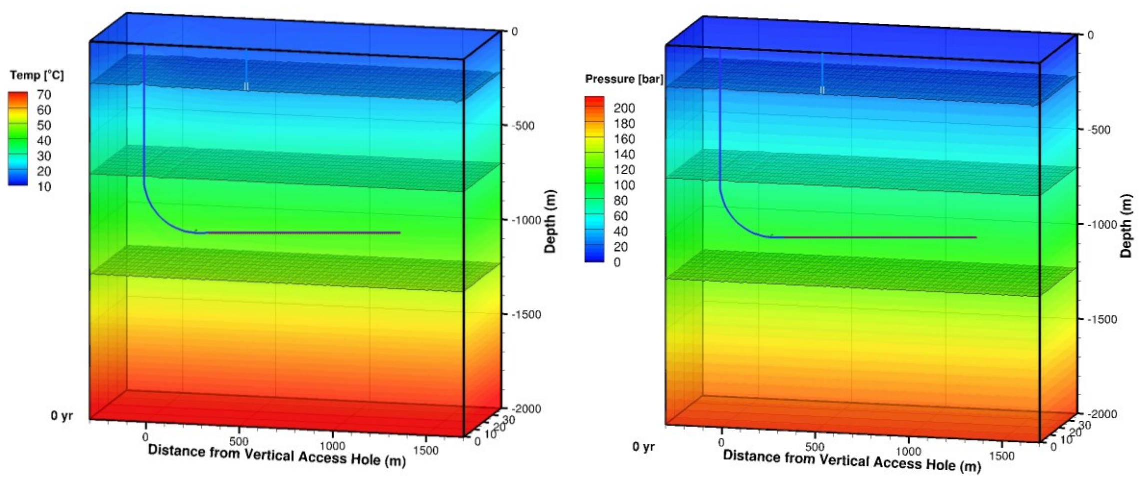

(a) (b)

---

construction and operation phases. The perturbations from drilling and waste emplacement operations are expected to be minor and to re-equilibrate quickly after repository closure; the details of these effects will be examined for site-specific conditions.

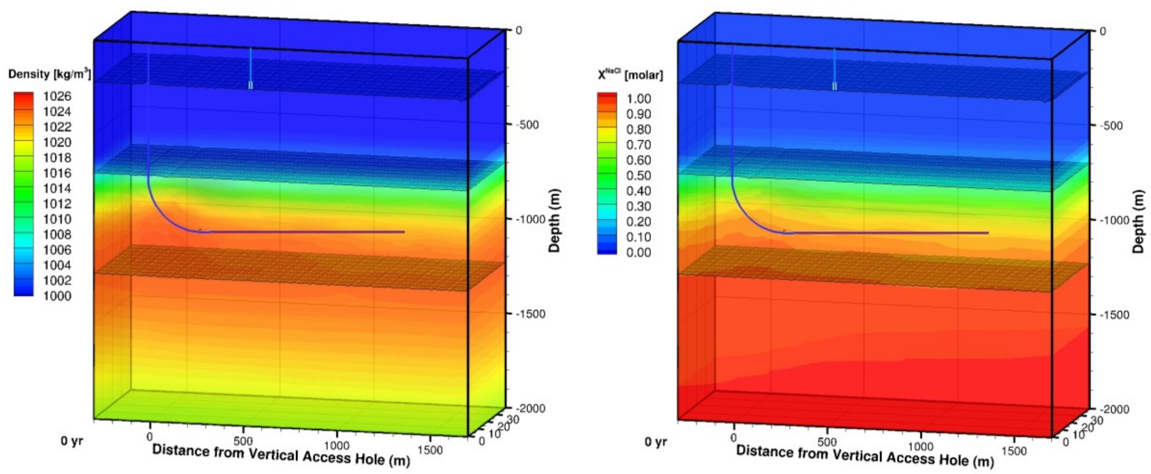

(c) (d)

Figure 6. Initial conditions: (a) temperature, (b) pressure (c), aqueous phase density, and (d) NaCl concentration.

4.5.11 Model Input Parameters

The general mathematical model described in Section 4.5.4 includes parameters that need to be specified to arrive at a physically meaningful, realistic and eventually site-specific model of the disposal system (see discussion in Section 2.2). Appendix B contains a complete set of hydrological, thermal, and transport properties specified for each of the natural or man-made materials included in the numerical model. Furthermore, other aspects of the repository system may be parameterized, including the initial inventory, waste degradation rates, fault geometry, and regional pressure gradient, among many other parameters that enter the numerical simulation.

A single value for each of these model input parameters is specified to define the nominal scenario (see Section 4.3.2). The selected parameter values are considered cautious, i.e., they do not overestimate repository performance but are not overly conservative so as to be unreasonable. In some instances, conservative assumptions are made because they simplify the model without having a large impact on simulation results.

Some of the parameters are poorly known or uncertain (especially prior to site-specific characterization), while others can be specified with confidence. In numerical modeling, a parameter's value can be fixed if (a) it is well known, i.e., it has a small range or small uncertainty standard deviation, or (b) it has a small influence on the predictions of interest, i.e., the calculated performance measures (see Table 1) do not change significantly if the parameter is changed within its uncertainty range. A parameter's influence can be determined by having a good general understanding of the system behavior, or by a formal sensitivity and uncertainty propagation analysis. The question whether a parameter is influential or not also depends on the level of prediction uncertainty that is considered acceptable.[*] In particular, stakeholders and regulators must have sufficient confidence that the model-predicted radiation dose is accurate enough to make a defensible assessment of the repository's long-term safety.

The influence of a single model input parameter on select model output variables could be assessed in a sensitivity analysis. More advanced methods examine multiple parameters at the same time, allowing to account for model nonlinearities and interactions among these parameters. Composite sensitivity measures can be calculated to rank parameter influence.

The aggregate impact of parameter uncertainties on the predicted performance measures is typically evaluated in an uncertainty propagation analysis, using one of several available methods, as discussed in Section 4.6. For each parameter that is considered uncertain and influential, additional information is needed, such as upper and lower bounds[†], the assumed

---

[*] A detailed discussion of the relations among uncertainty in characterization data, parameter estimation uncertainty, data sensitivity, parameter influence, and acceptable estimation and prediction uncertainties can be found in Finsterle (2015).

[†] Upper and lower bounds may designate the expected uncertainty of a parameter, but may also specify its physical range, which is needed to avoid generating unphysical conditions during stochastic sampling.

probability distribution, as well as a standard deviation or parameter scaling factor. This additional information is also included in the table of Appendix B.

4.5.12 Summary of Model Development

The numerical model resulting from the development process described in Sections 4.5.1 through 4.5.11 can be summarized as a three-dimensional, mechanistic model of the entire repository system, which includes 153 individually represented waste containers emplaced in the horizontal disposal section of a cased drillhole embedded in a sedimentary host formation that is bounded from below by a slightly overpressured saline formation, and from above by a generic overburden of higher permeability and higher porosity, which in turn is in contact with a near-surface aquifer, from which water is extracted and used as the sole source of drinking water for a potentially exposed individual. Figure 7 shows the hydrostratigraphic layering and heterogeneous porosity distribution of the model used to examine the nominal scenario.

The waste containers release radionuclides and decay heat using a time-dependent source term that is based on the radionuclide inventory contained in spent fuel assemblies from a pressurized water reactor. Once released, radionuclides migrate radially and axially by diffusion and advection through the near field, which includes the various components of the engineered barrier system. Radionuclides then enter the three-dimensional far-field model, which represents the geosphere and includes advective mixing in and extraction from the near-surface aquifer. A standard biosphere model is used to convert radionuclide concentrations in the drinking water to annual dose.

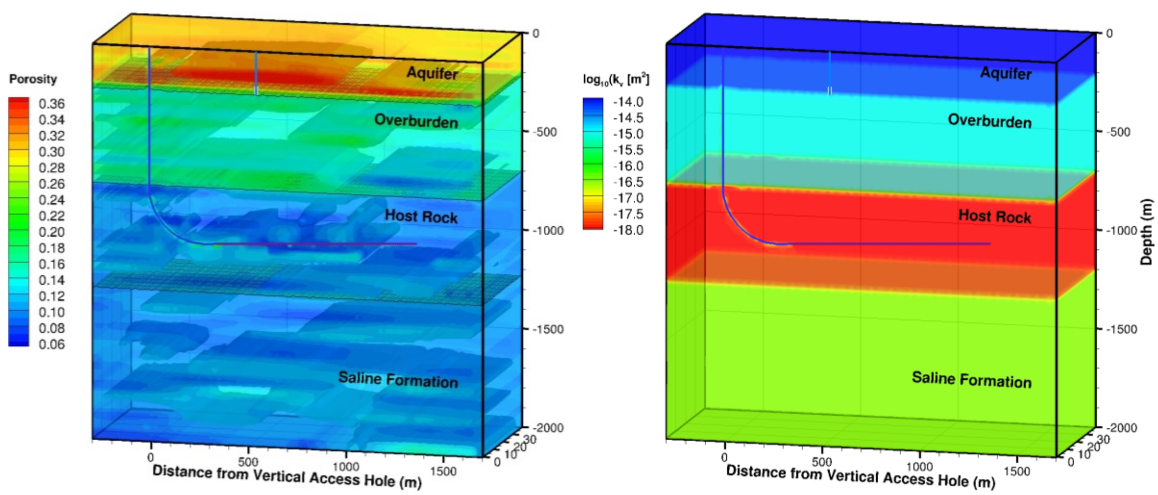

(a) (b)

Figure 7. Hydrostratigraphy, (a) porosity and (b) vertical permeability distribution for nominal scenario. Blue lines indicate the drillhole and the drinking water well; the 153 waste containers in the disposal section are shown in red.

4.6 Treatment of Variability and Uncertainty

The uncertainty in the quantitative evaluation of the long-term performance of a horizontal drillhole repository cannot be eliminated given incomplete knowledge and inherent variability of the repository system and the long time period involved in the projections; however, the uncertainty in the simulation results must be assessed.

There are multiple components contributing to the uncertainty in the calculated performance metrics, including uncertainties in the completeness and appropriateness of the conceptual model and the accuracy of its representation in the numerical model, uncertainties in model input parameters and the data used to determine them, as well as spatial variabilities and uncertainties in the estimates of occurrence probabilities. Some of these uncertainties are reducible, while others are inherently irreducible.*

Some of these uncertainties are best managed by a disposal concept and design decisions that lead to a robust repository system (see Section 5 for a summary of arguments in support of the robustness of the deep horizontal drillhole disposal strategy). The design can incorporate margins to encompass the inevitable uncertainties. The judicious selection of the repository location and host formation is equally essential for attaining an acceptably low assessment uncertainty of repository performance. The FEPs process (see Section 4.2) strives for conceptual completeness of the safety analysis, while research, technology development, testing, monitoring and site characterization aim at quantifying and reducing uncertainties due to incomplete knowledge.

In the absence of a specific site, a generic safety analysis must be based on general site selection criteria and a preliminary repository design. As a result, uncertainties are (a) managed by adopting a generally cautious approach (described in Section 2.2), and (b) estimated through a probabilistic analysis with appropriately adjusted input uncertainties that reflect the current knowledge about the generic repository system (Section 4.7.4).

The probabilistic analysis is based on the nominal scenario using the reference parameters of Appendix B. The disruptive events or the conservative assumptions examined in the sensitivity analyses of Section 4.7.3 are not exercised probabilistically. Because the reference model is realistic, the probabilistic results on a particular confidence level (e.g., the 99th percentile) can be considered to constitute a conservative measure of performance (NEA, 2002).

---

* Reducible and irreducible uncertainties are also referred to epistemic and aleatory uncertainties. In short, epistemic uncertainty reflects one's confidence in an outcome in the face of incomplete knowledge, whereas aleatory uncertainty can be interpreted as the relative frequency of a stochastic behavior or process. Epistemic uncertainty can be reduced by searching for patterns or causality, while aleatory uncertainty cannot be reduced but is managed by determining the relative propensity of the stochastic event (Fox and Ülkümen, 2011). For example, the level of epistemic uncertainty in mean porosity of the host formation can be reduced by site characterization; the spatial variability of porosity within the host formation is an external, random factor that cannot be reduced—it is thus an aleatory uncertainty. (Note that the uncertainty in a geostatistical parameter that describes the spatial variability of porosity can be reduced and is thus epistemic.)

One of the most frequently applied methods used for the assessment of repository performance under uncertainty is a sampling-based probabilistic analysis. A Monte Carlo approach[*] with Latin Hypercube Sampling (LHS)[†] is used for the probabilistic analysis reported in Section 4.7.4.[‡] It consists of repeatedly sampling each of the uncertain parameters from its assumed uncertainty distribution,[§] combining sampled parameters into n_{MC} random sets, and running the simulations n_{MC} times, producing n_{MC} realizations of the system evolution and corresponding performance metrics. The results can be statistically analyzed or simply visualized. Specifically, the mean, median, standard deviation, as well as select quantiles (e.g., the 5th and 95th percentiles) can be extracted from the probabilistic results. When averaging results, special attention must be given to the issue of risk dilution.[**]

[*] Monte Carlo (MC) simulation is a sampling-based computational method used here to integrate the uncertainty in the calculated performance metrics as a function of uncertainty in the input parameters. A distribution is determined for each uncertain input parameter. Then random samples are generated from each distribution (e.g., using the Latin Hypercube Sampling strategy), and these data are used as input for the safety analysis model to calculate the performance metrics. These two steps are repeated as many times as is reasonably necessary to achieve a sufficiently converged, informative output distribution.

[†] Latin Hypercube Sampling (LHS) is a statistical method for generating a near-random sample of parameter values from a probability distribution in the n-dimensional parameter space, where n is the number of uncertain parameters. In LHS, the parameter hypercube is subdivided into equally probable intervals, and a single random sample is taken within each of these intervals, thus making sure that the random parameter set closely represents the desired probability distribution. Specifically, it ensures that the tails of the n-dimensional distribution are properly represented even if n_{MC} is relatively small (for an example, see Figure 29).

[‡] There are alternative, computationally frugal methods that may be sufficiently informative and potentially more transparent than Monte Carlo simulations, specifically if the model underlying the Monte Carlo analysis has to be simplified or replaced by a network of highly abstracted submodels to make the calculations tractable. The mechanistic model developed to assess the safety of a deep horizontal drillhole repository is computationally efficient enough so it can be used directly (i.e., without further abstraction) in a sampling-based probabilistic safety analysis.

[§] Uncertain parameters may be statistically correlated to each other. For example, a rock with lower porosity tends to have lower permeability and lower effective diffusivity. As there is a random component inherent in such correlations, they may not be adequately described by deterministic relationships. If sufficient cross-data between the correlated parameters are available, a statistical correlation coefficient can be determined and accounted for during the Monte Carlo sampling step. Nevertheless, almost all probabilistic safety analyses assume that the parameters are uncorrelated, i.e., independent random samples are taken during Monte Carlo sampling. In this generic safety analysis, the random samples are also considered independent of each other. Note, however, that the Latin Hypercube Sampling algorithm implemented in the iTOUGH2 simulation-optimization framework (Finsterle et al., 2017) has the capability to account for correlations among uncertain input parameters, a feature that may be used in subsequent safety analyses should defensible information about the covariances become available.

[**] Risk dilution is a situation in which an increase in the uncertainty in the model input parameters leads to a (non-conservative) decrease in calculated risk (NEA, 2004). Risk dilution can arise

In addition to parametric uncertainties, stochastic spatial variability in porosity* is also accounted for. Porosity is selected as the spatially variable parameter because of its dominant influence on the effective diffusion coefficient and advective transport velocity, two key factors affecting radionuclide migration through the geosphere.† Random, spatially correlated porosity-modifier fields are generated using geostatistical simulation techniques based on an anisotropic, spherical semi-variogram.‡

The cautious approach is expected to result in dose estimates that are relatively high (and uncertainty bands that are relatively wide) compared to an analysis in which conservative assumptions and conservative parameter values were replaced—based on defensible arguments—by a more realistic representation. Once site-specific characterization data become available, assumptions can be replaced with mechanistic models that, because they are site-specific, are more accurate, and are based on reliable information. For the same reasons, parameter standard deviations may be lowered, leading to dose estimates that are potentially lower and are associated with narrower uncertainty bands.

The site-specific, detailed safety analyses to be performed at a later, more advanced stage of repository development may also address "reserve FEPs", which describe effects that are readily identified as being positive for repository performance, but are omitted from the model for these initial calculations. Table 4 is a partial list of cautious assumptions and reserve FEPs that are omitted from the current model for the sake of simplicity and computational efficiency, but also because their mechanistic inclusion is not warranted given the information available at the current stage of repository development.

---

when assigning overly large uncertainties to influential input factors, and then averaging consequences that are localized in space and time. Averaging cases or scenarios that have very different occurrence probabilities also leads to risk dilution. The method used for calculating peak dose (see Section 4.4), the separation of nominal, disruptive, and sensitivity cases, the visualization of all realized dose curves (see Section 4.7.4) rather than just reporting the mean, and the fact that the drinking water well captures the entire contaminant plume are attempts at minimizing risk dilution effects. The generally diffusion-dominated radionuclide transport processes result in dispersive dose estimates that leave little scope for risk dilution (NEA, 2004). Also see comments about the potential impact of parameter correlations.

* Porosity is the only parameter for which random heterogeneity on the small scale (i.e., within a material domain) is specified. All the other parameters are assumed homogeneous within an given material domain (i.e., they are only deterministically heterogeneous on the large scale).

† While permeability tends to be correlated to porosity, it is assumed homogeneous within each of the hydro-stratigraphic units of the model. This is justified as radionuclide transport is diffusion-dominated in the host rock and the overburden. It is advection-dominated in the aquifer; however, transit times in the aquifer are very short, rendering heterogeneity in permeability irrelevant.

‡ The parameters of the semi-variogram (i.e., correlation length, sill value, and anisotropy ratio) are considered uncertain and are subjected to probabilistic sampling during the Monte Carlo analysis.

Table 4: Cautious assumptions* potentially addressable by the inclusion of reserve FEPs.

#	**Assumption**	**Section**
1	No self-sealing of excavation disturbed zone or fault zone	4.5.7
2	Multiple, parallel drillholes with 100 m spacing	4.5.3
3	No retardation effect due to matrix diffusion	4.5.4.3
4	Effective diffusion coefficient calculated based on bulk porosity	4.5.4.3
5	No sorption on waste form or corrosion products of canister or casing	4.5.5.3
6	High fractional waste-form degradation rate	4.5.5.3
7	High solubility limits	4.5.5.4
8	High corrosion rates for canister and casing	4.5.7
9	Pressurized saline formation below repository horizon	4.5.10
10	Relatively high geosphere permeabilities for nominal case	4.5.11
11	Regional gradient parallel to drillhole pointing towards access hole	4.5.10
12	High annual water consumption rate	4.5.9
13	Unmonitored and untreated drinking water	4.5.9
14	Non-sealing fault	4.3.3.2

* The likely impact of a FEP on the maximum annual dose is used as the criterion to decide whether an assumption is cautious or optimistic.

4.7 Model Results

4.7.1 Introduction

Multiple simulations have been performed, each examining a particular scenario or alternative parameter sets that are perturbed as part of a sensitivity analysis or probabilistic uncertainty propagation analysis. Each of these numerical simulations calculates the evolution of the system state (i.e., pressures, temperatures, brine and radionuclide concentrations) throughout the three-dimensional model domain at many discrete points in time between repository closure and the simulation end time of 10 million years. In addition, quantities derived from a given system state (specifically flow rates, flux concentrations, peak dose, peak-dose times) and secondary properties (such as fluid density) are available at each spatial and temporal calculation point.

The performance metrics listed in Table 1 provide a means to condense the information from these simulations into concise composite measures that are suitable for the assessment of repository safety. The following subsections thus focus on a discussion of these performance measures (specifically the peak dose value); additional information and visualizations are provided to support the interpretation of the simulation results.

4.7.2 Nominal Scenario

The nominal scenario is described in Section 4.3.2. It provides a cautious assessment of repository performance under undisturbed conditions (i.e., the system is not affected by low-probability disruptive events).

The main performance measure of interest is the temporal evolution of annual dose and its peak value to which an individual is exposed by ingesting drinking water extracted from the aquifer located above the repository.

Figure 8 shows the annual dose as a function of time from the exposure to ^{129}I, ^{36}Cl, ^{79}Se in the nominal scenario (^{99}Tc is not shown because its contribution to dose is insignificant). The combined peak dose caused by these four radionuclides is 8.0×10^{-3} mrem yr^{-1}. This peak dose, which occurs after 1.6 million years, is dominated by ^{129}I. The peak doses of ^{79}Se and ^{36}Cl are 1.3×10^{-4} and 4.5×10^{-6} mrem yr^{-1}, respectively. Peak dose of ^{79}Se is higher than that of ^{36}Cl because of its larger inventory (see Table 2) and its higher dose coefficient (see Table 3). Both radionuclides reach their peak dose after approximately 775,000 years. Peak doses as well as peak-dose times are curtailed by the decay of these two radionuclides as they migrate through the geosphere. ^{99}Tc does not arrive at the drinking water aquifer in any significant concentration despite its large inventory. This is mainly due to its shorter half-life, solubility limit and retardation by adsorption to the solids of the geosphere. The total dose from the four radionuclides tracked in this simulation is essentially identical to that from ^{129}I. The dominance of ^{129}I is explained by its long half-life, which leads to minimal decay despite the very long travel time from the repository to the accessible environment. The peak dose for the nominal scenario is more than three-orders of magnitude below a typical dose standard (Figure 8 indicates 10 mrem yr^{-1} as a reference value).

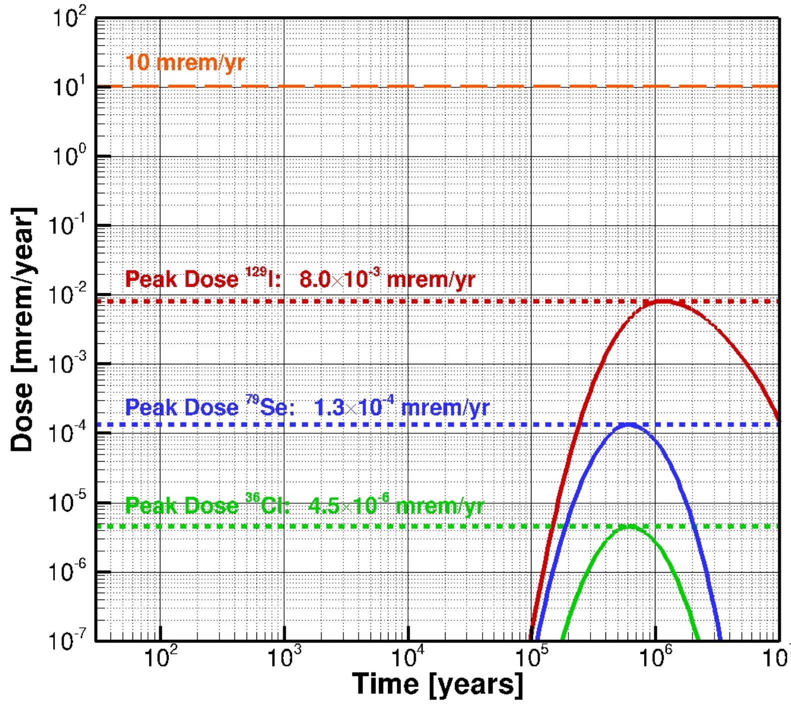

Figure 8. Performance Metric 1: Dose as a function of time for nominal scenario.

Figure 9 shows the second relevant performance measure, which is the maximum radionuclide concentration (expressed as an activity) in groundwater. Two sets of curves are shown: the activities of each of the radionuclides within the waste canister, and the maximum concentrations in the aquifer. The concentration in the waste itself depends on the inventory (see Table 2), the specific activity (see Table 3), and the fractional waste degradation rate (see Section 4.5.5.3). Concentrations respond to the release of radionuclides from the degrading waste matrix and their dissolution in the aqueous phase* within the canister. As long as the canister is intact, concentrations increase (slightly moderated by radioactive decay). Note that the activity of dissolved ^{99}Tc is low because of the imposed solubility limit.

* If there were no solubility limit, the maximum aqueous-phase concentration of ^{99}Tc that would be reached inside the canister is approximately 3×10^{-3} mol L^{-1}, i.e., far above the solubility limit of Tc under reducing conditions (Nagra, 2002b, Table A3.5-1; a conservatively high solubility limit of 10^{-8} mol L^{-1} is assumed in the simulations). The Tc concentration reaches the solubility limit almost immediately after waste degradation begins, and falls below the solubility limit after approximately 800,000 years, at which point release becomes diffusion-limited, and a source-term model based on the fractional waste degradation rate is invoked. The maximum concentration of ^{79}Se is approximately 4×10^{-5} mol L^{-1}, which is close to the solubility limit of Se; no solubility limit is imposed for ^{79}Se. The ^{129}I and ^{36}Cl concentrations are far below the high solubility limits of these elements. Selecting a relatively high solubility limit (as is done for ^{99}Tc) or ignoring it altogether (as is done for ^{129}I, ^{36}Cl, and ^{79}Se) is conservative as these assumptions increase radionuclide mobilization from the waste matrix (see Section 4.5.5.4).

Once corrosion perforates the canister (which is assumed to occur after 10,000 years), the radionuclides are released to the near field, leading to a sharp drop in concentrations within the canister. Mobilization of radionuclides declines with time as the degradation rate decreases because the inventory is reduced by radioactive decay and the leaching process itself. Moreover, the release is diffusion limited with a decreasing concentration gradient.

Radionuclide concentrations in the near-surface aquifer are substantially lower compared to their activities in the drillhole repository. This is a result of the diffusion process, which spreads the radionuclides over a large volume within the geosphere, drastically reducing concentrations. Moreover, transport times are sufficiently long compared to the half-lives of most radionuclides (with the exception of ^{129}I) that decay further reduces the concentrations.*

As expected, the time when peak dose is reached (see Figure 8) coincides with the time when groundwater concentrations reach their maximum (see Figure 9).† The peak concentrations are substantially lower than typical regulatory limits set for radionuclide contamination in groundwater.‡

* Note that the well extracting drinking water from the aquifer (used as a basis for the dose calculation) reduces or prevents the accumulation of radionuclides in the aquifer. Accumulation may be possible under certain conditions (e.g., in arid regions with no run-off, erosion, pumping, or other loss mechanisms); the presence and relevance of such conditions will be evaluated using a more detailed biosphere model that is based on site-specific information. Conversely, any sink terms that reduce radionuclide concentrations in the groundwater are also excluded from this analysis. These factors and a comprehensive list of exposure pathways will be included in a site-specific safety assessment, when the local geographical, topographical, and climatological factors that affect each exposure pathway are sufficiently characterized.

† The differences in the ratios between the peak-dose values (see Figure 8) of the various radionuclides and the respective ratios in peak groundwater concentrations (see Figure 9) are a result of the different dose coefficients that convert concentrations to effective dose (see Table 3).

‡ The radionuclide concentrations in groundwater reported here can be converted to total body or organ dose equivalents as prescribed by an applicable regulation (e.g., 40 CFR 141.66(d)(2)).

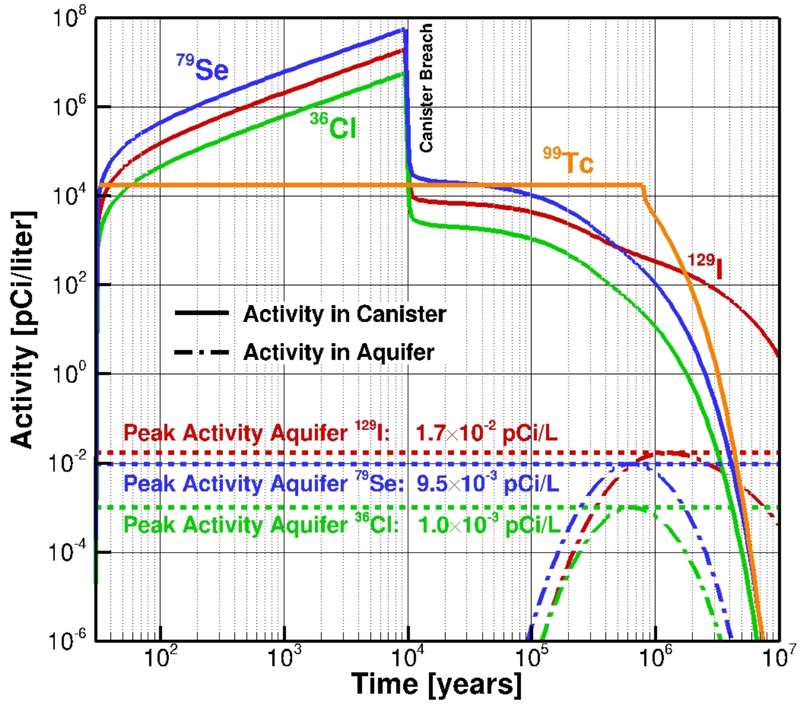

Figure 9. Performance Metric 2: Aqueous radionuclide activities in canister and aquifer as a function of time for nominal scenario.

Figure 10 shows radionuclide flow rates across three interfaces:* (1) from the drillhole into the geosphere, (2) through the circular cross section of the drillhole and the surrounding excavation disturbed zone at a depth of -725 m, i.e., where radionuclides traveling in axial direction along the drillhole enter the vertical access hole, and (3) into the aquifer from the underlying formation and from the access hole. The flow rates are expressed in units of pCi s^{-1} to account for the different activities of the radionuclides.

After the canisters have been breached (at 10,000 years), radionuclides are released (mainly by diffusion) from the drillhole to the excavation-disturbed zone of the surrounding host rock (solid lines in Figure 10), from where they migrate through the geosphere. These flow rates into the geosphere are close to the diffusion-limited release rates from the breached canisters.

* The flow rates at these three locations represent performance metrics 3 through 5 of Table 1.

Radionuclides migrate through the host rock and the overburden, and eventually enter the aquifer. The rate into the aquifer shown in Figure 10 is the total influx of contaminants to the near-surface aquifer across the entire interface between the overburden and the aquifer (an area larger than the footprint of the repository, which is about 10^5 m^2 *); radionuclide fluxes entering the aquifer from the vertical access hole are also included.

The maximum activity flow rate from ^{129}I is approximately 0.03 pCi s^{-1}. The groundwater in the aquifer dilutes contaminants as radionuclides migrate towards the extraction well. The maximum rate of ^{79}Se of 0.02 pCi s^{-1} is similar to that of ^{129}I. The higher activity of ^{79}Se compensates for its smaller inventory and shorter half-life. Much less ^{36}Cl is initially present in the repository, and the mass concentration flux into the aquifer is very small; however, ^{36}Cl has a high specific activity, so its contribution to the total aquifer activity reaches 5% at its peak value after 770,000 years. ^{99}Tc does not reach the aquifer, mainly because it is adsorbed to the grain surfaces in the geosphere.

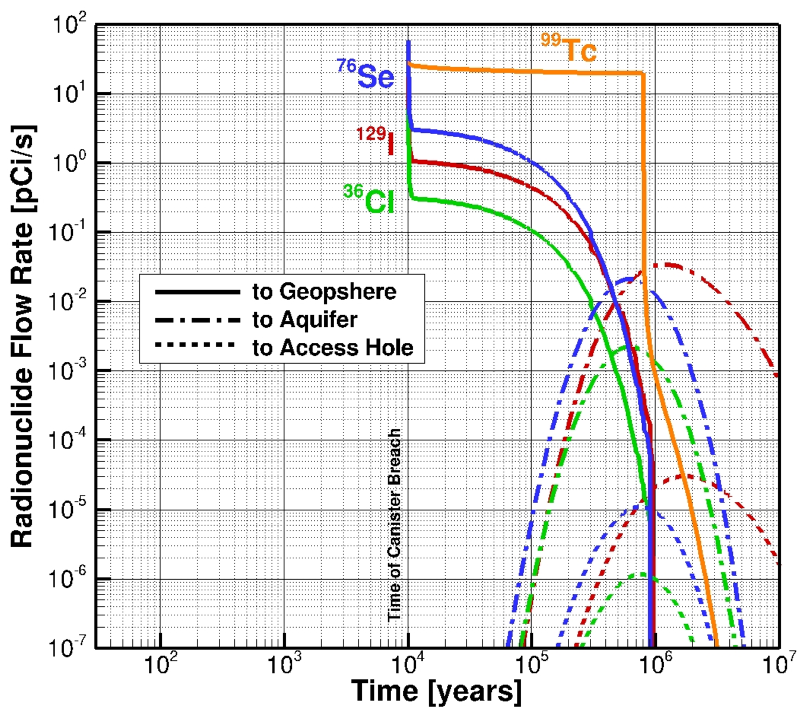

Figure 10. Performance Metrics 3–5: Radionuclide flow rate as a function of time for nominal scenario.

* The footprint of the repository is defined here as the length of the disposal section (approximately 1000 m) times the separation distance between drillholes (100 m). The actual flow rate shown in Figure 10 is the sum of the flow rates across the entire model interface between the overburden and the aquifer, which is 5,750 × 50 × 2 = 575,000 m^2 (the factor of 2 is due to symmetry).

Figure 11 shows the temperature in the buffer material within the disposal section of the drillhole and in the host rock immediately at the drillhole wall as a function of time in response to the decay heat generated in the waste form. As shown in Figure 5, the early-time heat output after the pre-disposal cooling time of 30 years (shaded in Figure 5) is mainly due to the decay of ^{137}Cs and ^{90}Sr. The temperature in the drillhole initially increases. The relatively short half-lives of these key fission products (approximately 30 years) lead to rapidly declining heat output, which—combined with cylindrical heat dissipation—prevents temperatures from rising to very high values. Ten years after disposal, temperatures reach a maximum of approximately 99°C.* This temperature is far below the boiling temperature under the high in-situ pressures (see Figure 3). After 1,000 years, the temperature is still approximately 10°C above the ambient temperature of 40°C.

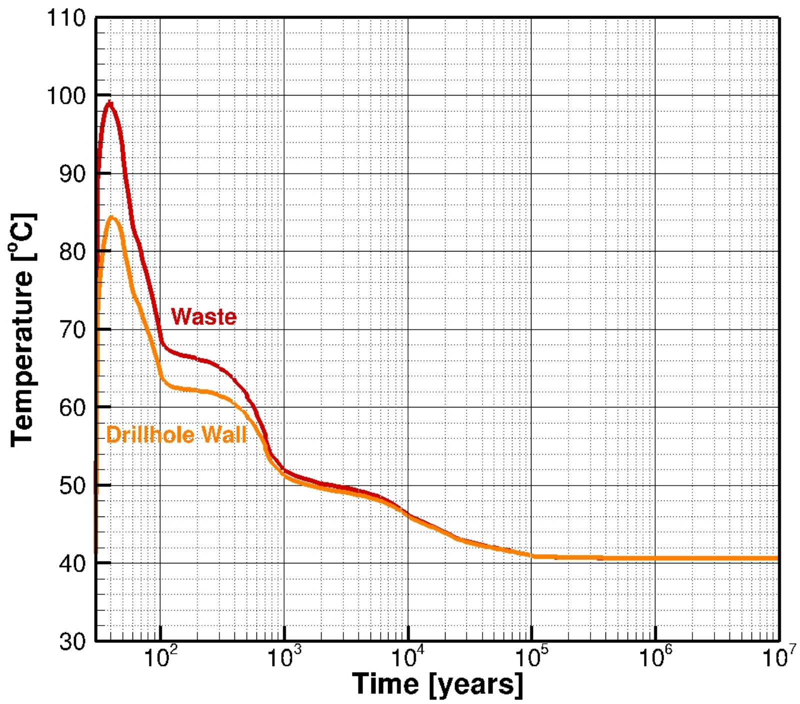

Figure 11. Performance Metric 6: Temperature as a function of time for nominal scenario.

* A 100°C thermal limit is imposed by most nuclear waste disposal programs that consider mined repositories and use bentonite as a buffer material. At higher temperatures, several potential issues have been identified that may degrade the bentonite's barrier performance. These concerns are mainly related to chemical alterations (illitization and cementation by silica) that may reduce the buffer's swelling capacity and plasticity, but also include potential effects from water boiling, dry-out and salinity changes. While bentonite or bentonite slurries may also be used in a deep horizontal drillhole repository, the horizontal drillhole disposal concept does not rely on the bentonite's swelling capacity, and desiccation or boiling is prevented by the waste being emplaced under fully saturated, high-pressure conditions.

The temperature rise induces fluid expansion,* leading to a pore pressure increase. Figure 12 shows that the temperature-induced pressure change in the drillhole is on the order of a few bars, values that are not expected to adversely affect the engineered components or lead to additional fracturing or significant fracture dilation in the excavation disturbed zone. The perturbation reaches its maximum a few years after repository closure, coincident with the temperature maximum. Reduced heat output from the waste and thermal dissipation lead to cooling and contraction of the fluid and the pore space. As a result, pressures temporarily drop below the initial pressure and eventually re-equilibrate by back-flowing water. These pressure perturbations are constrained to the thermal period. They induce flows along the backfilled drillhole and into the host rock. These flow rates are, however, small and are reversed during the cool-down period.† Moreover, in the nominal scenario, the canister is assumed intact during the thermal period, i.e., no thermally induced advective radionuclide transport will occur.‡

* As an example, the density of the 0.86 molar brine at the initial repository condition of P = 100 bar and T = 42 °C is 1,024 kg m^{-3}; the density at a pressure of P = 104 bar and a temperature of T = 98°C is 992 kg m^{-3}, which corresponds to a volume increase of about 3%. However, the effects of thermal fluid expansion are partly countered by an increase in porosity, which is caused by the thermal expansion of the solid skeleton and elastic deformation due to the pressure increase; see Sections 4.5.4.2 and 4.5.4.5. This reduces the heat-induced volumetric flow during the thermal period.

† During heating, water is pushed out by the overpressure caused by thermal expansion; during cooling, the water is sucked back in by the underpressure caused by the contraction of the cooling water. The advective contribution of the thermal effects to radionuclide transport are thus reversed; however, this cycle leads to a more disperse contaminant plume.

‡ Thermal expansion may lead to heave at the land surface. This process is not analyzed as heave is not one of the radiological performance metrics examined here (see Table 1).

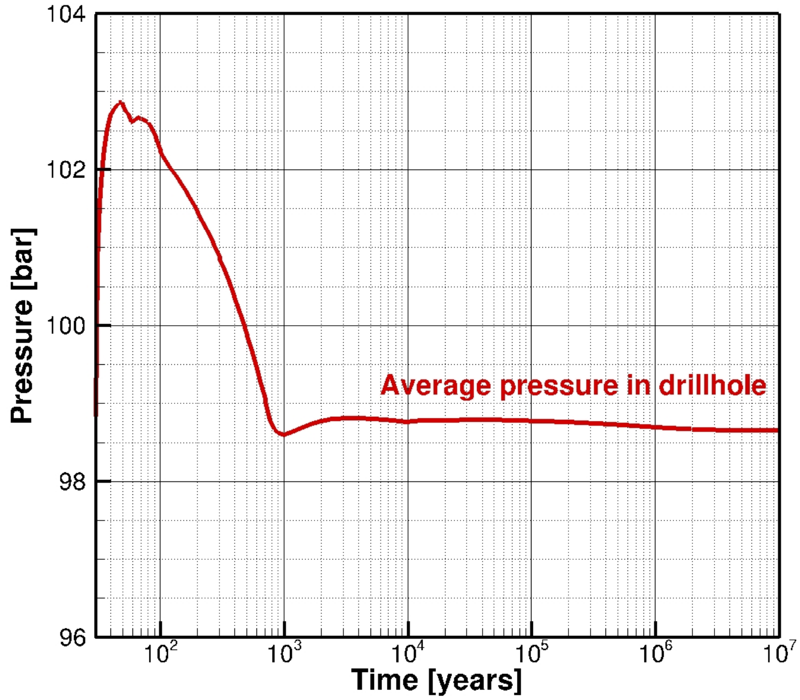

Figure 12. Performance Metric 7: Average pressure in disposal section as a function of time for nominal scenario.

As described in Section 4.7.1, the performance measures are derived from the time-dependent system state calculated at each point in the model domain. To better understand the evolution of the repository system (specifically the migration of radionuclides from the repository to the accessible environment), state variables are visualized at select times.

Figure 13 shows the temperature and fluid-density distributions during the thermal period. It indicates that the repository-induced thermal perturbation is spatially limited relative to the domain size and with respect to the natural geothermal gradient. Nevertheless, the temperature increase influences fluid flow and radionuclide transport in various direct and indirect ways, including (a) reduced fluid density (see right column of Figure 13), which leads to a pressure increase with associated elastic porosity changes (Delage, 2013; Ghabezloo and Sulem, 2009) and potential advective fluid flow, (b) porosity increase due to thermal expansion of the rock skeleton, (c) increased diffusivity according to the Stokes-Einstein equation (direct effect) and due to increased porosity (indirect effect), and (d) reduced fluid viscosity. Temperature changes also affect corrosion rates, waste form degradation, radionuclide solubilities, geochemical reaction rates, and coupled thermal-hydrological-mechanical effects; however, these effects are not accounted for in the current model.

Figure 14 through Figure 17 show the radionuclide plumes of ^{129}I, ^{36}Cs, ^{79}Se and ^{99}Tc at six select times. (In the figures, radionuclide concentration is converted to radioactivity in pore water and represented using an exponential scale.) In general, the plumes indicate a diffusion-dominated transport process within the low-permeable host rock. At late times, the pressure perturbation imposed by the constantly producing drinking water well combined with the slight overpressure in the deepest strata induces an advective flow and transport component and thus an advective activity pattern in the overlying formations.

Even for the weakly-sorbing, long-lived ^{129}I (see Figure 14), the bulk of the radionuclide mass remains in the shale host rock up to and beyond the time when peak dose is reached (at around 1.5 million years). After very long times (10 million years), the activity has been slowly dispersed by diffusion and slow advective transport, driven by the regional pressure gradient in the underlying saline formation. Recall that peak dose is dominated by the activity of ^{129}I in the near-surface aquifer.

The activity concentrations of ^{36}Cl and ^{79}Se show qualitatively a similar evolution (see Figure 15 and Figure 16). The activity of ^{79}Se is generally higher than that of ^{36}Cl (despite its activity coefficient being lower by a factor of about 2; see Table 3) because of its larger inventory (by a factor of 20; see Table 2). Both radionuclides have approximately the same half-live (of 300,000 years), i.e., most of their initial mass has decayed[*] by the time peak dose is reached. No discernable activity can be found at the end of the simulation period of 10 million years.

Finally, despite its large inventory, the release of ^{99}Tc from the waste form is limited by its poor solubility in pore water, and its transport is considerably retarded due to adsorption of this radionuclide to the grains of the shale. As a result, most of the ^{99}Tc is retained in the waste form and near field of the repository, where it is essentially immobilized, and where it is reduced by radioactive decay[†] (see Figure 17).

The evaluation of the performance measures for the nominal scenario suggests that radioactive waste disposed in a horizontal drillhole repository is sufficiently isolated from the accessible environment. The maximum radiation exposure of an individual is likely far below a typical, stringent dose standard, despite making cautious assumptions about the properties of the engineered and natural barrier systems. Radionuclide releases from the repository and transport rates along potential migration pathways are exceedingly small, leading to very low levels of contamination in the geosphere and specifically in the near-surface aquifer. Finally, perturbations due to repository construction and operation as well as post-closure thermal loading are small to moderate and are unlikely to induce detrimental effects that jeopardize the integrity of the engineered or natural barrier systems.

[*] The half-lives of ^{36}Cl and ^{79}Se are 301,000 and 295,000 years, respectively; after 1.5 million years (the approximate time when peak dose is reached), radioactive decay reduced the total activity of ^{36}Cl and ^{79}Se in the repository system by a factor of about 30.

[†] The half-life of ^{99}Tc is 211,000 years; after 1.5 million years (the time peak dose is reached), radioactive decay reduced the total activity of ^{99}Tc in the repository system by a factor of about 140.

Figure 14 through Figure 17 also show that the radionuclide activity field is essentially two-dimensional within the *X*-*Z* plane, i.e., concentrations in *Y* direction* between the symmetry planes defined by the neighboring parallel disposal section are uniform. As a result, for drillhole separation distances of less than about 100 m, the results (activities and dose) scale approximately inversely proportional to drillhole spacing. If the repository consists of a single drillhole or multiple drillholes that are relatively far apart, the radionuclide plume spreads in a more three-dimensional fashion, leading to reduced concentrations.

* Note that in Figure 14 and all similar figures, the *Y* axis is rendered with an exaggeration of 10.

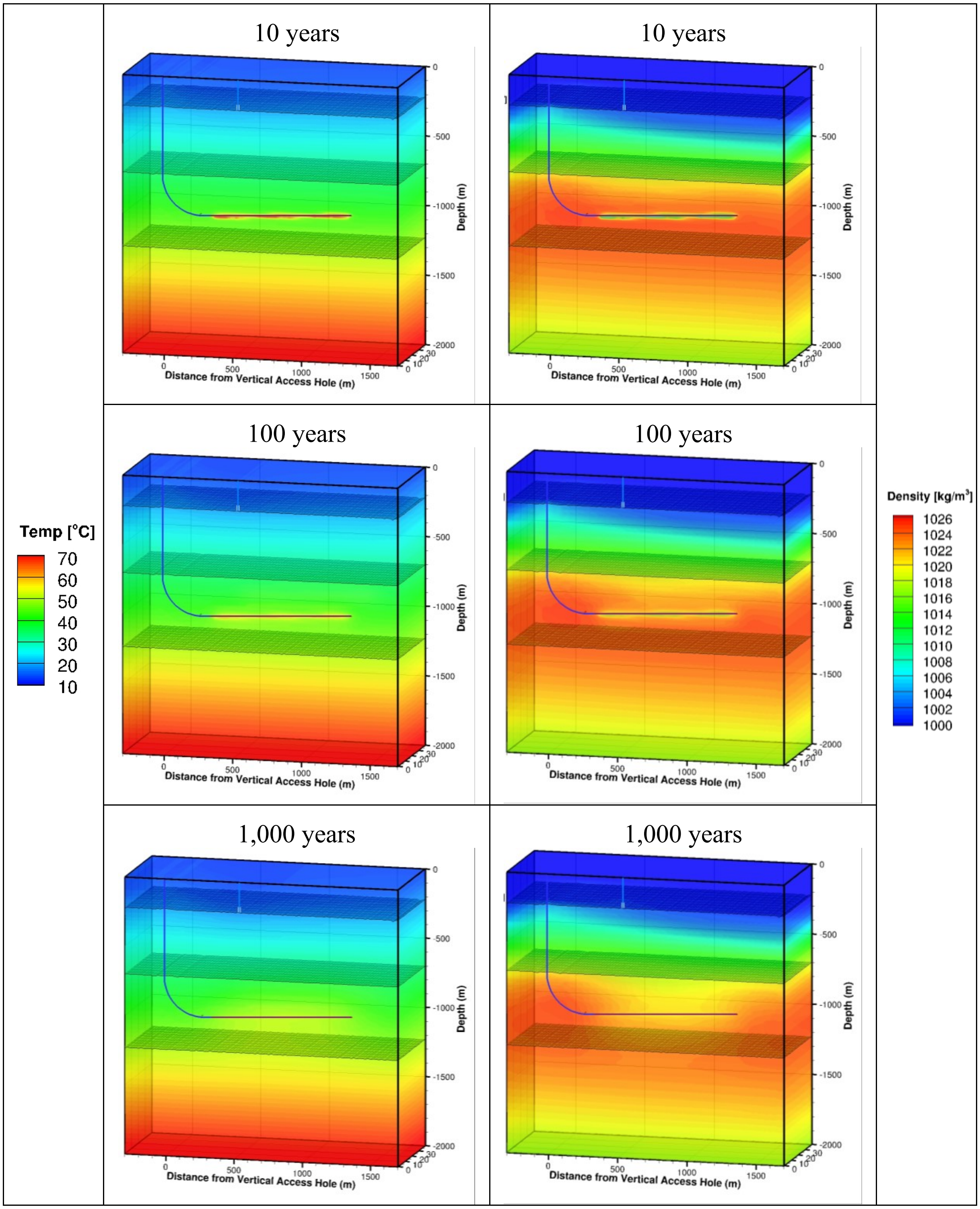

Figure 13. Temperature (left column) and fluid density (right column) distribution throughout repository system.

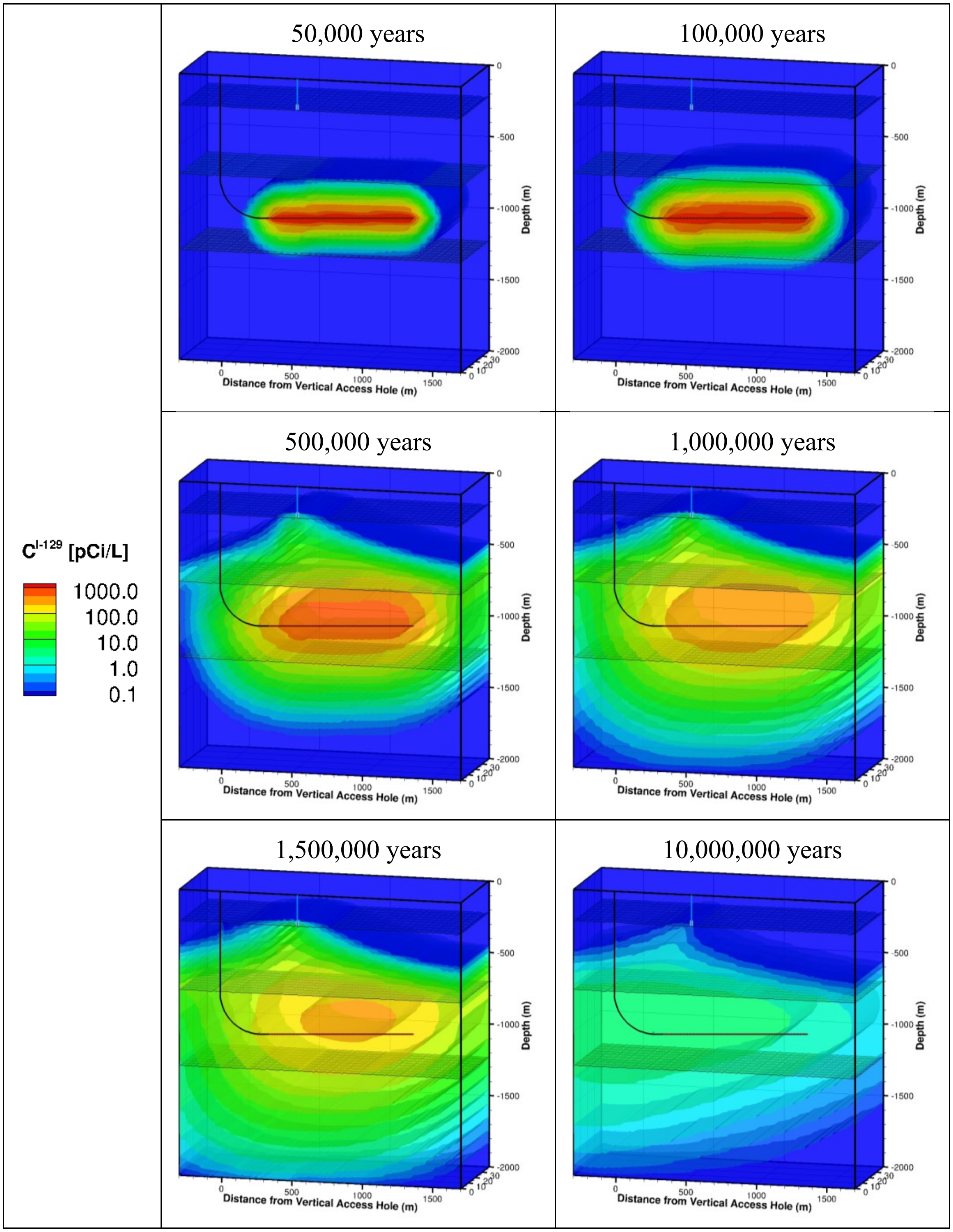

Figure 14. Simulated ^{129}I activity distribution throughout repository system.

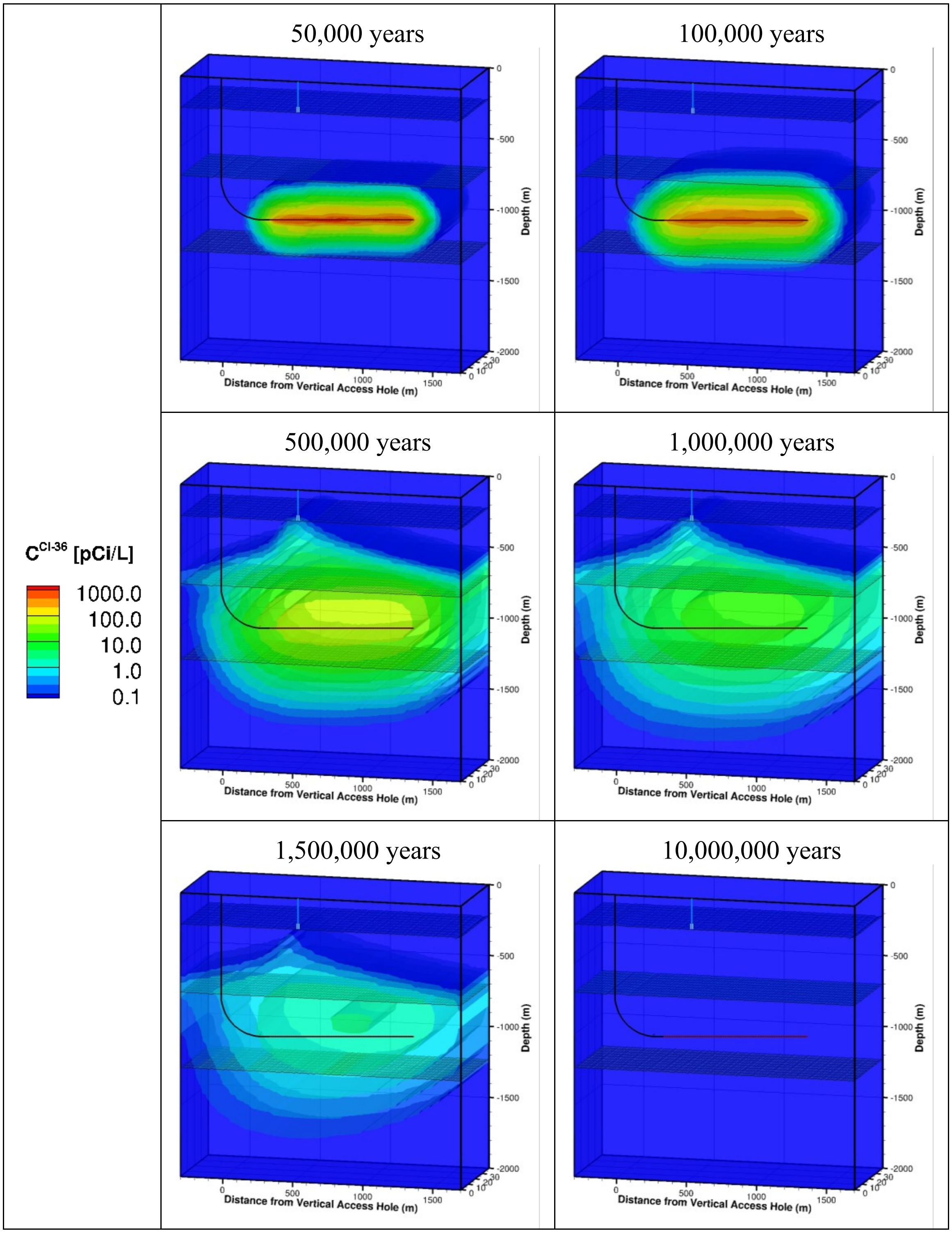

Figure 15. Simulated ^{36}Cl activity distribution throughout repository system.

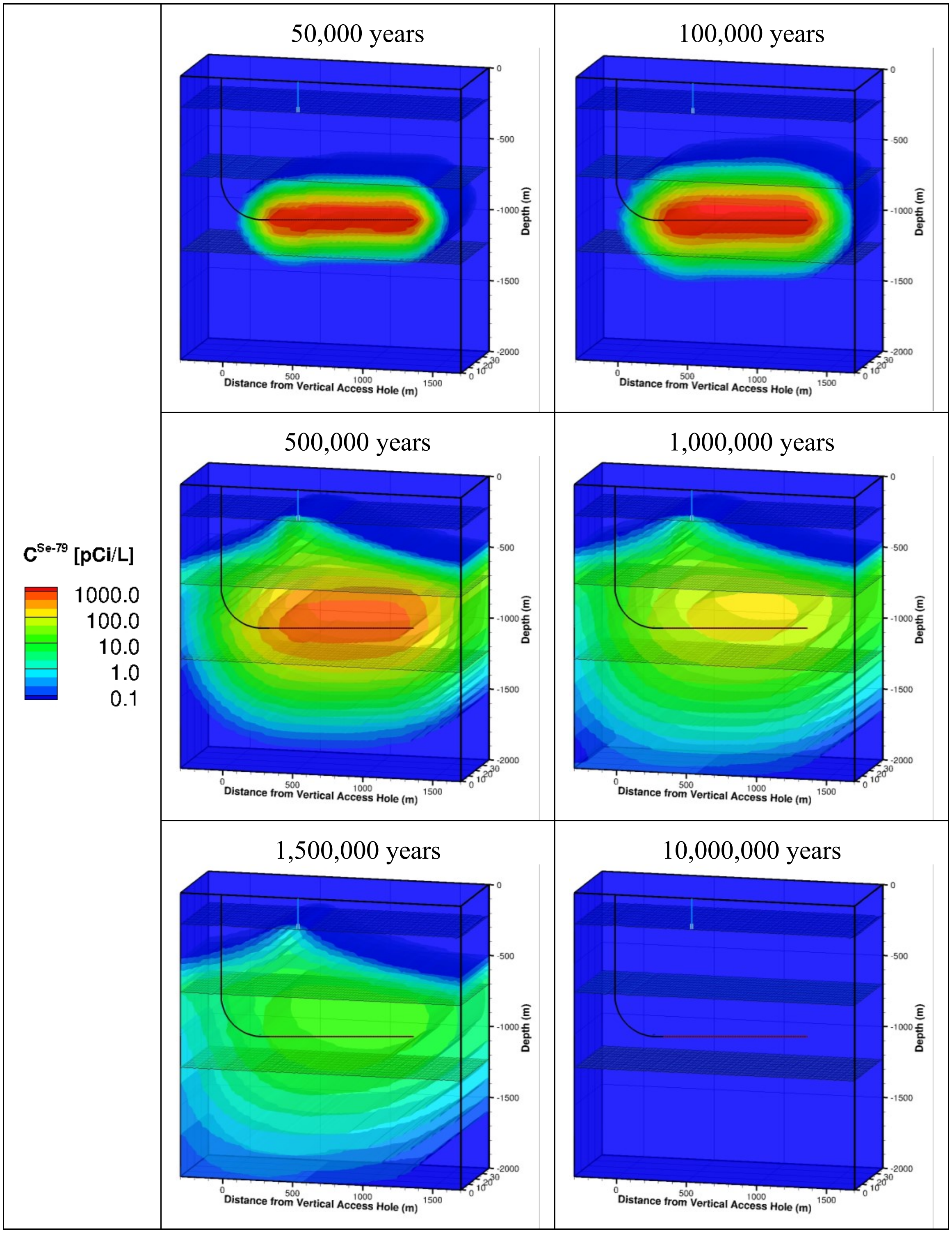

Figure 16. Simulated ^{79}Se activity distribution throughout repository system.

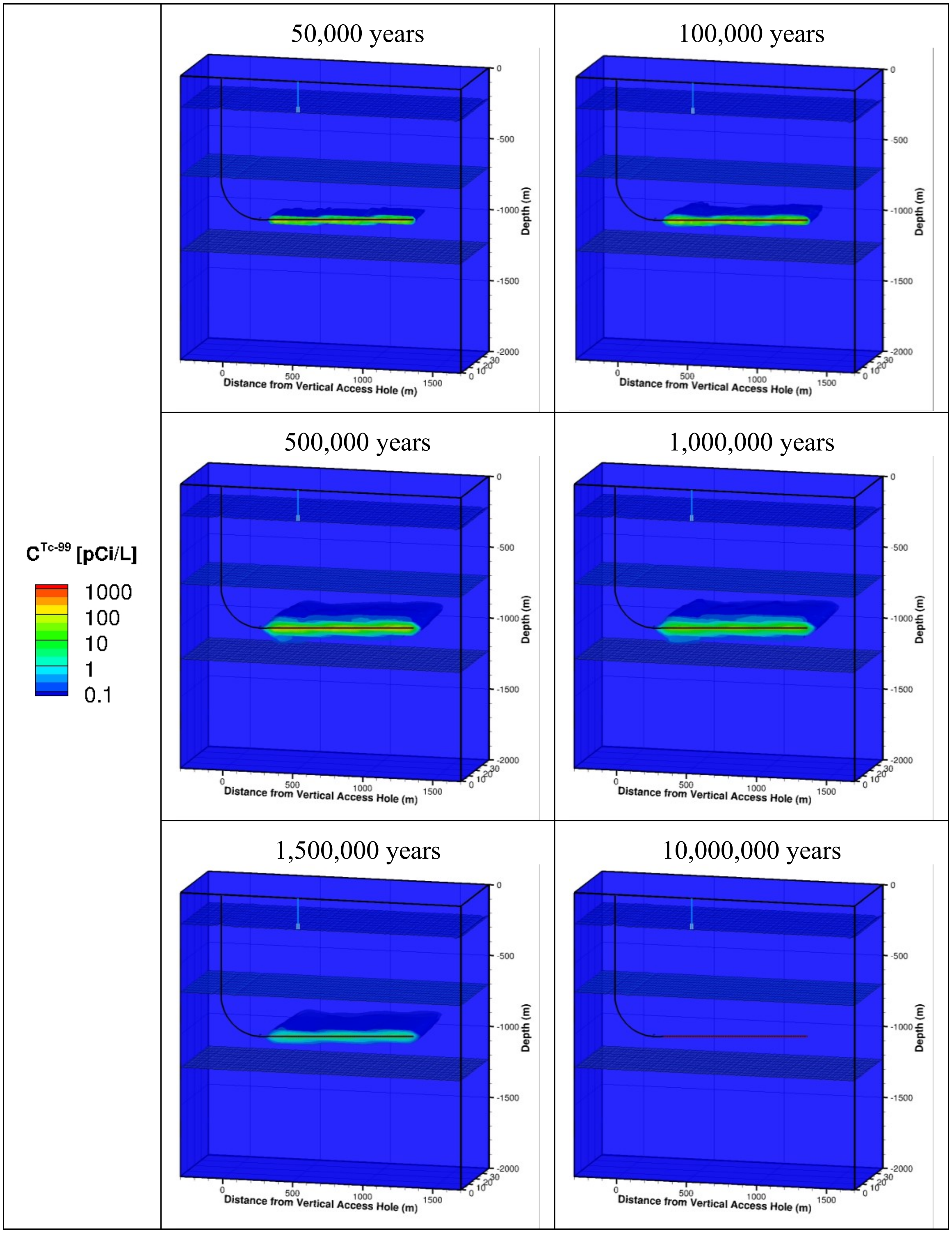

Figure 17. Simulated ^{99}Tc activity distribution throughout repository system.

4.7.3 Sensitivity Analyses

The following subsections describe the results of sensitivity analyses performed mainly to improve the understanding of the system behavior and the influence of specific factors. All sensitivity analyses are local,* with the nominal scenario used as the reference point.

4.7.3.1 Waste Degradation Rate, Instant Release Fraction, and Instant Mobilization

The fractional waste degradation rate determines the rate with which radionuclides encapsulated in the waste matrix are released and become potentially mobile by dissolution in the water that is present within the canister (see Section 4.5.5.3). Degradation of the solid waste matrix is the result of complex radiolytic oxidation and transport processes that depend on the characteristics of the waste form itself as well as the geochemical environment. The SNF matrix is very stable†, making it difficult to experimentally determine its degradation rate; this explains the wide range of rates reported in the literature.

To examine the importance of an accurate determination of the waste degradation rate, a sensitivity analysis is performed by lowering the somewhat conservative estimate of 10^{-5} yr^{-1} used in the nominal scenario to 10^{-7} yr^{-1} (SKB, 2006; Table 10-2).

The results are shown in Figure 18. Reducing the fractional waste degradation rate from 10^{-5} to 10^{-7} yr^{-1} delays the peak-dose time from 1.6 to 4.0 million years and reduces the peak dose by a factor of six from 8.0×10^{-3} to 1.4×10^{-3} mrem yr^{-1}.

Some radionuclides are concentrated on pellet and crack surfaces and in the gap between the fuel and cladding (Roth, 2015). This enrichment is the result of enhanced release from the fuel matrix during in-reactor irradiation. This fraction of the inventory is leached rapidly, a phenomenon that is captured by specifying an instant release fraction (IRF).

For SNF with a burn-up of 60 GWd/MTIHM, the IRF for ^{129}I is approximately 20% of the initial inventory (Nagra, 2002a; Table A2.2.1). Because an IRF is omitted in the reference scenario, it is examined in this sensitivity analysis. Accounting for a 20% instant release‡ of ^{129}I slightly increases the peak dose from 8.0×10^{-3} to 8.3×10^{-3} mrem yr^{-1} (Figure 19).

* See footnote in Section 4.3.4 for an explanation.

† The encapsulation of radionuclides in the very stable waste matrix fulfills one of the main barrier functions of the repository system.

‡ The instant release fraction of 20% is implemented in the model by assuming 20% of the initial inventory is instantaneously dissolved in the canister's pore water. The corresponding radionuclide mass fraction in the liquid phase is calculated and specified as initial conditions for the appropriate primary variable in all elements representing the waste form. Moreover, the initial inventory is reduced by 20% and used as the starting point for the standard fractional waste degradation calculation as described in Section 4.5.5.3.

This small influence can be explained by the "spreading in time" phenomenon (Nagra, 2002; Section 6.6.3)* and the stronger concentration gradient associated with the instant release pulse, which disperses the ^{129}I plume over a larger region, thus reducing the peak concentration. The relative insignificance of the IRF is also explained by the high waste degradation rate used in the nominal scenario, which leads to the release of most of the radionuclides at early times, i.e., an effect similar to that of specifying a instant release fraction.

A bounding case is also simulated to demonstrate the importance of the source-term model for estimating peak dose. In this scenario, the entire ^{129}I inventory is assumed to be instantaneously released from the waste matrix (corresponding to an IRF of 100%). Furthermore, the released radionuclides dissolve immediately and completely into the pore water (i.e., no solubility limit is applied). Finally, it is assumed that the canister and casing have degraded instantaneously, i.e., they do not inhibit fluid flow nor diffusive transport of dissolved radionuclides from the waste form to the near field. This extreme scenario thus assumes immediate and complete mobilization of the entire ^{129}I inventory. While unrealistic, this bounding case demonstrates the relative importance of the engineered and natural barrier systems for waste isolation.

Figure 20 shows that while instant radionuclide mobilization leads to an earlier arrival of the plume at the receptor, peak dose is not significantly affected (in comparison with the nominal scenario). Peak dose is only weakly affected by the temporal details with which radionuclides are released from the waste form and canisters. This insensitivity is mainly related to the already conservative assumptions made in the nominal case, where a high waste degradation rate combined with a short lifetime of the canisters and casing lead to a pulse-like release of the inventory. The details of the pulse are of little influence because its overall duration is short compared to the time needed for the radionuclides to diffusively migrate to the aquifer. The result is also consistent with the relative insensitivity of peak dose to the instant release fraction (see Figure 19) and early canister failure (see Section 4.7.5.2).

* The "spreading in time" phenomenon refers to the fact that a pulse (such as the instantaneous release of a fraction of radionuclides) becomes less pronounced as it travels by diffusion through the engineered and natural barrier system, reducing its contribution to peak concentration fluxes with time.

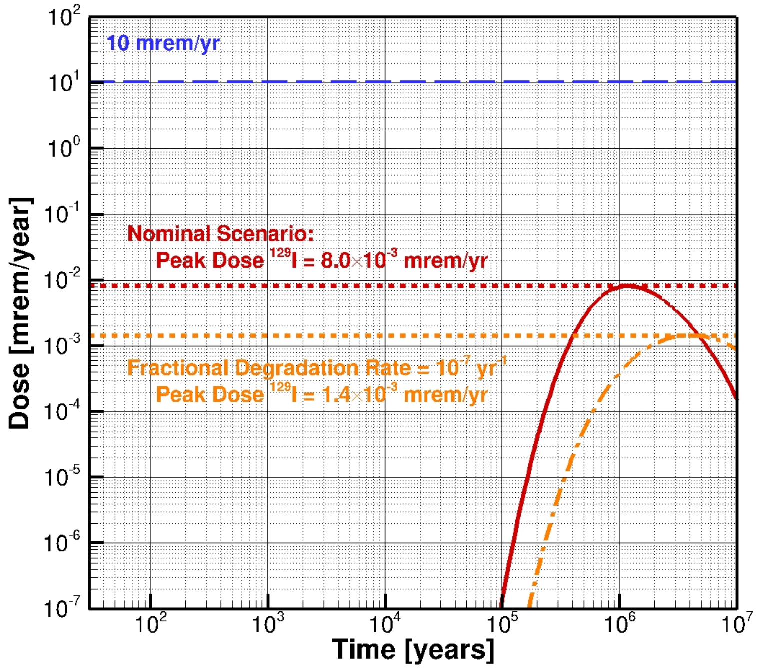

Figure 18. Comparison of annual dose from ^{129}I exposure with fractional waste degradation rates of 10^{-5} yr^{-1} (nominal scenario) and 10^{-7} yr^{-1}.

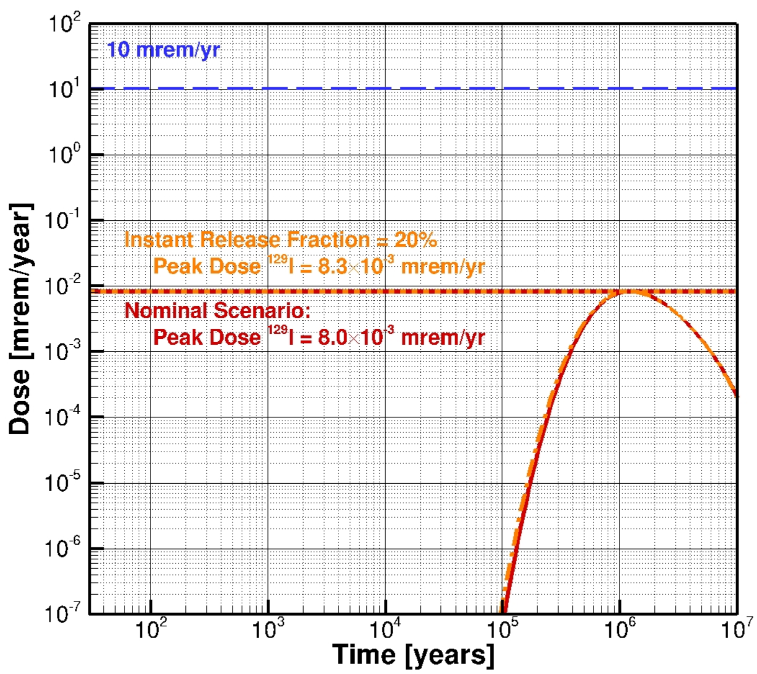

Figure 19. Comparison of annual dose from ^{129}I exposure with instant release fraction of 0% (nominal scenario) and 20%.

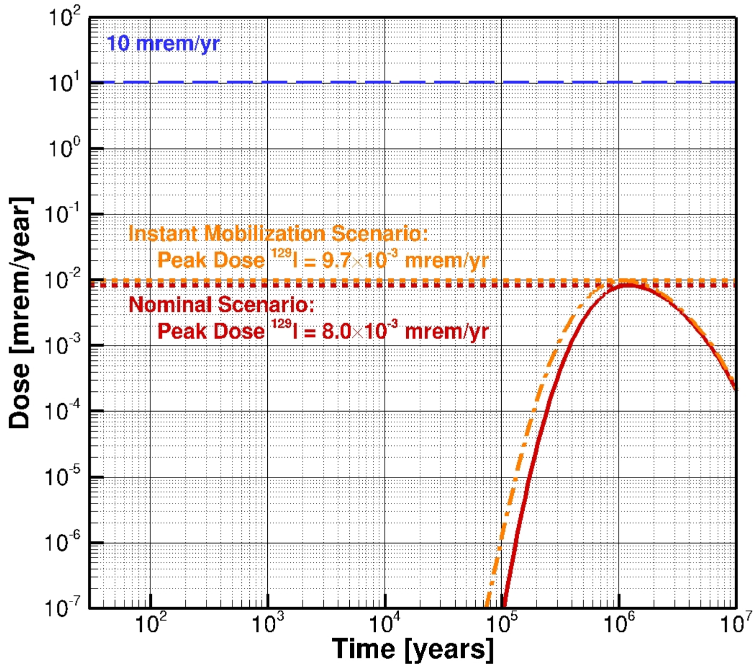

Figure 20. Comparison of annual dose from ^{129}I exposure for nominal scenario and assuming that radionuclide mobilization is instant (IRF = 100%; no barrier function assigned to canister and casing) and complete (no solubility limit enforced).

The sensitivity analysis of waste degradation parameters indicates that determining the source term is only important for the estimation of peak dose if there is a need to relax the conservative assumptions made in the current nominal scenario.* Specifically, if the rate with which the waste form degrades—releasing the radionuclides previously encapsulated in its solid matrix—is lower than the assumed rate of 10^{-5} yr^{-1}, the peak dose is reduced. Conversely, peak dose is not significantly increased by accounting for the instant release of a fraction of the radionuclides, or assuming (as an unrealistic bounding case) that the entire inventory is mobilized immediately after repository closure. The small influence of the temporal release function, which is part of the source-term model, is a result of the dampening that occurs due to the diffusive nature of radionuclide transport and the long migration times.

These observations have significant implications. They demonstrate that the repository is robust to uncertainties in the performance of the engineered barrier system. For example, waste degradation and canister corrosion rates are difficult to determine with confidence for the range of geochemical, thermal, and mechanical conditions that might be encountered over the expected lifetime of these engineered barrier components. However, if the barrier functions of the waste form and canisters do not significantly contribute to the long-term

* Currently there is no need to relax conservative assumptions made in this generic safety analysis, as the calculated peak dose is below a dose standard of 10 mrem yr^{-1} by a large margin.

safety of the repository, peak dose can be estimated despite uncertainties in the source-term model.

4.7.3.2 Advection and Diffusion

Once released from their containment within the engineered barrier system, radionuclides are transported from the repository to the biosphere by diffusion and advection (potentially retarded by sorption). A key safety function of the geosphere is to ensure diffusive spreading of the radionuclides and slow advective transport.* The key parameters affecting these two processes are the effective diffusion coefficient as well as permeability and hydraulic gradients. This sensitivity analysis looks at the impact of these two parameters on radionuclide migration and annual dose.

The effective diffusion coefficient includes the combined effects of molecular diffusion (in bulk water) and the properties of the porous medium (specifically porosity and tortuosity). While the molecular diffusion coefficient for various radionuclides can be determined relatively accurately, the formation-specific porous-medium component is more difficult to estimate.

Permeability may also vary considerably.† In a generic safety analysis, the range of permeabilities to be examined does not only reflect estimation uncertainty, but should also include the fact that the type of the formation has not been determined yet. The sensitivity analysis therefore examines one-order-of-magnitude changes in the effective diffusion coefficient and in the reference permeability of all hydrogeological layers.‡

Figure 21 shows the ^{129}I activity distributions after one million years for the reference case (middle row) and for diffusion coefficients and permeabilities reduced or increased by a factor of 10 (top and bottom rows, respectively).

Reduced diffusion leads to a more concentrated activity plume, with the bulk of ^{129}I remaining within the shale. The front between the plume and the uncontaminated groundwater is relatively sharp. By contrast, increasing the diffusion coefficient spreads the ^{129}I over a considerably larger volume. The concentration front reaches the near-surface aquifer

---

* As demonstrated below, advective transport may be beneficial for repository performance as it may promote mixing and plume dispersion, or make the plume bypass the compliance boundary.

† Diffusion coefficients and permeabilities tend to be positively correlated (i.e., formations with a higher permeability typically have higher effective diffusion coefficients, with porosity being the link between the two factors). This means that systems with low (or high) permeability and low (or high) diffusion coefficients are more likely to occur than systems with opposing parameter combinations. Such correlations may need to be included in future probabilistic performance assessments to properly calculate the likelihood of extreme parameter combinations—and correspondingly extreme outcomes. Accounting for parameter correlations also helps avoid risk dilution effects (see Section 4.6).

‡ For simplicity, the same permeability perturbation factor is applied to all hydrogeological layers. Once site-specific characterization data become available, this artificial correlation between permeabilities in different units will no longer be applied.

sooner, but at lower activity values because of the substantially enhanced dispersion and mixing of the plume. In summary, a low-diffusion environment leads to a smaller, more compact (i.e., higher average activity) radionuclide plume, whereas high diffusion leads to a larger plume with on average lower activity. Which of the two situations is beneficial clearly depends on other transport properties (specifically advection) as well as the selected performance metric and the location of the performance boundary (see discussion below).

Reducing permeabilities in the geosphere by an order of magnitude keeps the center of the ^{129}I plume near the disposal section of the drillhole repository. Increasing the geosphere permeabilities by a factor of 10 shows an upward migration of the plume center (driven by the overpressure from the deep saline formation, and the underpressure in the near-surface aquifer due to the continuous pumping). The horizontal flow component from the regional pressure gradient is also visible.

The relatively small differences between the high-permeability case and the reference case indicate that the system is diffusion dominated, at least for the reference diffusion coefficient and reference permeability.* Diffusion-dominance appears true specifically for the (low permeability) host formation, but is less pronounced for the overburden; the potable aquifer is advection-dominated. Advective flow patterns become apparent if the permeability is increased by an order of magnitude.

The influence of the different plume evolutions on peak annual dose is visualized in Figure 22. As expected, the smaller the effective diffusion coefficient, the later the plume arrives at the drinking water well, and the later the peak annual dose is reached. Because the well extracts radionuclides only from the edge of the plume, the higher-diffusivity case yields a higher peak dose (by approximately a factor of three) despite the lower average concentration of the plume. For the low-diffusivity case, the response of a sharper plume activity front arriving later and with a slower migration velocity leads to a peak dose that is almost identical to that for the reference case.

The response to different permeabilities is shown in Figure 23. As mentioned above, for the reference permeability as well as lower permeability values, the system is diffusion-dominated, thus yielding almost identical dose curves. If geosphere permeabilities are increased by an order of magnitude, peak dose is reduced considerably (by a factor of approximately 20). This is a result of increased mixing and dilution and partially of the plume's advective bypassing of the drinking water well. These effects are likely to be site-specific, i.e., for alternative configurations, where the compliance boundary† is downstream of the advective plume migration pathway, peak dose is likely to increase with increasing permeability.

---

* The same conclusion can be reached by noting the comparatively large differences seen when changing the diffusion coefficient over two orders of magnitude, while permeability is kept constant at its reference value.

† The compliance boundary can be defined as the location where the performance metrics are evaluated and compared to the regulatory standard; it is the spatial equivalence to the (temporal) performance period.

The system (even in its simplified, generic form) is rather complex, with dose estimates depending on two- and three-dimensional flow effects that lead to interactions between formations with different dominant transport processes. Furthermore, the resulting plume characteristics may have opposing benefits depending on the chosen performance metrics or the precise location of the performance boundary. This behavior is typical for most performance metrics that depend on the breakthrough curve, where the magnitude of the concentration values depends on timing, the strength of plume dispersion processes and the relative position of the observation point with respect to the plume center (i.e., whether the well extracts water from the advancing front, center, or receding tail of the plume).

This simple[*] sensitivity analysis also demonstrates that the influence of parameter changes on repository safety is difficult to assess without performing mechanistic simulations using a model that includes the salient features of the entire repository system without undue oversimplifications.[†]

[*] This is a local sensitivity analysis of only two adjustable factors, in which the parameters are changed one at a time, the other being kept fixed at its reference value. While non-linear effects along each of the parameter axes are evident (see Figure 21), no parameter interactions are accounted for. Global sensitivity analysis methods (see, e.g., Saltelli et al. 2008) can be used to study effects from non-linearity and parameter interactions.

[†] "Undue oversimplifications" are often driven by the need for computational efficiency (specifically that demanded by sampling-based probabilistic performance assessments). It is preferable to maintain high conceptual and numerical fidelity of the model—even at the expense of running fewer Monte Carlo simulations—to make sure key features and processes affecting the dose calculation are properly captured. Systematic errors introduced by oversimplifications directly propagate through the Monte Carlo analysis, rendering the resulting uncertainty estimates questionable. The modeling and analysis approach described in Section 4.5.1 attempts to avoid this pitfall.

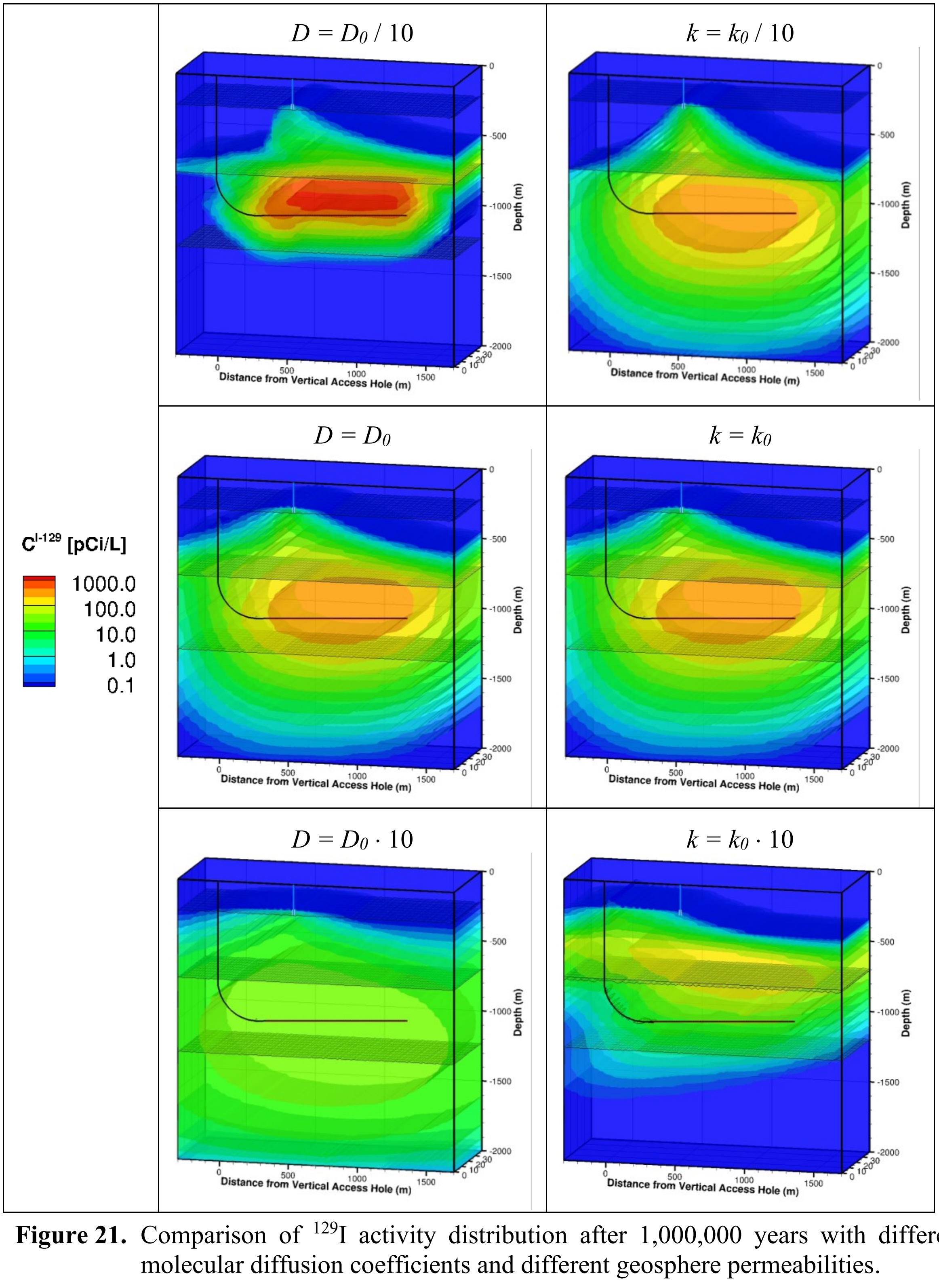

Figure 21. Comparison of ^{129}I activity distribution after 1,000,000 years with different molecular diffusion coefficients and different geosphere permeabilities.

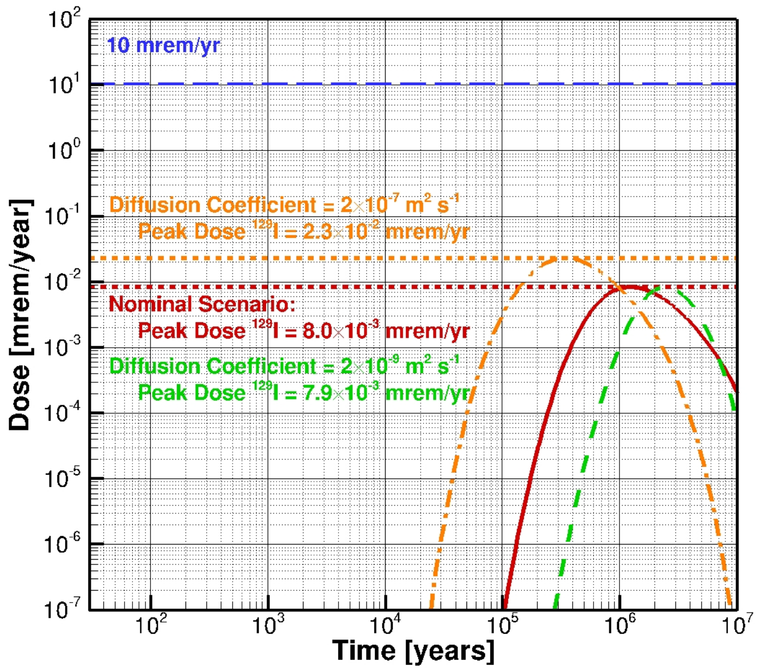

Figure 22. Comparison of annual dose from ^{129}I exposure with different molecular diffusion coefficients and different geosphere permeabilities.

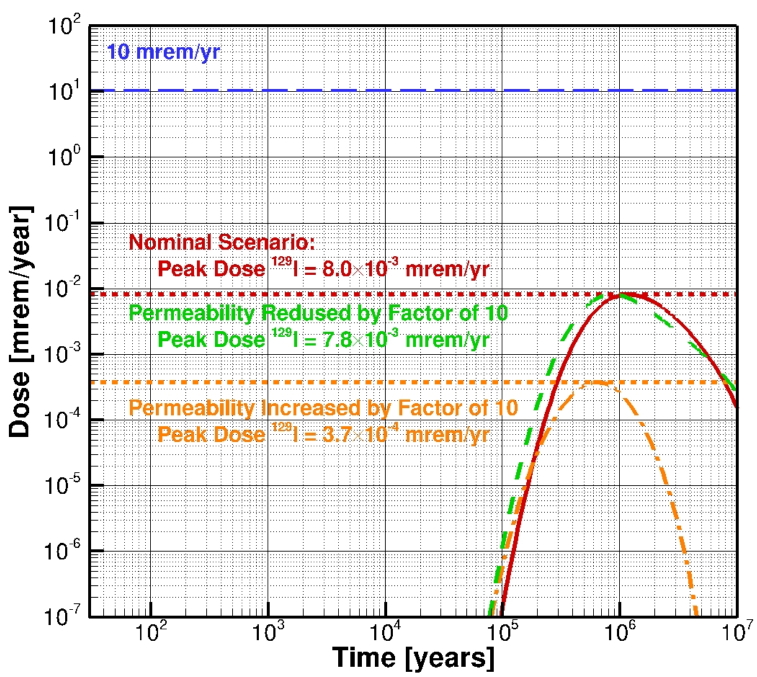

Figure 23. Comparison of annual dose from ^{129}I exposure with different geosphere permeabilities.

4.7.3.3 Overpressured or Underpressured Saline Formation

The pressure in the formation underlying the host rock (here denoted as a saline formation) determines the regional flow field, which may induce advective radionuclide transport in both downward or upward direction.

A downward vertical component can be expected if the repository site is located in a large-scale recharge zone, i.e., where topographic highs on the regional, basin, or continental scale lead to the recharge of deep aquifer systems (see, for example, Condon and Maxwell, 2015). This situation is likely beneficial for repository performance (unless the underpressure in the saline formation is caused by fluid extraction[*]). Conversely, an overpressured saline formation may lead to upward fluid flow and radionuclide transport. A deep formation may be overpressured naturally, e.g., by hydrothermal or igneous activities, by erosion and deposition of sediments,[†] by glacial loading[‡], or if located in a large-scale discharge zone.[§] Human activities (e.g., waste-water injection, geologic carbon sequestration, or the operation of an enhanced geothermal system (EGS)) may also pressurize deep formations, potentially on a large scale (see, for example, Zhou and Birkholzer, 2011; Celia et al., 2015).

Figure 24 illustrates the advective displacement of the ^{129}I activity plume depending on the pressure in the saline formation underlying the repository. In the underpressured situation (Figure 24a), the center of the plume is pulled towards the lower right corner, with its upper fringe being drawn into the drinking water well. In the overpressured situation, the center of the activity plume is vertically displaced from the host formation into the overburden (Figure 24b). In these simulations, advective plume migration is slow, with an approximate velocity of less than 500 m per one million years.

---

[*] Fluids may be extracted from deep saline formations by geothermal wells or wells installed for pressure management of a nearby geologic carbon sequestration project (Gonzalez-Nicolas et al., 2019).

[†] Large-scale geomorphological changes induce complex responses in both shallow and deep formations. Erosion (or deposition) leads to unloading (or loading) of the rocks' skeleton with associated pore volume and fluid pressure changes; the same processes also lead to changes in water table elevations and associated local and regional groundwater flow. Rapid sedimentation rates in marine environments can pressurize deposits.

[‡] Glacial loading induces to overpressures due to the compaction of the rock skeleton. However, it only leads to an upward pore pressure gradient if the compressibility of the saline formation is higher than the compressibilities of the overlying units. Over long time periods, the compression by glacial loading is partially reversed by the elastic component of decompression during glacial retreat and the associated unloading, inducing underpressures that may persist for a considerable time in low-permeability formations. While such cycling may keep the plume location—on average—at the same elevation, it increases the dispersion of the contaminant plume. Glaciation may also directly impact pore-water pressures and groundwater flow depending on the many factors that influence the glacier's liquid water content.

[§] Artesian pressures arise from the effects of differential relief of the recharge zone.

Figure 25 shows the annual dose curves for (1) the reference case with a slight overpressure of +2 bars is imposed on the lower right quarter of the model domain, for (2) a saline formation overpressured by +20 bars, and (3) a saline formation underpressured by -5 bars. Overpressurization by +20 bars—a value possible under natural conditions and also consistent with the carbon sequestration scenarios studied by Zhou and Birkholzer (2011)—leads to advective upward transport of radionuclides and increases the peak dose of the reference case (which exhibits an overpressure of +2 bars) from 8×10^{-3} to 5×10^{-2} mrem yr^{-1}. A slight underpressure (of -5 bars) leads to downward advective transport at a rate that is, however, smaller than the diffusive transport (which occurs in all directions). For this beneficial case, peak dose is reduced about seven-fold.

The sensitivity of advective radionuclide transport to changes in the magnitude and direction of the regional pressure gradient can be mitigated by siting the repository in a large-scale recharge zone, by avoiding locations with overpressures in underlying formations, or by selecting a host formation of sufficiently low permeability.

This sensitivity analysis indicates that it is worthwhile to study the state and evolution of the regional hydrological flow field, as is typically done either as part of the screening process during repository siting and subsequent site characterization efforts.

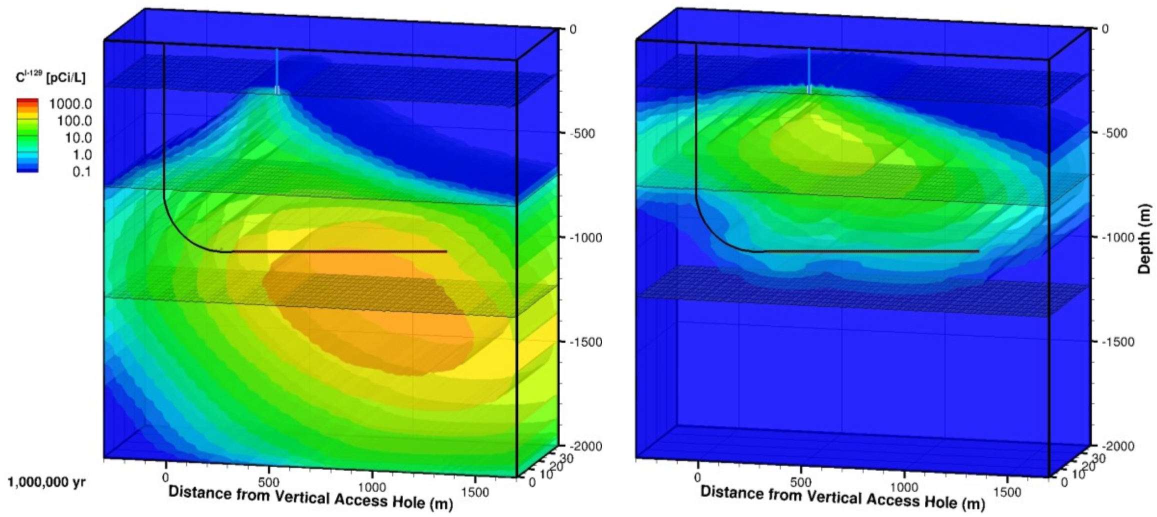

(a) (b)

Figure 24. Comparison of ^{129}I activity distribution after 1,000,000 years with saline formation being (a) underpressured by 5 bars, (b) overpressured by 20 bars.

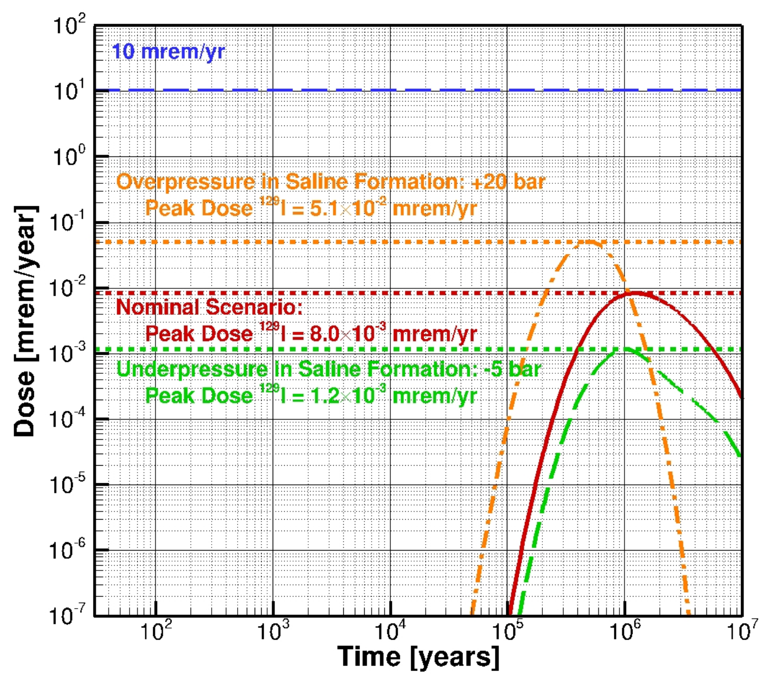

Figure 25. Comparison of annual dose from ^{129}I exposure with different pressures in underlying saline formation.

4.7.3.4 Depth

Repository depth is expected to be an important safety factor. In the reference scenario, a relatively shallow depth of the waste disposal section of 1.0 km was chosen. Drilling to greater depths is not considered a particular challenge.

In this sensitivity analysis, the depth of the horizontal disposal section was increased to 1.5 km. A new numerical grid was generated using the approach described in Appendix C. The hydrogeologic layers were the same as in the reference case, with the thickness of the overburden increased from 500 m to 1,000 m. The mesh and stratigraphic units are visualized in Figure 26.

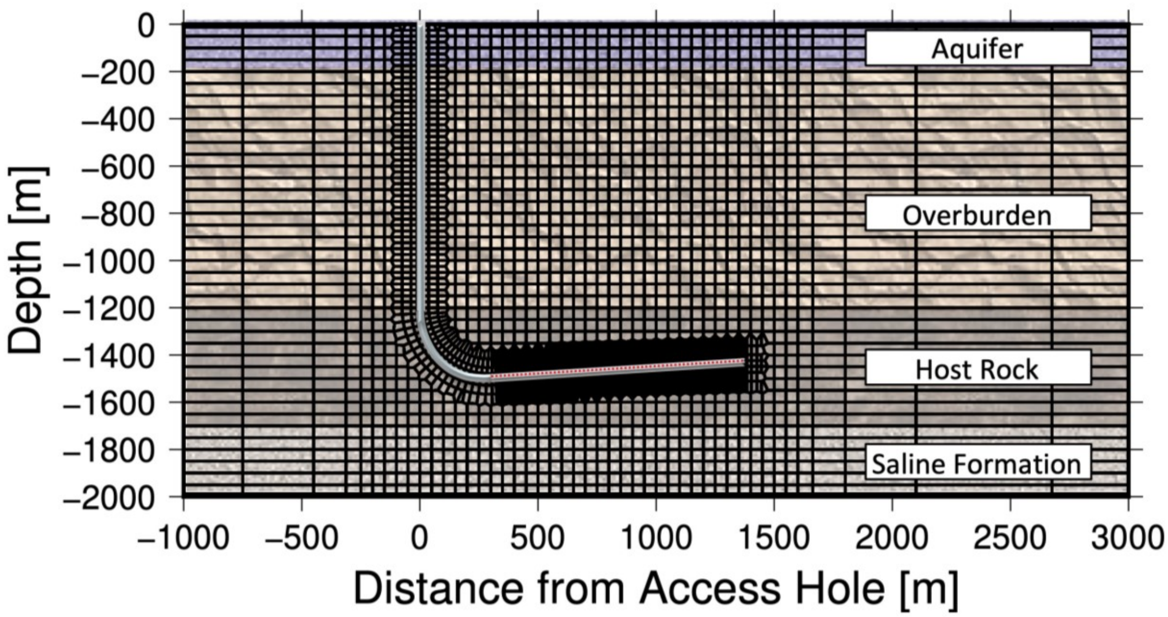

Figure 26. Numerical grid for a disposal depth of 1.5 km.

The ^{129}I distributions after 1.5 and 3.3 million years are shown in Figure 27; Figure 28 shows a comparison of the dose curves with the waste disposal sections at depths of 1.0 and 1.5 km. The greater depths leads to a longer travel distance and thus later arrival time at the drinking water aquifer. Radionuclide concentrations are lower because the plume is more disperse. Consequently, a 50% increase in depth leads to a reduction of peak dose by a factor of approximately three. Peak dose is reached after about 3.3 million years.

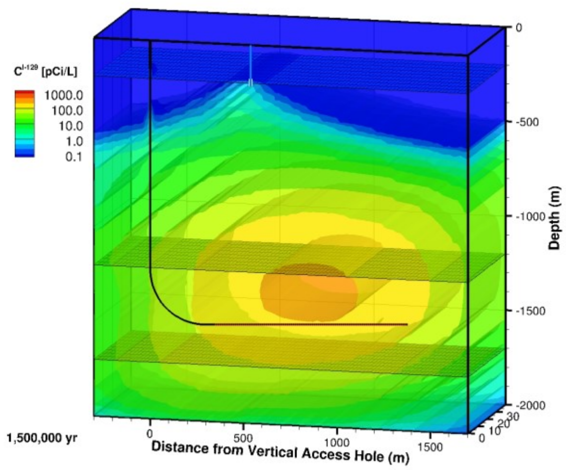

Figure 27. Distribution of ^{129}I activity after 1.5 and 3.3 million years with the disposal section at a depth of 1.5 km.

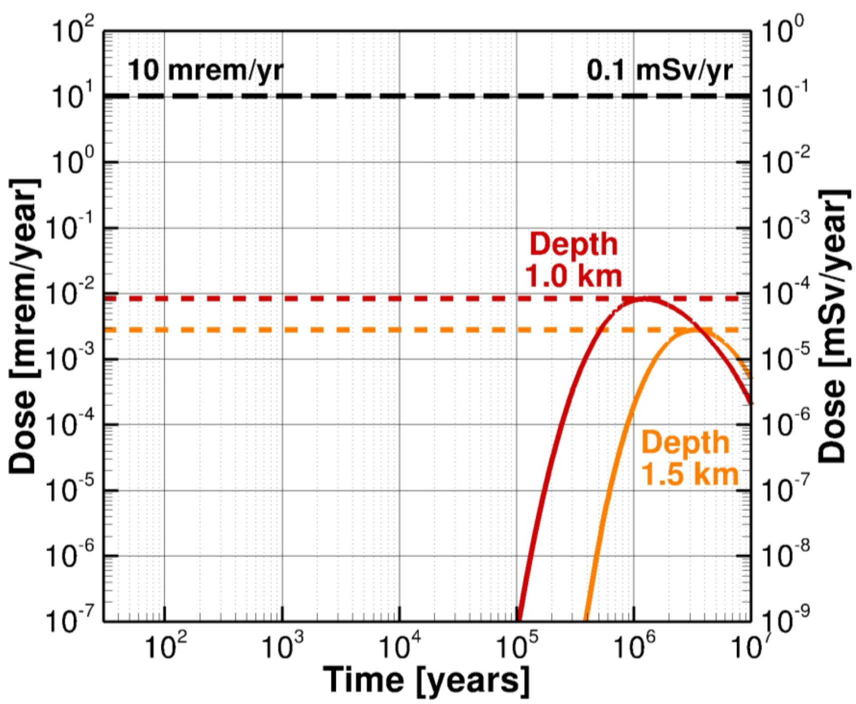

Figure 28. Comparison of annual dose from ^{129}I exposure for a disposal depth of 1.0 km and 1.5 km.

4.7.4 Probabilistic Safety Analysis

As discussed in Section 4.6, the calculated performance metrics of Table 1 are uncertain because of uncertainty in the model's input parameters, which represent material properties affecting the flow and transport of fluids, radionuclides and heat through the repository system, but also initial and boundary conditions as well as spatial variability in the porosity field. Probability distributions are specified for 38 individual parameters and parameter groups. The chosen probability distributions (uniform, triangular, log-triangular, normal, or log-normal) as well as their statistical parameters (lower and upper bounds, mean or mode, and standard deviation) are summarized for each parameter in Appendix B.

These distributions either represent epistemic uncertainty or a range of possible property values that reflect design alternatives (e.g., regarding the yet unspecified backfill material). Latin Hypercube Sampling (LHS)* is employed to sample these probability distributions. Design parameters (such as properties of the engineered barrier system, initial radionuclide inventory, or pumping rates) are typically represented by triangular, log-triangular, or uniform distributions, whereas uncertain properties of the natural barrier system are represented by normal or log-normal distributions. If needed, the normal or log-normal distributions are truncated to respect the physical bounds of the parameter. Histograms of the sampled parameters (for a sample size of $n_{MC} = 400$) are shown in Figure 29, demonstrating that the prescribed, theoretical distributions of Appendix B are well reproduced by the histograms of the actual values sampled by LHS.

Four hundred independent† samples of the parameters or parameter groups are taken and randomly combined to yield 400 realizations to be examined by the Monte Carlo‡ uncertainty propagation analysis. Each realization also has its unique seed number to be used by the internal random number generator. Before each Monte Carlo simulation, a new, spatially correlated, random porosity-modifier field is generated and mapped onto the numerical grid to include the impact of unidentifiable spatial variability of this key parameter on the simulation results. The resulting porosity fields are unique not just because of the random number generator used in the sequential Gaussian simulation process, but also because the reference porosity as well as the parameters of the underlying spherical semi-variogram (i.e., correlation length, sill value, and anisotropy ratio)§ are randomly sampled

---

* See footnote on Latin Hypercube Sampling in Section 4.6.

† See footnote on parameter correlations in Section 4.6.

‡ See footnote on Monte Carlo methods in Section 4.6.

§ The spherical semi-variogram is defined by the following equation:

$$\gamma(h) = c \cdot sph\left(\frac{h}{a}\right) = \begin{cases} c \cdot \frac{3}{2} \cdot \frac{h}{a} - \frac{1}{2} \cdot \left(\frac{h}{a}\right)^3, & h \le a \\ c, & h > a \end{cases}$$

where h is the lag (or separation) distance, a is the correlation length (or range), and c is the sill value (related to the variance of spatially uncorrelated sample values), which can be anisotropic according to the orientation of the separation vector $\boldsymbol{h}$. Each seed number (the starting number of a random number generator) produces a unique series of pseudo-random real values.

from their respective probability distributions. For illustration, Figure 30 shows a few realizations of the porosity field, generated for three correlation lengths and the seed numbers.*

Each of the 400 Monte Carlo simulations is run to the end time of 10 million years. The calculated doses for each of the four considered radionuclides are determined and summed up to give the total dose. Furthermore, the time when peak dose occurs is extracted. Histograms are developed for these two composite performance measures (peak dose and peak-dose time).

The results are displayed in Figure 31. The red curves show the total dose transients of the 400 Monte Carlo realizations. Calculated peak dose values range widely (over approximately six orders of magnitude). However, only peak doses at the high end of the distribution are of interest. Just 5% of the realizations yield peak dose values that are higher than 0.1 mrem yr^{-1}; the maximum peak dose obtained in this probabilistic analysis is 0.5 mrem yr^{-1}. These highest values are lower than the typical dose standard of 10.0 mrem yr^{-1} (indicated by the horizontal, orange line) by a factor of 20 or more. The light blue curve is the total dose of the realization that corresponds to the median peak dose, which has a value of less than 0.01 mrem yr^{-1}. This curve is essentially identical to the curve obtained with the base-case parameter set for the nominal scenario (see Figure 8).

The spread of first arrival times† (between approximately 10,000 years and more than 5 million years) is considerable, but of little relevance for safety, which is mainly characterized by peak dose rather than travel time. The earliest time when peak dose is reached is approximately 100,000 years; the median is at about 1.5 million years. A few realizations do not reach a peak dose within 10 million years (i.e., the dose curve is still rising at the end of the simulation period); however, the trajectories of these curves suggest that the peak doses of these realizations (once they are reached in the far distant future) would be very low.

This initial probabilistic safety analysis—conducted without the need for additional abstractions of the mechanistic flow and transport model—indicates that while the calculated annual dose is uncertain, the peak dose—even for the most unfavorable parameter combinations considered—remains well below the typical dose standard of 10 mrem yr^{-1} (0.1 mSv yr^{-1}).‡ For the generic conceptual model considered here and its numerical implementation, and for the assumptions made about the distributions of uncertain and variable input parameters, the uncertainty analysis does not invalidate the conclusions of the deterministic nominal scenario, which appear to be reasonably robust.

---

* The range of porosity variability used in the probabilistic analysis is significantly more pronounced than shown in Figure 30, because the porosities are further modified by randomly sampled values for reference porosities, sill values, and anisotropy ratios.

† "First arrival" is defined here as the time when the total dose first exceeds the somewhat arbitrary value of 10^{-7} mrem per year, i.e., eight orders of magnitude below a typical dose standard of 10 mrem yr^{-1}.

‡ See, for example, Becker et al. (2009; Table 5.8).

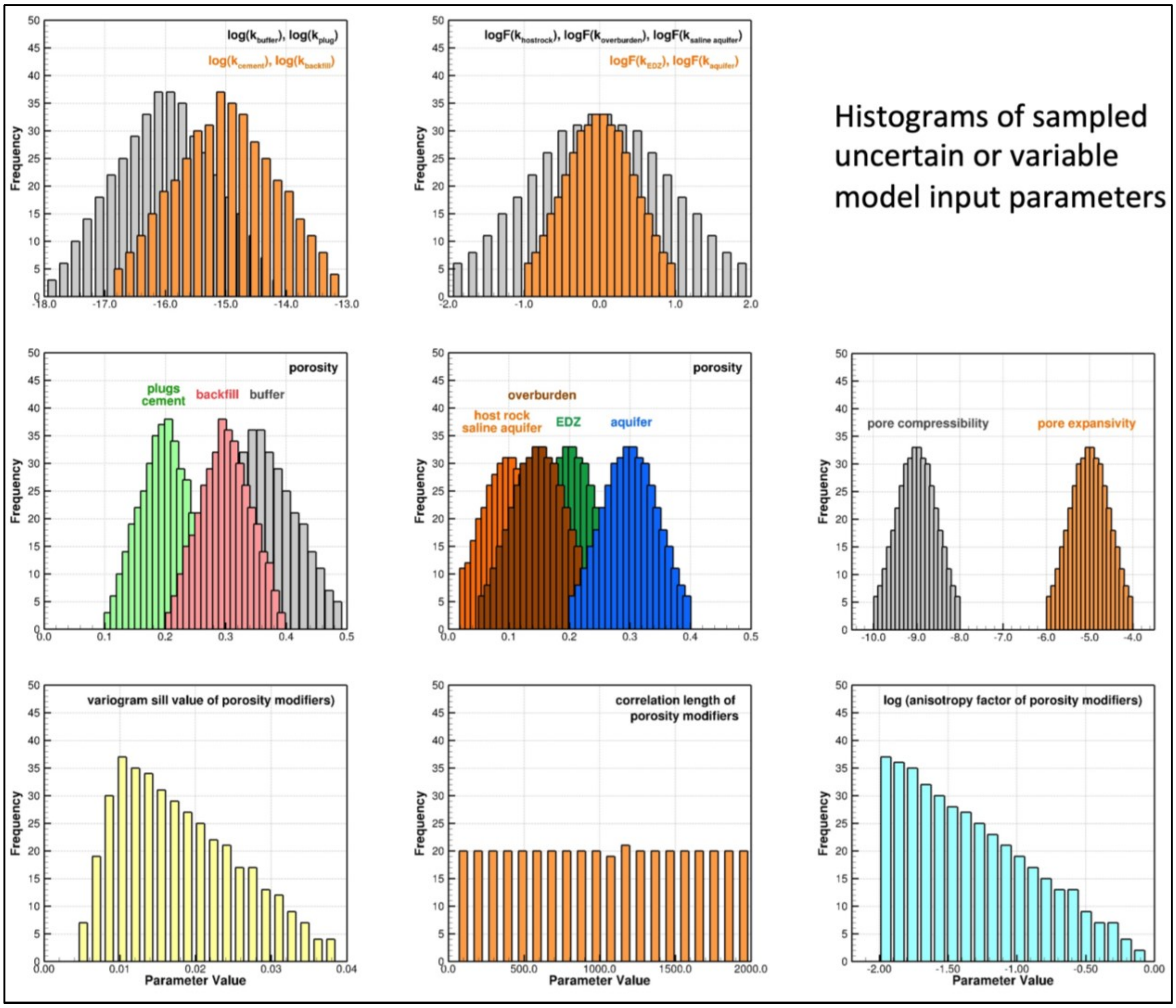

Figure 29. Sampling histograms of input parameters.

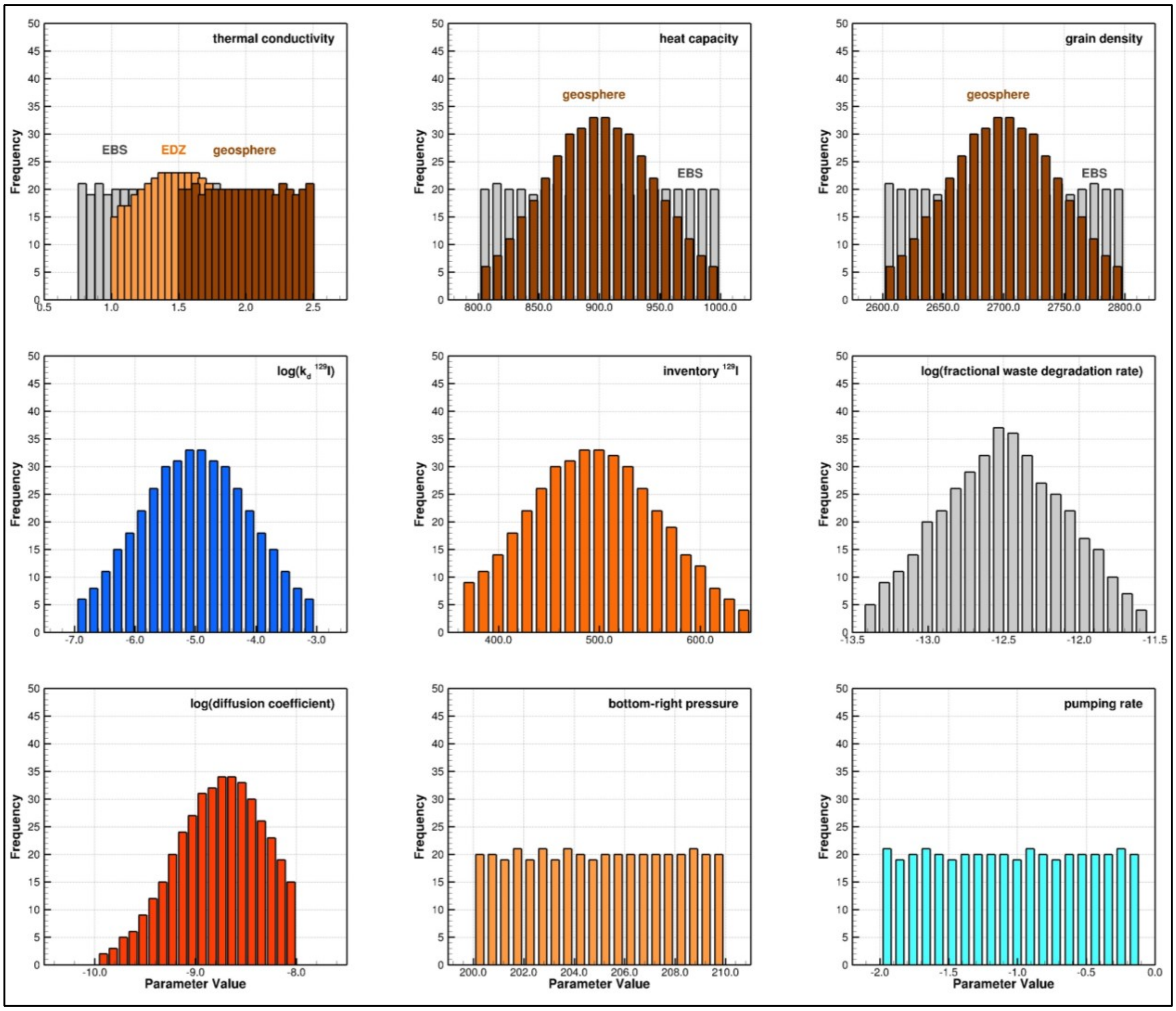

Figure 29 (cont.). Sampling histograms of input parameters.

#	corr. length = 50 m	corr. length = 500 m	corr. length = 2,000 m	
1	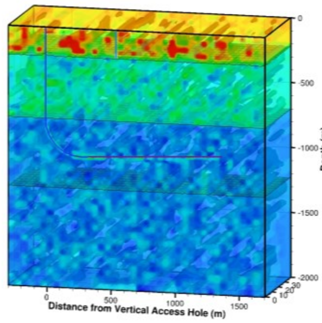	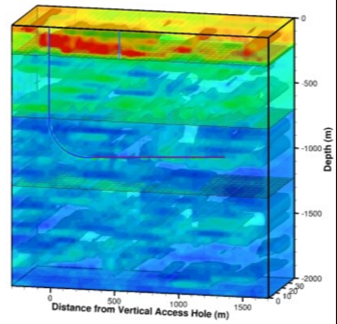	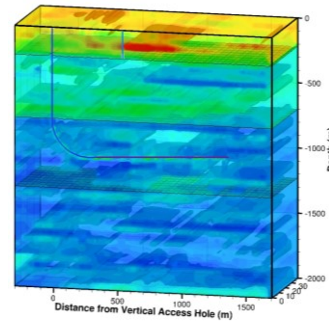	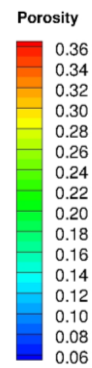
2	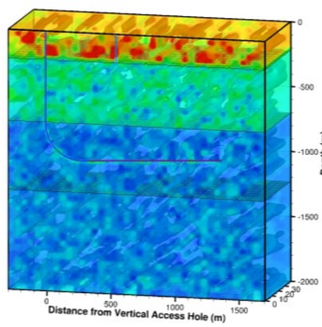	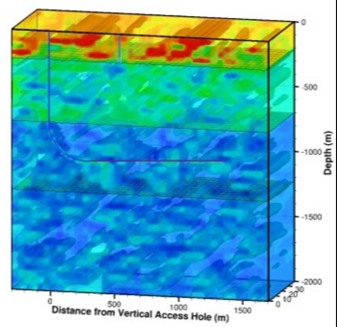	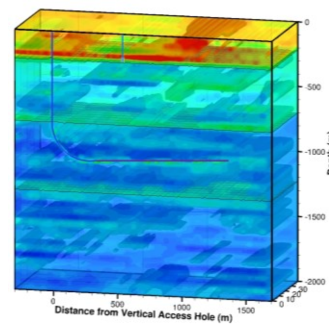	
3	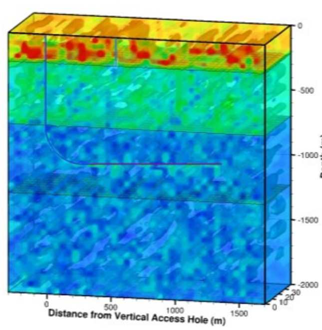	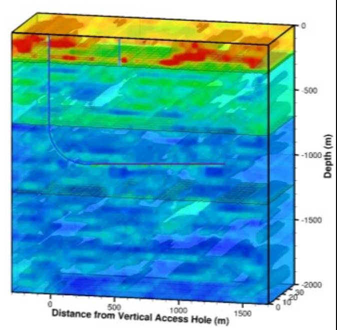	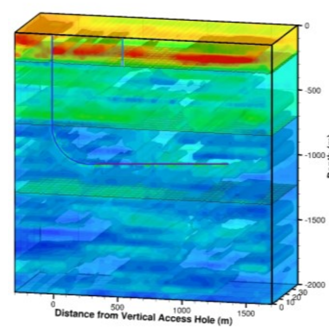	

Figure 30. Porosity field realizations for three correlation lengths and three seed numbers of random number generator.

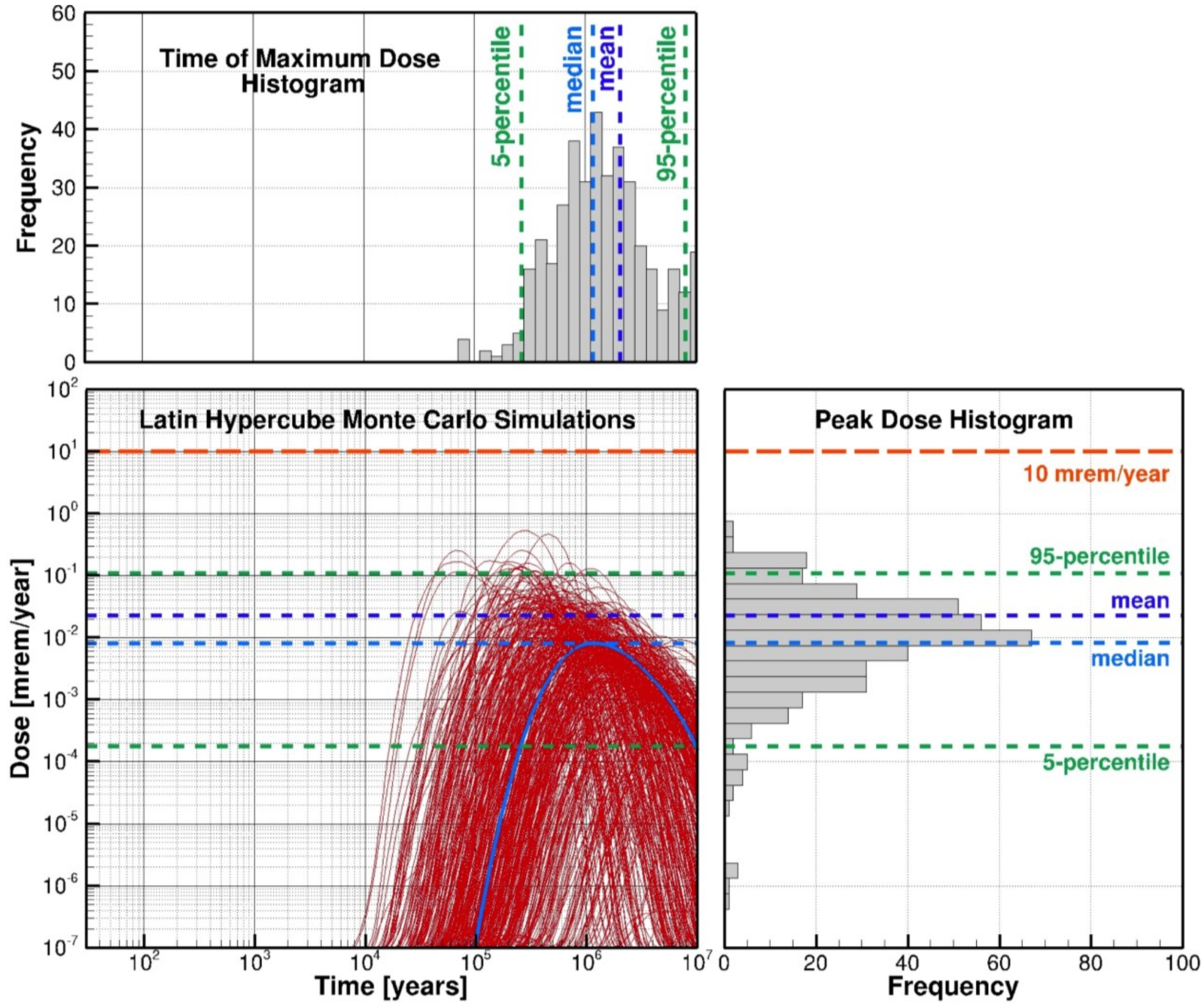

Figure 31. Probabilistic dose based on 400 Monte Carlo simulations.

4.7.5 Disruptive Scenarios

Two disruptive event scenarios are considered as part of this generic analysis: (1) fault (re)activation caused by a seismic event, and (2) early waste canister failure. Other disruptive scenarios (such as igneous events and human intrusion) will be evaluated in subsequent safety analyses once site-specific conditions are known and the regulatory requirements regarding human intrusion for a drillhole repository have been clarified.

4.7.5.1 Seismic Fault Activation Scenario

The fault activation scenario is described in Section 4.3.3.2. To summarize, it is assumed that a large tectonic or seismic event causes the activation (or reactivation) of a new (or existing*) sub-vertical fault and generates an associated fracture zone that intersects the central part of the repository's disposal section. The fault extends from the deep strata to the aquifer and reaches the surface near the location of the drinking water well (see Figure 32). The seismic event occurs shortly after repository closure. The fault and fractures remain highly conductive throughout the performance period.

At its center, the fault has a vertical permeability of 10^{-13} m^2, which tapers off (using a spherical function) towards the edge of the fracture zone, where it reaches the respective permeability of the formation it cuts through.† The Fracture zone is 25 m wide on either side of the fault line. Porosity is treated in an analogous manner, with a reference value of 0.1 at the center of the fault, which represents the transport porosity along the fast-flow pathways within the fault zone. All other hydrologic, thermal, and transport parameters as well as initial and boundary conditions are identical to the base values of the nominal scenario.

* This assumes that the existing fault remained undetected during site characterization.

† See Section 4.5.8 for additional comments on this conceptualization of the fault.

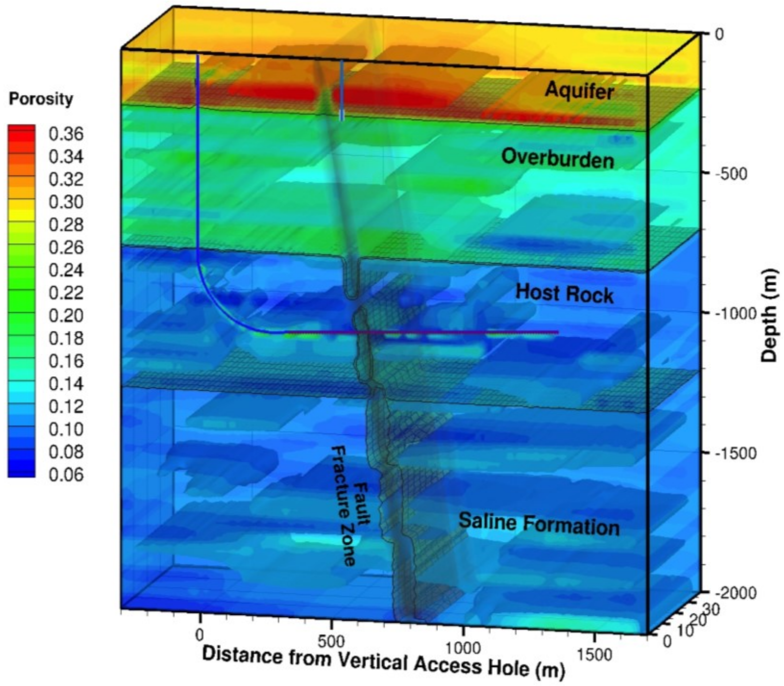

Figure 32. Hydrostratigraphy and porosity distribution with subvertical fault intersecting the repository's disposal section and extending to the aquifer.

Figure 33 visualizes the migration of the ^{129}I plume* for the seismic fault activation scenario. The activity evolution shows that the fault acts as a preferential fast-flow pathway for fluid, which is slightly pressurized from the overpressure in the saline formation. Radionuclides are thus transported advectively through the fault and associated fracture zone towards the near-surface aquifer. Advective fluid flow is also visible below the repository, where uncontaminated brine enters the shale formation, flushing ^{129}I upwards, and eventually dividing the diffusive plume into two parts.

* The discussion focuses on ^{129}I because it is the dominant contributor to peak dose.

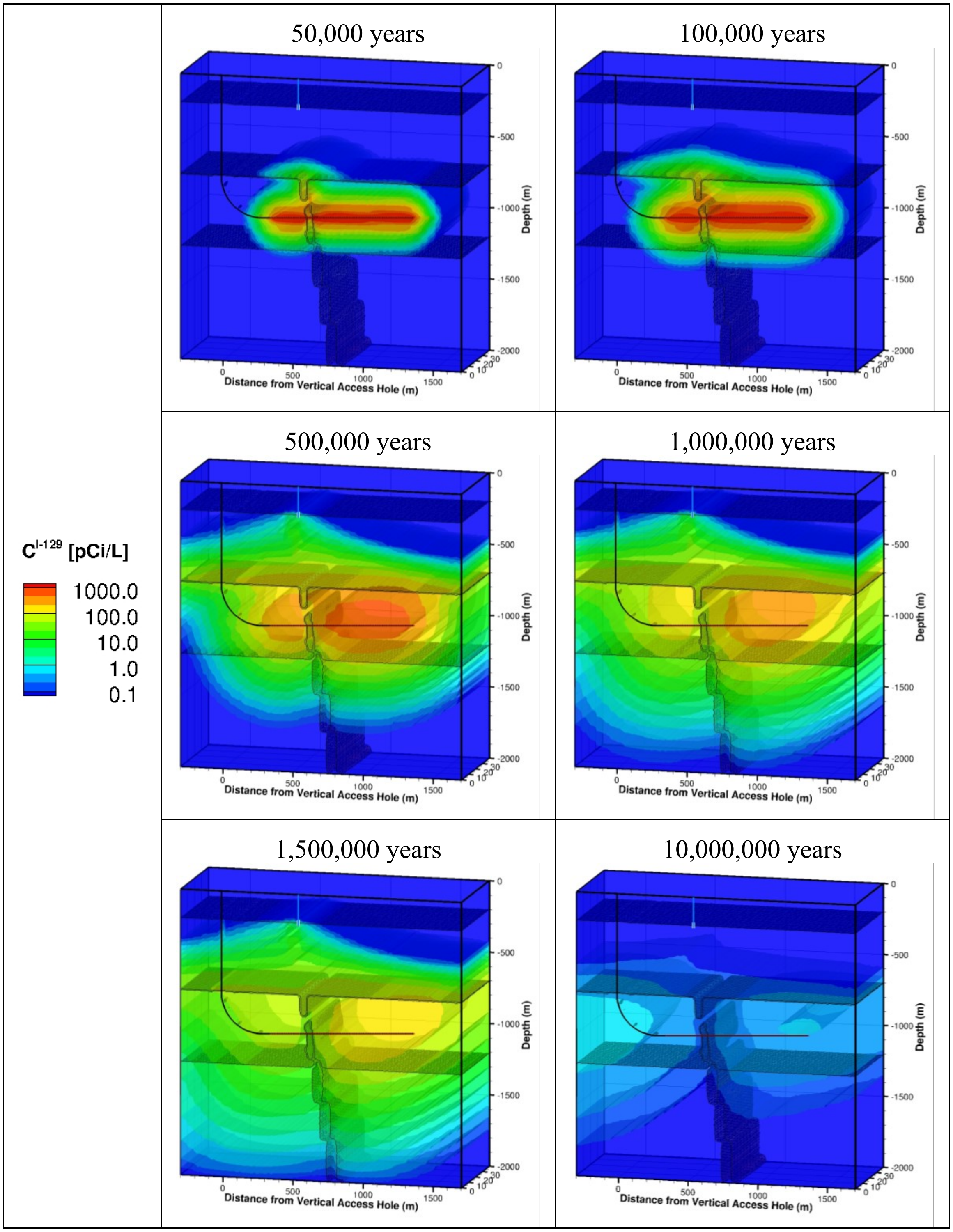

Figure 33. Simulated ^{129}I activity distribution throughout repository system with subvertical fault intersecting disposal section of the repository.

Finally, it is assumed that fault displacement ruptures the waste container that is directly intersected by the fault. However, early radionuclide releases from this single waste package can be ignored, and other waste packages are not directly affected by the seismic event.*

Figure 34 shows the dose curves with and without a fault. As expected, preferential flow and radionuclide transport along the fault leads to an earlier arrival of ^{129}I in the water supply system and an earlier peak-dose time. The peak dose of 1.3×10^{-2} mrem yr^{-1} is higher than that of the nominal scenario by a factor of 1.6, but still almost three orders of magnitude below a typical dose standard. In comparison to the uncertainty range of the peak dose determined by the probabilistic safety analysis (see Section 4.7.4), the increase in dose due to fault (re)activation is very small and statistically not significant.

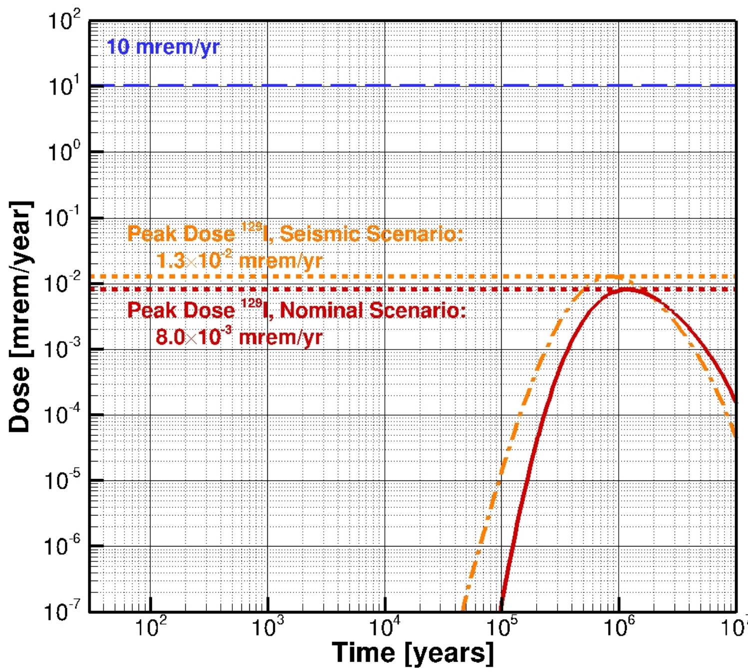

Figure 34. Comparison of annual dose from ^{129}I exposure with and without subvertical fault intersecting disposal section of the repository.

---

* These assumptions are considered justifiable for this generic case, because (a) the assumptions are irrelevant if the seismic event occurs any time after 10,000 years, which is the time when the canisters are breached by corrosion even without a disruptive event, (b) the waste form's barrier function may only be slightly affected even if the canister is breached, and (c) the inventory of a single canister is sufficiently small to not significantly affect the total dose. The impact of early canister failure on dose is further discussed in Section 4.7.5.2.

Figure 35 shows the maximum ^{129}I activity in the aquifer with and without the presence of a fault; the activity in the canister is also plotted for reference. The average activity in all the canisters (which is controlled by waste form degradation) is unaffected by the fault, i.e., essentially the same source term applies to both scenarios. As expected, the point where the maximum activity is observed coincides with the location where the fault enters the aquifer (see Figure 33). While the activity is higher than that of the nominal scenario, the impact on dose is smaller than the ratio of the maximum aquifer activities, unless drinking water were extracted directly and exclusively from the fault (i.e., without further dilution by less contaminated groundwater from the aquifer).*

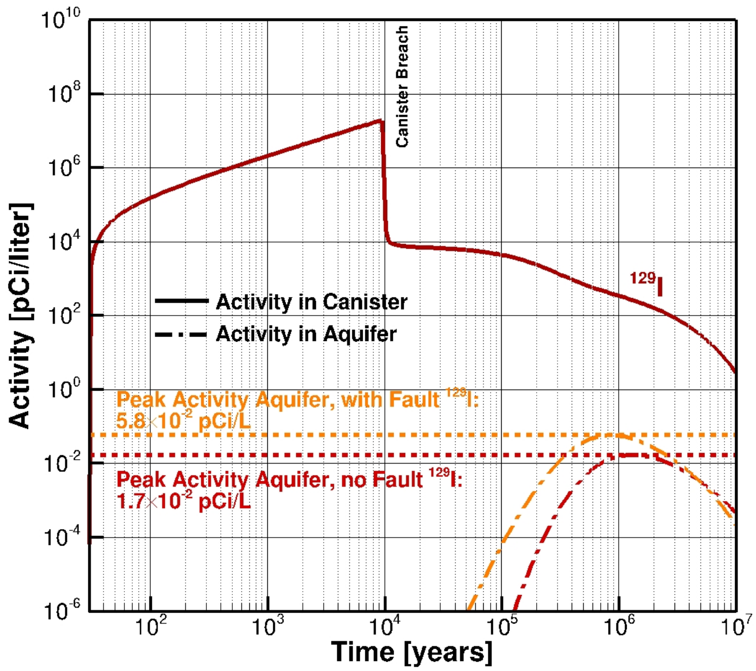

Figure 35. Comparison of ^{129}I activity with and without subvertical fault intersecting disposal section of the repository.

This initial evaluation of the disruptive seismic event scenario suggests minor impacts on repository performance. The scenario needs to be refined using site-specific information about the large-scale, tectonic processes, the regional stress field, the structure and properties of the formations, and other factors that may be used to assess the probability and impact of a seismic event occurring at or near the disposal site.

* Limiting extraction of drinking water from the location immediately above the intersection of the fault with the aquifer without dilution by less contaminated water from the aquifer is physically and technically unrealistic.

4.7.5.2 Early Canister Failure Scenario

The early canister failure scenario is described in Section 4.3.3.3. As a bounding calculation, it is assumed that radionuclide containment by the containers (and casing) fails immediately after repository closure and affects all canisters. This early failure scenario is implemented by setting the permeabilities and diffusivities of the canisters and casing to constant values that are identical to those of the surrounding backfill material.* Note that the waste form is assumed to retain its retention properties, i.e., radionuclides are released at the same rate as determined by the fractional waste degradation rate and (as applicable) solubility limits of the nominal scenario (see Section 4.5.5).

Figure 36 shows the impact of early canister failure on peak dose. Peak dose is only very slightly higher as a result of the earlier release of the radionuclides, insignificant if compared to the prediction uncertainty as evaluated by the probabilistic uncertainty propagation analysis of Section 4.7.4, but also relative to the difference between the calculated peak dose and the typical dose standard value of 10 mrem yr^{-1}.

The low influence of early canister failure on peak dose can be explain by containment time (assumed to be 10,000 years) which is very short compared to the time in takes radionuclides to migrate from depth through the geosphere to the exposed individual. It is also a result of the cautious assumption regarding corrosion rate made in the nominal scenario.

The early canister failure scenario suggests that safety of a deep horizontal drillhole repository is mainly provided by the natural barrier system, which is effective due to the depth of the repository and its overall configuration. This lowers the requirements that each component of the engineered system has to fulfill regarding its barrier function. The main engineered barrier is provided by the confinement of radionuclides in the stable waste form. Nevertheless, as demonstrated in Section 4.7.3.1, even if the entire inventory is mobilized at the time of repository closure, the peak dose remains very close to that calculated by the nominal scenario.

* In the nominal scenario, these permeabilities and diffusivities increase as a function of time; they exhibit a discrete jump after 100 and 10,000 years to reflect the onset of perforation of the casing and canisters, respectively (see Section 4.5.7).

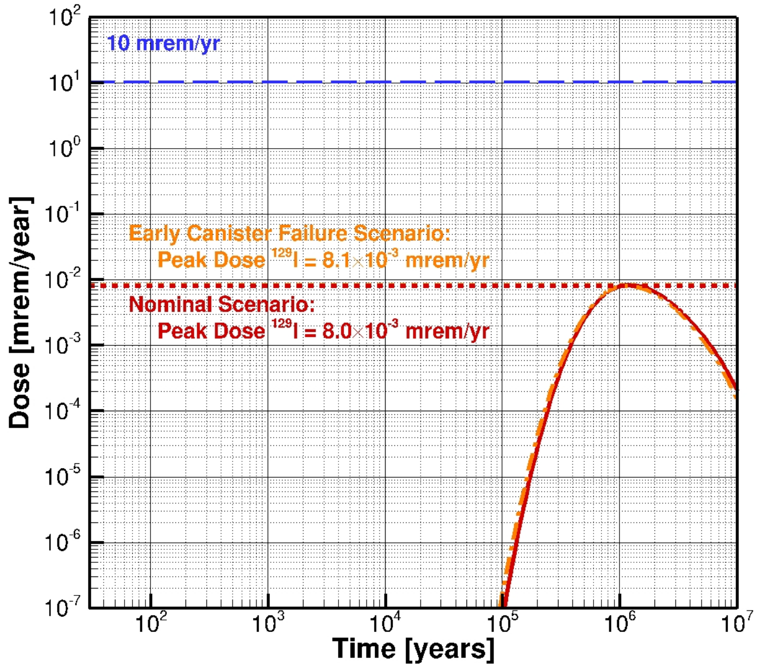

Figure 36. Comparison of annual dose from ^{129}I exposure for nominal scenario and early canister failure scenario.

5 Integration of Safety Arguments

5.1 Summary

The deep horizontal drillhole disposal concept consists of a system of multiple engineered and natural barriers. The performance of this barrier system with respect to waste isolation from the accessible environment has been quantitatively evaluated using numerical modeling and associated safety-analysis methods as described in Section 4. The disposal concept has been evaluated for a relatively wide range of conditions and alternative system evolutions. Moreover, it has been shown that the insights gained from the analyses are valid even if accounting for considerable variability and uncertainty in key factors that potentially affect repository performance.

The evaluation of the performance measures for the nominal scenario suggests that radioactive waste disposed in a horizontal drillhole repository is sufficiently isolated from the accessible environment. For the given assumptions, the maximum radiation exposure of an individual is likely far below regulatory dose standards, despite making cautious assumptions about the properties of the engineered and natural barrier systems. Radionuclide releases from the repository and transport rates along potential migration pathways are exceedingly small, leading to very low levels of contamination in the geosphere and specifically in the near-surface aquifer. Finally, perturbations due to repository construction and operation as well as post-closure thermal loading are small to moderate and are unlikely to induce detrimental effects that jeopardize the integrity of the engineered or natural barrier systems.

5.2 Main Arguments in Support of Safety Case

The deep horizontal drillhole disposal concept has a number of attributes that intrinsically support the safety case. The following is a list of safety arguments that can be made even for a generic repository design and host formation:

- *Depth* – The great depth of the repository effectively isolates the radioactive waste from the accessible environment. The total thickness of the overlying formations protects the host rock and repository from the influence of dynamic processes occurring at and near the land surface, and leads to long transport distances to the accessible environment, associated with long radionuclide migration times and large fluid volumes available for dilution. Careful siting and great disposal depth make it unlikely that the repository will be exposed to disruptive events and to processes unfavorable to long-term stability. Moreover, a great depth considerably decreases the likelihood of inadvertent human intrusion because of the low economic viability of recovering natural resources and the low likelihood of conflict with future infrastructure projects. Depth also poses high technical and economic barriers to discourage the malicious retrieval of the waste. Great depth in combination with the geologic stability and fluid isolation in the host rock and underlying formations represent the essence of geologic waste disposal, as described, for example, in DOE (1980) and NEA (1995).

- *Compact Geometry* – The repository has a compact geometry but a locally lower waste density. The small diameter of the disposal drillhole reduces the size of engineered barrier components, simplifying their construction and, consequently, increasing their robustness. The cross-sectional area available for potentially preferential fluid flow and radionuclide transport along the drillhole and excavation disturbed zone is substantially smaller than in a mined repository. The relatively low waste density in the linear drillhole arrangement distributes heat production and radionuclide releases. Compartmentalization of the waste in individual, unconnected drillholes within modular, geographically separated drillhole repositories decreases the consequences associated with disruptive events.
- *Orientation* – Waste is emplaced in the horizontal disposal section of the drillhole, which extends laterally for a considerable distance from the vertical access borehole. The horizontal separation distance from the waste to the vertical access hole reduces the potential that radionuclides migrate upwards to the biosphere. Moreover, the driving forces for radionuclide transport along the drillhole would need to have components that are oriented in two directions: (1) a horizontal component aligned with the drillhole and pointing towards the access hole rather than towards the dead-end of the disposal section, and (2) a considerable vertical component, pointing upwards. It is unlikely that natural gradients or repository-induced effects, such as thermally driven buoyancy (see discussion below), generate this particular gradient pattern, i.e., where driving forces are aligned with the orientation of the drillhole as a potential migration pathway. The repository is strictly linear. More complex, two-dimensional repository layouts (consisting of arrays of disposal tunnels, which are linked to each other and to the surface through access ramps, connection tunnels and ventilation shafts) provide additional opportunities for circulation or through flow of potentially contaminated water (even if backfilled). Because each individual drillhole terminates in a dead-end, axial water flow rates are strictly limited by the small permeability of the host formation.
- *Potential Pathway along Access Hole* – Access to the disposal section needed for waste emplacement occurs through the vertical and curved sections of the drillhole. This access structure is a potential pathway for radionuclides back to the biosphere. However, the repository layout and its design drastically reduce the risk that the access structure becomes a preferential transport pathway for radionuclides. These inherent design features include: (a) the cross-section of the access structure is small[*]; (b) the access structure is long due to the depth of the repository; (c) the vertical access structure is spatially offset from the horizontal waste disposal section; (d) the orientation of the access structure is orthogonal to that of the

[*] The diameter of the drillhole and associated excavation disturbed zone is smaller than that of a typical mined repository by a factor of at least 10, reducing the cross-sectional area by a factor of at least 100. However, this factor needs to be reduced by the ratio of the number of drillholes needed to store an equivalent amount of nuclear waste, which is also a function of the length of the disposal section.

disposal section, requiring a peculiar pattern of the driving force to enable radionuclide transport from the waste canisters to the land surface; (e) the access hole can be effectively backfilled and sealed; (f) drilling leads to a small excavation disturbed zone; (g) the excavation disturbed zone is often less permeable than the surrounding formation or it can be sealed*; and (i) the access structure can be monitored during the performance evaluation period.

- *Confinement and Containment* – The stability of the waste form (consisting of uranium dioxide pellets) in the expected geochemical environment assures long-term encapsulation of radionuclides. Many radionuclides released from the slowly degrading waste matrix remain relatively immobile due to a low solubility limit or geochemical retardation processes. Moreover, the high-integrity waste canisters protect the waste form and provide additional containment. Even if released from the waste containers, migration through and away from the engineered barriers is slow. During confinement within the engineered barrier system and the immediately surrounding rock, much of the inventory's activity will have decayed even before migration towards the accessible environment and associated diffusion, dispersion and dilution processes are initiated.
- *Low Permeability* – The targeted host rock exhibits a low hydraulic conductivity so that movement of dissolved radionuclides is predominantly by diffusion rather than advection. This attenuates and limits the concentration of radionuclides in the geosphere. Repository-induced and natural fractures are expected to have low transmissivity due to the self-sealing capacity of argillaceous formations, providing a strong natural barrier to radionuclide transport. In the absence of transmissive fractures and in the presence of a sufficiently high clay content, argillaceous formations tend to be relatively homogeneous, reducing uncertainties in safety assessment due to limited spatial variability. Low permeability prolongs travel times, allowing radionuclides to decay, which further and considerably reduces activity in potable groundwater.
- *Reducing Environment* – In general, the geochemical conditions in a deep, saturated host rock and surrounding formations are reducing. Such conditions decrease or inhibit the dissolution of spent fuel pellets, offset potential deleterious effects of radiolysis, and favor the immobilization of several long-lived transuranic and fission product radionuclides in the waste form. The latter occurs through formation of relatively insoluble secondary phases, and through preferential adsorption on reducing minerals, thereby enhancing their retardation during transport through the engineered and natural barrier system. Reducing conditions also afford the opportunity to design long-lasting engineered barriers that could isolate the waste from

* Reduced permeability is characterized by a so-called "positive skin factor," a parameter that can be determined through standard hydraulic testing. An excavation disturbed zone of increased permeability exhibits a "negative skin factor"; such a zone can be plugged using permeation grouting. The excavation disturbed zone around a hole drilled in shale may self-seal (Fjær et al., 2016).

chemical attack by saline waters until most fission-product radionuclides have decayed to insignificant levels.

- *Saturated, High-Pressure Environment* – The repository is located in the saturated zone far below freshwater aquifers. Critically, the repository is never desaturated, severely underpressured, or exposed to significant oxidizing conditions* even during the construction and operation phases. The high *in situ* pressure prevents boiling of water during the thermal period. It also inhibits phase separation of gaseous corrosion products or at least minimizes the volume of any evolving free gas phase, thereby preventing the development of continuous gas flow paths. No transport of volatile radionuclides through the unsaturated pore space to the atmosphere occurs.
- *Multi-Barrier Concept* – The safety and security of the repository is strengthened by a multi-barrier concept, which is the combination of natural barriers (consisting of the host rock and surrounding formations) and the engineered barrier system, which includes ceramic UO_2 fuel pellets, zirconium alloy cladding of the assemblies, any material that fills the space within the canisters, canisters made of corrosion-resistant alloy, buffering material between the canisters and the casing, carbon steel casing, cement or other filling between the casing and the drillhole wall, backfilling and plugs that seal the horizontal disposal section and vertical access hole. The engineered barrier system protects the repository from external disturbances, provides a suitable environment for the canisters and waste form, and serves as a barrier to radionuclide release and transport away from the repository. The compactness of the relatively small-diameter access and disposal sections of the drillhole repository strengthens these engineered components and drastically reduces their vulnerability. The great depth of the drillhole repository and its sub-horizontal orientation along the bedding of a suitable argillaceous host formation makes the geosphere a reliable natural barrier system, drastically reducing the requirements that otherwise need to be imposed on the barrier functions of the engineered components. The drillhole may thus be designed for optimal safety during waste emplacement and the early post-closure period, without having the burden to take on long-term safety functions. Finally, the multi-barrier system provides passive safety, i.e., once the disposal facility has been closed, no further human action is required.
- *Perturbations* – Construction and operation of a drillhole repository is considerably less intrusive than that of a mined repository. The host rock and its environment are much less perturbed—hydrologically, mechanically, and chemically. In addition to preserving the integrity of the host rock, this has considerable advantages regarding characterization of the near field. Not only is the excavation damage zone smaller

* Radiolysis can induce a net oxidation in the vicinity of the waste, because the hydrogen generated by this process is transiently inert, and diffuse away from the waste, leaving a net increase in oxidation state.

and less disturbed, its hydraulic and transport performance can be readily tested.* Furthermore, observations and measurements made in the disposal section do not need to be corrected or extrapolated to vastly different post-closure conditions, as is often the case in a depressurized, ventilated, and mechanically damaged large-diameter waste emplacement tunnel. This reduction in complexity makes host-rock characterization more accurate and robust. Reduced perturbation of the natural barrier system also reduces the requirements for the components of the engineered barrier system.

- *Flexibility* – The drillhole repository concept offers considerable flexibility, both globally and locally. Drillhole repositories of different sizes can be built in a modular fashion, tailored to the specifics of the waste inventory, waste package characteristics as well as geographical and geological conditions. In particular, relatively small repositories can be built on the sites where the waste is produced, limiting or avoiding transportation. Locally, the design of the repository can be adapted to the geologic conditions and/or tailored to the design specifications desired by the host community by changing the number, length, orientation and inclination of the disposal sections, geologic conditions permitting. This global and local flexibility allows for a staged approach, with short implementation times and rapid site closure after waste emplacement. Furthermore, it facilitates the flexible incorporation of new knowledge, data and findings from on-going site characterization studies, fundamental scientific research, research in generic or dedicated underground rock laboratories, and international collaborations. Small repositories built in a staged manner can respond to changes in the waste inventory. In general, drillhole repositories can be adapted to stakeholder feedback; they can be continually improved and optimized, increasing overall safety and likely decreases cost.
- *Logistical Simplicity* – The simplicity, compactness and flexibility of the drillhole disposal concept also reduce logistical complexity. Specifically, no humans need to be underground, transportation is reduced or avoided and established drilling technology can be used. This reduces the need to build and license additional, complex infrastructure. Logistical simplicity increases operational safety and reduces costs.

5.3 Other Issues

The safety assessment of a deep horizontal drillhole repository is in its early stages. Therefore, the current calculations are for a generic repository system; consequently, the conclusions are preliminary and cannot be applied to a specific site without further analyses. As demonstrated throughout the report and summarized in Section 5.2, the conclusions about the safety of the horizontal drillhole disposal concept are valid even if accounting for considerable variabilities and uncertainties in site characteristics and deviations from the expected repository evolution. Consequently, the main challenges facing the further

* The relevant properties of the excavation disturbed zone can be determined, for example, by standard well tests, axial multi-packer borehole hydraulic interference and tracer tests.

development of the concept tend to be non-technical in nature; they can be summarized as follows:

- *Characterization* – Characterization by direct inspection of the host rock by humans working underground is not possible in a drillhole concept. However, the suite of advanced borehole-based coring, logging, testing and characterization methods provides sufficient information about the safety-relevant properties of the host formation. Drillholes can also be visually inspected remotely, providing comparable information about the integrity of the drillhole and the characteristics of the formation. By contrast, the data collected in drained, ventilated, large underground openings[*] are difficult to interpret and may not accurately reflect post-closure repository conditions. Furthermore, a large component of site characterization for mined repositories consists of regional geological studies as well as surface-based geophysical surveys and geological mapping (mainly used for identification of a suitable host formation for repository allocation and characterization of the regional groundwater flow field) and exploratory boreholes and associated core analyses. In addition, relevant processes can be examined in underground rock laboratories and at research institutions, complementing field investigations. This shows that site investigations for a drillhole repository and a mined repository have access to the same data that are used to increase fundamental process understanding; many of these common data are used identically for the characterization of the site-specific natural barrier system. It should also be noted that less characterization of the near field is needed for a drillhole repository compared to a mined repository, because drillhole repositories are generally simpler, have smaller engineered components, and perturb the host rock to a much lesser degree, leading to an excavation disturbed zone that is not only smaller, but also much less complex and easier to characterize and test.

- *Public Confidence* – Scientists, engineers, regulators, stakeholders and the public need to gain confidence in the safety of the repository. This is only possible after a comprehensive performance assessment study and a related safety case have been presented. Developing a defensible license application depends—in part—on the legal and regulatory framework, which may need to be adapted to accommodate the deep horizontal drillhole concept. While waste disposal in deep horizontal drillholes is a novel concept with historically limited consideration by the nuclear industry, its components and implementation procedures are solidly based on established technologies and processes. Moreover, many aspects of the proposed concept are based on decades of research, testing, engineering analyses and worldwide experience by independent institutions, nuclear waste management organizations, as well as the oil, gas and geothermal industries.

[*] Repositories mined from argillaceous host rocks often require liners and other ground-support measures during or immediately after excavation, limiting visual inspection and direct observation of the host formation.

5.4 Addressing Main Objectives

The overall goal of the model, analyses, and interpretations documented in this report is to identify some of the factors that affect the key safety features of a deep horizontal drillhole repository, and to obtain an initial estimate of the repository system's long-term performance. The report also addresses the following objectives:

- To the extent possible (within the confines of a generic analysis), safety-relevant aspects were quantitatively evaluated or qualitatively discussed (see Section 4). If an aspect is strongly related to the details of the repository design or site-specific conditions, their inclusion in the safety analysis was deferred to the time when such information is available.
- It has been demonstrated that long-term safety of a deep horizontal drillhole repository can be evaluated using established simulation tools and analysis methods (see Section 4.5).
- Defensible arguments have been provided as a basis for a subsequent, site-specific safety assessment and license application for such a repository (see Section 5.2).
- This report may serve as a template for documenting a site-specific safety analysis.
- The initial modeling results and related analyses and interpretations can be used as a technical basis for discussions with the public, stakeholders, regulators, and collaborators.
- The suitability of argillaceous formations to host a repository for heat-generating nuclear waste has been corroborated (see Section 4.7.2).
- The understanding of the safety functions assigned to each component of the multi-barrier system of the deep horizontal drillhole repository has been improved (see Section 4.7.3).
- The robustness of the analyzed disposal system to uncertainties as well as adverse events has been assessed (see Section 4.7.4).
- The limits of a generic safety analysis to support a site-specific safety analysis have been recognized.

5.5 Conclusions

A horizontal drillhole repository is a viable concept for the disposal of spent nuclear fuel. This conclusion is contingent on the assumptions as well as the representativeness and accuracy of the simulation results of the nominal scenario (see Sections 4.3.2, 4.5.2 and 4.7.2). The validity and robustness of this conclusion is further corroborated by (a) performing sensitivity analyses that examine the influence of specific assumptions and parameters (see Section 4.7.3), (b) accounting for uncertainty and spatial variability in a probabilistic uncertainty propagation analysis (see Section 4.7.4), and (c) considering disruptive events (see Section 4.7.5).

The post-closure radiological consequences—calculated using a simplified representation of a generic deep horizontal drillhole repository located in shale—show for both the nominal case and disruptive-event scenarios that (a) the estimated maximum annual dose is low, and (b) the dose estimate is robust to key assumptions as well as uncertainties inherent in the analysis. Furthermore, the calculations suggest that the key safety function of long-term isolation from the accessible environment is provided by the depth of the repository and the attributes of its configuration (i.e., linear arrangement of waste canisters in a drillhole with small cross-sectional area, small perturbation of the host formation). Long-term confinement of radionuclides in the stable waste matrix and long migration times allow for radioactive decay to occur within the repository system, considerably reducing the activity of radionuclides potentially being released to the accessible environment. Retardation and spreading of radionuclides in the geosphere, dilution in the near-surface aquifer and attenuation in the biosphere lead to low annual doses that are calculated to be significantly below a dose standard of 10 mrem yr^{-1}. The calculated maximum radioactivity in the aquifer's groundwater is also very low and unlikely to exceed the limits of 40 CFR Part 141.66.[*]

The above conclusions are contingent on the stated model assumptions, i.e., they are only pertinent to a potential or actual site if the geological environment at that site exhibits similar characteristics, and if the repository system is carefully constructed, operated, and sealed as is assumed in the simulations. The calculations are preliminary and do not derive from a specific geographic location or geological site. The layout and design of the repository represent only the general disposal concept as no site-specific characterization data or detailed technical designs are available. The conceptual and numerical models, as well as assumptions and parameters and their uncertainties, are reflective of this context. It is understood that repository performance has to be reassessed as new information becomes available, and reevaluated for each potential disposal site, accounting for the final repository design and site-specific conditions. Nevertheless, such generic calculations are considered a useful if not necessary step toward developing a comprehensive, site-specific safety analysis which will support the safety case of a deep horizontal drillhole repository in compliance with all applicable regulations. They could also serve as a basis for successive stages in repository planning, siting, and development, and to provide a sound platform for interactions with interested parties and stakeholders.

[*] 40 CFR Part 141.66, *Maximum Contaminant Levels for Radionuclides*, lists separate maximum contaminant levels for different radionuclides (^{226}Ra, ^{228}Ra, gross alpha particle activity, beta particle and photon radioactivity, and uranium). The regulation requires the calculation of the concentration of man-made radionuclides causing 4 mrem total body or organ dose equivalents using a specific protocol. This detailed calculation will be performed as part of a site-specific safety analysis to demonstrate compliance with the requirements of 40 CFR Part 141.66.

References

AMEC (2014): *Sealing Deep Site Investigation Boreholes: Phase 1 Report*, Report 201257/002 Issue B, RWMD/03/042, AMEC, Oxfordshire, United Kingdom.

Andra (Agence nationale pour la gestion des déchets radioactifs) (2005): *Dossier 2005 Argile: Synthesis—Evaluation of the Feasibility of a Geological Repository in an Argillaceous Formation—Meuse/Haute-Marne Site*, pp. 241, Paris, France.

Ansolabehere, S., J. Deutch, M. Driscoll, J.P. Holdren, P.L. Joskow, R.K. Lester, E.J. Moniz, and N.E. Todreas (2003): *The Future of Nuclear Power: An Interdisciplinary MIT Study*, Massachusetts Institute of Technology, Cambridge, Massachusetts.

Anttila, M. (1999): *Criticality Safety Calculations of the Nuclear Waste Disposal Canisters for Twelve Spent Fuel Assemblies*, Working Report 99-03, VTT Energy, Espoo, Finland, pp. 20.

Arnold, B.W., P.V. Brady, S.J. Bauer, C. Herrick, S. Pye, S., and J. Finger (2011): *Reference Design and Operations for Deep Borehole Disposal of High-Level Radio-active Waste*, Report SAND2011-6749, Sandia National Laboratories, Albuquerque, New Mexico.

Babadagli, T., and S. Al-Salmi (2004): A review of permeability-prediction methods for carbonate reservoirs using well-log data, Society of Petroleum Engineering, Reservoir Evaluation & Engineering, *7*(2), SPE-87824-PA, doi: 10.2118/87824-PA.

Bates, E.A., M.J. Driscoll, R.K. Lester, and B.W. Arnold (2014): Can deep boreholes solve America's nuclear waste problem? *Energy Policy*, *72*, 186–189, doi: 10.1016/j.enpol.2014.03.003.

Becker, D.A., J.L. Cormenzana, A. Delos, Delos, L. Duro, J. Grupa, J. Hart, J. Landa, J. Marivoet, J. Orzechowski, T.-J. Schröder, A. Vokal, J. Weber, E.Weetjens, J. Wolf (2009): *PAMINA–Performance Assessment Methodologies in Application to Guide the Development of the Safety Case–Safety Indicators and Performance Indicators*, Deliverable 3.4.1, European Commission.

Berkowitz, B. and H. Scher (1995): On characterization of anomalous dispersion in porous and fractured media, *Water Resources Research*, *31*(6), 1461–1466.

Bethke, C.M., and P.V. Brady (2000): How the K_d approach undermines ground water cleanup, *Groundwater*, *38*(3), 435–443.

Blümling, P. (2005): Borehole sealing project at the Grimsel Test Site, *Geotech. Geol. Eng.* 23**,** 843–858, doi: 10.1007/s10706-004-2144-9.

Blümling, P., and J. Adams (2008): *Grimsel Test Site Investigation Phase IV Borehole Sealing*, Nagra Technical Report NTB 07-01, Nagra, Wettingen, Switzerland.

Bock, H., B. Dehandschutter, D.C. Martin, M. Mazurek, A. De Haller, F. Skoczylas, and C. Davy (2010): *Self-sealing of Fractures in Argillaceous Formations in the Context of Geological Disposal of Radioactive Waste Review and Synthesis Report*, OECD NEA 6184, Waste Management, Paris, France, ISBN 978-92-64-99505-1.

Bracke, G., F. Charlier, A. Liebscher, F.R. Schilling, and T. Röckel (2017): About the possibility of disposal of HLRW in deep boreholes in Germany, *Geosciences*, *7*, doi: 10.3390/geosciences7030058.

Brady, P.V., B.A. Arnold, G.A. Freeze, P.N. Swift, S.J. Bauer, J.L. Kanney, R.P. Rechard, and J.S. Stein (2009): *Deep Borehole Disposal of High-Level Radioactive Waste*, Report SAND2009-4401; Sandia National Laboratories, Albuquerque, New Mexico.

Brady, P., B. Arnold, S. Altman, and P. Vaughn (2012): *Deep Borehole Disposal of Nuclear Waste: Final Report*, Report SAND2012-7789 Sandia National Laboratories, Albuquerque, New Mexico.

BRC, Blue Ribbon Commission on America's Nuclear Future (2012): *Report to the Secretary of Energy, January 2012*, Available online (accessed on 4 February 2019): https://www.energy.gov/sites/prod/files/2013/04/f0/brc_finalreport_jan2012.pdf.

Carter, J.T., A.J. Luptak, J. Gastelum, C. Stockman, and A. Miller (2012): *Fuel Cycle Potential Waste Inventory for Disposition*, Report FCR&D-USED-2101-00031 Rev 5., U.S. Department of Energy, Office of Used Fuel Disposition, Washington, D.C.

Celia, M.A., S. Bachu, J.M. Nordbotten, and K.W. Bandilla (2015): Status of CO2 storage in deep saline aquifers with emphasis on modeling approaches and practical simulations, *Water Resour. Res.*, *51*(9), 6846–6892, doi: 10,1002/2015WR017609.

Clayton, D., G. Freeze, T. Hadgu, E. Hardin, J. Lee, J. Prouty, R. Rogers, W.M. Nutt, J. Birkholzer, H.H. Liu, L. Zheng, and S. Chu (2011): *Generic System Modeling—Fiscal Year 2011 Progress Report*, Report FCRF-USED-2011-000184, U.S. Department of Energy, Office of Used Fuel Disposition, Washington, D.C.

Condon, L.E., and R.M. Maxwell (2015): Evaluating the relationship between topography and groundwater using outputs from a continental-scale integrated hydrology model, *Water Resour. Res., 51*, 6602–6621, doi: 10.1002/2014WR016774.

Davis, J.A., and D.B. Kent (1990): Surface complexation modeling in aqueous geochemistry, In: Hochella, M.F., and A.F. White (eds.), Mineral-water interface geochemistry, Mineralogical Society of America, *Reviews in Mineralogy*, *23*, 177–260.

Delage, P. (2013): On the thermal impact on the excavation damaged zone around deep radioactive waste disposal, J*ournal of Rock Mechanics and Geotechnical Engineering*, *5*(3), 179–190, doi: 10.1016/j.jrmge.2013.04.002.

de Marsily, G. (1986): *Quantitative Hydrogeology*, Academic Press, Orlando, Florida.

Deep Isolation (2020): *Features, Events, and Processes for the Deep Horizontal Drillhole Disposal Concept*, Report DI-FEP-20-02, Deep Isolation Inc., Berkeley, Calif.

DOE, U.S. Department of Energy (1980): *Environmental Impact Statement on Management and Disposal of Commercially Generated Radioactive Wastes*, Report DOE/EIS-0046, U.S. Department of Energy, Office of Nuclear Waste Management, Washington, D.C.

DOE (2008): *Yucca Mountain Repository License Application, Safety Analysis Report*, Report DOE/RW-0573, Rev. 1, U.S. Department of Energy, Office of Civilian Radioactive Waste Management, Washington, D.C.

Deutsch, C.V., and A.G. Journel (1992): *GSLIB, Geostatistical Software Library and User's Guide*, Oxford University Press, New York, New York.

Darcy, H. (1856). *Les fontaines publiques de la ville de Dijon*. Victor Dalmont, Paris, France.

Finsterle, S. (1998): *Parallelization of iTOUGH2 Using PVM*, Report LBNL-42261, Lawrence Berkeley National Laboratory, Berkeley, Calif.

Finsterle, S. (2015): Practical notes on local data-worth analysis, *Water Resour. Res.*, *51*(12), 9904–9924, doi: 10.1002/2015WR017445.

Finsterle, S. (2017): *iTOUGH2-EOS1nT: A Nonisothermal Two-Phase Flow Simulator for Water and Multiple Tracers—User's Guide*, Report FGC-17-01, Finsterle GeoConsulting, Kensington, Calif.

Finsterle, S. (2019): *Enhancements to the TOUGH2 Simulator Implemented in iTOUGH2*, Report LBNL-7016E, Lawrence Berkeley National Laboratory, Berkeley, Calif.

Finsterle, S., and M.B. Kowalsky (2007): *iTOUGH2-GSLIB User's Guide*, Report LBNL/PUB-3191, Lawrence Berkeley National Laboratory, Berkeley, Calif.

Finsterle, S., M. Commer, J. Edmiston, Y. Jung, M.B. Kowalsky, G.S.H. Pau, H. Wainwright, and Y. Zhang (2017): iTOUGH2: A multiphysics simulation-optimization framework for analyzing subsurface systems, *Computers and Geosciences*, *108*, 8–20, doi:10.1016/j.cageo.2016.09.005.

Finsterle, S., R.A. Muller, R. Baltzer, J. Payer, and J.W. Rector (2019): Thermal evolution near heat-generating nuclear waste canisters disposed in horizontal drillholes, *Energies*, *12*(4), 596, doi: 10.3390/en12040596.

Fjær, E., J.S. Folstad, and L. Li (2016): How creeping shale may form a sealing barrier around a well, Paper ARMA-2017-482, 50th U.S. Rock Mechanics/Geomechanics Symposium, 26–29 June, 2016, Houston, Texas.

Fox, C.R., and G. Ülkümen (2011): Distinguishing two dimensions of uncertainty, In: Brun, W. H. Keren, G. Kirkebøen, and K. Montgomery (Eds.): *Perspectives on Thinking, Judging, and Decision Making.* ISBN 978-82-15-01878-2, Universitetsforlaget, Oslo, Norway.

Freeze, R.A. and J.A. Cherry (1979): *Groundwater*, Prentice-Hall, Englewood Cliffs, New Jersey.

Freeze, G. A., P. E. Mariner, J. E. Houseworth, and J. C. Cunnane 2010. Used Fuel Disposition Campaign Features, Events, and Processes (FEPs): FY10 Progress Report. SAND2010-5902. Sandia National Laboratories, Albuquerque, New Mexico.

Freeze, G., and P. Vaughn, P. (2012): *Development of an Advanced Performance Assessment Modeling Capability for Geologic Disposal of Nuclear Waste: Methodology* *and Requirements*, Report SAND2012-10208, Sandia National Laboratories, Albuquerque, New Mexico.

Freeze, G., M. Voegele, M., P. Vaughn, J. Prouty, W.M. Nutt, E. Hardin, and S.D. Sevougian (2013): *Generic Deep Disposal Safety Case*, Report SAND2013-0974P, Sandia National Laboratories, Albuquerque, New Mexico.

Freeze, G., E. Stein, L. Price, R. MacKinnon, and J. Tillman (2016): *Deep Borehole Disposal Safety Analysis*, Report FCRD-UFD-2016-000075 Rev. 0, SAND2016-10949R, Sandia National Laboratories, Albuquerque, New Mexico.

Freeze, G.A., E. Stein, and P.V. Brady (2019a): Post-closure performance assessment for deep borehole disposal of Cs/Sr capsules, *Energies*, *12*, 1980, doi: 10.3390/en12101980.

Freeze, G.A., E. Stein, P.V. Brady, C. Lopez, D. Sassani, D., K. Travis, F. Gibb, and J. Beswick (2019b): Deep borehole disposal safety case, *Energies*, *12*, 2141, doi: 10.3390/en12112141.

Geng, Z., A. Bonnelye, M. Chen, Y. Jin, P. Dick, C. David, X. Fang, and A. Schubnel (2018), Time and temperature dependent creep in Tournemire shale, *J. Geophys. Res. Solid Earth*, *123*, 9658–9675, doi: 10.1029/2018JB016169.

Ghabezloo, S., and J. Sulem (2009): Stress dependent thermal pressurization of a fluid-saturated rock, *Rock Mechanics and Rock Engineering*, *42*(1), 1–24.

Gonzales, S. and K.S. Johnson (1984): *Shale and Other Argillaceous Strata in the United States,* Report ORNL/Sub/84-64794/1, Oak Ridge National Laboratory, Oak Ridge, Tennessee, doi: 10.2172/5927124.

Gonzalez-Nicolas, A., A. Cihan, R. Petrusak, Q.L. Zhou, R. Trautz, D. Riesenberg, M. Godec, and J.T. Birkholzer (2019): Pressure management via brine extraction in geological CO_2 storage: Adaptive optimization strategies under poorly characterized reservoir condition, *Int. J. Greenhous Gas Control*, *83*, 176–185, doi: 10.1016/j.ijggc.2019.02.009.

GRS, Gesellschaft für Anlagen- und Reaktorsicherheit (GRS) mbH (2008): *Assessment of the Long-Term Safety of Repositories, Scientific Basis*, GRS Report GRS-237, Gesellschaft für Anlagen- und Reaktorsicherheit, Köln, Germany.

Haukwa, C.B. (1998): *AMESH—A Mesh Creating Program for the Integral Finite Difference Method—User's Manual*, Report LBNL-45284, Lawrence Berkeley National Laboratory, Berkeley, Calif., 53 pp. doi:10.2172/892927.

Heath, R.C. (1983): *Basic Ground-Water Hydrology,* U.S. Geological Survey Water-Supply Paper 2220, 86 pp., ISBN 0-607-68973-0, Denver, Colorado, USA.

Herbert, A.W., C.P. Jackson, and D.A. Lever (1988): Coupled groundwater flow and solute transport with fluid density strongly dependent on concentration, *Water Resour. Res.*, *24*(10), 1781–1795.

IAEA, International Atomic Energy Agency (1981): *Safety Assessment for the Underground Disposal of Radioactive Wastes,* IAEA Safety Fundamentals, Safety Series No. 56, International Atomic Energy Agency Vienna, Austria.

IAEA (1983): *Concepts and Examples of Safety Analyses for Radioactive Waste Repositories in Continental Geological Formations,* IAEA Safety Fundamentals, Safety Series No. 58, International Atomic Energy Agency, Vienna, Austria.

IAEA (1985): *Performance Assessment for Underground Radioactive Waste Disposal Systems*, IAEA Safety Fundamentals, Safety Series No. 68, International Atomic Energy Agency, Vienna, Austria.

IAEA (2003): *"Reference Biospheres" for Solid Radioactive Waste Disposal*, Report IAEA-BIOMASS-6, International Atomic Energy Agency, Vienna, Austria.

IAEA (2006): *Fundamental Safety Principles*, IAEA Safety Standards Series No. SF-1, International Atomic Energy Agency, Vienna, Austria.

IAEA (2011a): *Disposal of Radioactive Waste*, IAEA Safety Standards Series No. SSR-5, International Atomic Energy Agency, Vienna, Austria.

IAEA (2011b): *Radiation Protection and Safety of Radiation Sources: International Basic Safety Standards — Interim Edition*, IAEA Safety Standards Series No. GSR Part 3 (Interim), International Atomic Energy Agency, Vienna, Austria.

IAEA (2012): *The Safety Case and Safety Assessment for the Disposal of Radioactive Waste,* IAEA Specific Safety Guide No. SSG-23, International Atomic Energy Agency, Vienna, Austria.

IAEA (2016): *Safety Assessment for Facilities and Activities*, IAEA Safety Standards Series No. GSR Part 4 (Rev. 1), International Atomic Energy Agency, Vienna, Austria.

IAEA (2017): *Generic Post-Closure Safety Assessment for Disposal of Disused Sealed Radioactive Sources in Narrow Diameter Boreholes*, IAEA-TECDOC-1824, International Atomic Energy Agency, Vienna, Austria.

IAEA (2019): *IAEA Safety Glossary, Terminology Used in Nuclear Safety and Radiation Protection, 2018 Edition*, STI/PUB/1830, International Atomic Energy Agency, Vienna, Austria.

Johnson, L.H., and J.C. Tait (1997): *Release of Segregated Radionuclides from Spent Fuel*, SKB Technical Report 97-18, Svensk Kärnbränslehantering (SKB), Stockholm, Sweden.

Juhlin, C., and H. Sandstedt (1989): *Storage of Nuclear Waste in Very Deep Boreholes: Feasibility Study and Assessment of Economic Potential*, SKB Technical Report 89-39, Svensk Kärnbränslehantering (SKB), Stockholm, Sweden.

Lemmens, K., E. González-Robles, B. Kienzler, E. Curti, D. Serrano-Purroy, R. Sureda, A. Martínez-Torrents, O. Roth, E. Slonszki, T. Mennecart, I. Günther-Leopold, and Z. Hózer (2017): Instant release of fission products in leaching experiments with high burnup nuclear fuels in the framework of the Euratom project FIRST- Nuclides, *Journal of Nuclear Materials, 484*, 307–323, doi: 10.1016/j.jnucmat.2016.10.048.

McKinley, I.G., and A. Scholtis (1993): A comparison of radionuclide sorption databases used in recent performance assessments, *J. Contam. Hydrol*., *13*, 347–363.

Miller, W., R. Alexander, N.A. Chapman, I.G. McKinley, and J. Smellie (2000): Geological disposal of radioactive wastes and natural analogues: lessons from nature and archaeology, *Waste Management Series*, *2*, pp. 316, Pergamon, Amsterdam, The Netherlands.

Millington, R.J., and J.P Quirk (1961): Permeability of porous solids, *Trans Faraday Soc.*, *57*, 1200–1207.

Muller, R.A., S. Finsterle, J. Grimsich, R. Baltzer, E.A. Muller, J.W. Rector, J. Payer, and J. Apps (2019): Disposal of high-level nuclear waste in deep horizontal drillholes, *Energies*, *12*(11), 2052, doi: 10.3390/en12112052.

Nagra, National Cooperative for the Disposal of Radioactive Waste (2002a): *Project Opalinus Clay, Safety Report, Demonstration of Disposal Feasibility for Spent Fuel, Vitrified High-Level Waste and Long-Lived Intermediate-Level Waste (Entsorgungsnachweis),* Nagra Technical Report NTB 02-05, Nagra, Wettingen, Switzerland.

Nagra (2002b): *Project Opalinus Clay: Models, Codes and Data for Safety Assessment. Demonstration of Disposal Feasibility for Spent Fuel, Vitrified High-Level Waste and Long-Lived Intermediate-Level Waste (Entsorgungsnachweis)*, Nagra Technical Report NTB 02-06. Nagra, Wettingen, Switzerland.

Nagra (2002c): *FEP Management for the Opalinus Clay Safety Assessment*, Nagra Technical Report NTB 02-23, Nagra, Wettingen, Switzerland.

Nagra (2002d): *SMA/WLB: Bohrlochversiegelung/-verfüllung SB4a/s,* Nagra Technical Report NTB 02-24, Nagra, Wettingen, Switzerland.

NAS, National Academy of Sciences (1957): *The Disposal of Radioactive Waste on Land*. Available online: http://www.nap.edu/openbook.php?record_id=10294

NAS (2001): *Disposition of High-Level Waste and Spent Nuclear Fuel: The Continuing Societal and Technical Challenges,* National Academy of Sciences–National Research Council, National Academy Press, Washington, DC.

NDA, Nuclear Decommissioning Agency (2010): *Geological Disposal, Radioactive Wastes and Assessment of the Disposability of Waste Packages*, NDA Report NDA/RWMD/039, Nuclear Decommissioning Agency, Radioactive Waste Management Directorate, Didcot, United Kingdom.

NEA, Nuclear Energy Agency (2000): *Features, Events and Processes (FEPs) for Geologic Disposal of Radioactive Waste, An International Database*, OECD/NEA Nuclear Energy Agency, Paris, France.

NEA/IAEA (2002): *An International Peer Review of the Yucca Mountain Project TSPA-SR*, OECD/NEA Nuclear Energy, Paris, France, and International Atomic Energy Agency, Vienna, Austria.

NEA (2004): *Management of Uncertainty in Safety Cases and the Role of Risk*, Workshop Proceedings, Stockholm, Sweden, 2–4 February 2004, OECD/NEA Nuclear Energy Agency, Paris, France, ISBN 92-64-00878-0.

NEA (2006): *NEA Feature, Event and Process (FEP) Database*, available on-line at https://oecd-nea.org/feppd.

NEA (2011): *Reversibility and Retrievability (R&R) for the Deep Disposal of High-Level Radioactive Waste and Spent Fuel*, NEA/RWM/R(2011)4. Organization for Economic Co-Operation and Development, Paris, France.

NEA (2012): *Reversibility of Decisions and Retrievability of Radioactive Waste—Considerations for National Geological Disposal Programmes*, NEA No. 7085, Organization for Economic Co-Operation and Development, Paris, France.

Monlouis-Bonnaire, J.P., J. Verdier, and B. Perrin (2004): Prediction of the relative permeability to gas flow of cement-based materials, *Cement and Concrete Research*, *34*, 737744, doi: 10.1016/S0008-8846(03)00071-1.

Milodowski, A.E., W.R. Alexander, J.M. West, R.P. Shaw, F.M. McEvoy, J.M. Scheidegger and L.P. Field (2015): *A Catalogue of Analogues for Radioactive Waste Management*, British Geological Survey Commissioned Report CR/15/106, 184 pp., Keyworth, Nottingham, United Kingdom.

Neuzil, C.E. (2019): Permeability of clays and shales, *Annu. Rev. Earth Planet. Sci.*, *47*, 247–273, doi: 10.1146/annurev-earth-053018-060437.

Nirex (2003): *Generic Repository Studies–Generic Post-Closure Performance Assessment*, Report No. N/080, United Kingdom Nirex Limited, Harwell, United Kingdom.

Nirex (2004): *A Review of the Deep Borehole Disposal Concept for Radioactive Waste* Report No. N/108, United Kingdom Nirex Limited, Harwell, United Kingdom.

NWMO, Nuclear Waste Management Organization (2012): *Used Fule Repository Conceptual Design and Postclosure Safety Assessment in Crystalline Rock,* Report NWMO TR-2012-16, Toronto, Ontario, Canada.

NWMO (2013): *Postclosure Safety Assessment of a Used Fuel Repository in Sedimentary Rock,* Report NWMO TR-2013-07, Toronto, Ontario, Canada.

NWTRB, Nuclear Waste Technical Review Board (2015): *Transcript Fall 2015 Board Meeting*, NWTRB, Arlington, Virginia. Available online: https://www.nwtrb.gov/docs/default-source/meetings/2015/october/15oct21.pdf

NWTRB (2016): *Survey of National Programs for Managing High-Level Radioactive Waste and Spent Nuclear Fuel: A Report to Congress and the Secretary of Energy*. Available online (accessed 10/14/19): https://www.nwtrb.gov/docs/default-source/reports/survey_report_2016.pdf.

NWTRB (2018): *Geological Repositories: Performance Monitoring and Retrievability of Emplaced High-Level Radioactive Waste and Spent Nuclear Fuel*, A Report to U.S> Congress and the Secretary of Energy, Available online (accessed 10/18/19): https://www.nwtrb.gov/docs/default-source/reports/nwtrb_perfmonitoring.pdf.

O'Brien, M.T., L.H. Cohen, T.N. Narasimhan, T.L. Simkin, H.A. Wollenberg, H.A., W.F. Brace, S. Green, and H.P. Pratt (1979): *The Very Deep Hole Concept: Evaluation of an Alternative for Nuclear Waste Disposal*, Report LBL-7089, Lawrence Berkeley Laboratory, Berkeley, Calif.

Ollila, K. (2011). *Influence of Radiolysis on UO_2 Fuel Matrix Dissolution under Disposal Conditions, Literature Study*. Working Report 2011-27. Posiva Oy, Eurajoki, Finland.

Payer, J.H., S. Finsterle, J.A. Apps, and R.A. Muller (2019): Corrosion performance of engineered barrier system in deep horizontal drillholes, *Energies*, *Energies, 12*(8), 1491, doi: 1020193390/en12081491.

Pruess, K., C. Oldenburg, and G. Moridis (2012): *TOUGH2 User's Guide, Version 2.1*, Report LBNL-43134, Lawrence Berkeley Laboratory, Berkeley, California.

Posiva (2007): *Safety Assessment of a KBS-3H Spent Nuclear Fuel Repository at Olkiluoto, Complementary Evaluations of Safety*, Report POSIVA 2007-10, Posiva Oy, Eurajoki, Finland.

Rechard, R.P., L.C. Sanchez, C.T. Stockman, and H.R. Trellue (2000): *Improbability of Nuclear Criticality when Disposing Transuranic Waste at the Waste Isolation Plant*, Report SAND2000-16105,; Sandia National Laboratories, Albuquerque, New Mexico, USA, pp. 72.

Robertson, E.C. (1988): *Thermal Properties of Rocks*, USGS Open-File Report 88-441, Unitest States Geological Survey, Reston, Virginia, USA.

Roth, O. (2015): *A Study of Instant Release Fractions and Matrix Dissolution Rate of Two Fuel Samples Irrariated in Olkiuoto 1*, Report 2015-19. Posiva Oy, Olikluoto, Finland.

Sapiie, B., and M.J. Driscoll (2009): *A Review of Geology-Related Aspects of Deep Borehole Disposal of Nuclear Wastes*, Report MIT-NFC-TR-109, MIT, Cambridge, Massachusetts.

Saltelli, A., M. Ratto, T. Andres, F. Campolongo, J. Cariboni, D. Gatelli, M. Saisana, and S. Tarantola (2008): *Global Sensitivity Analysis: The Primer*, John Wiley & Sons, West Sussex, England.

SKB, Svensk Kärnbränslehantering AB (2006): *Long-Term Safety of KBS-3 Repositories at Forsmark and Laxemar – a First Evaluation*, SKB Technical Report TR-06-09, Svensk Kärnbränslehantering AB, Stockholm, Sweden.

SKB (2015): *Safety Analysis for SFR Long-Term Safety, Main Report for the Safety Assessment SR-PSU*, SKB Technical Report TR-14-01 (revised edition), Svensk Kärnbränslehantering AB, Stockholm, Sweden.

SKB (2018): Sealing of Investigation boreholes—Full Scale Field Test and Large-Scale Laboratory Tests, SKB Technical Report TR-18-18, Svensk Kärnbränslehantering AB, Stockholm, Sweden.

SNL, Sandia National Laboratories (2009): *Deep Borehole Disposal of High-Level Radioactive Waste*, Report SAND2009-4401, Sandia National Laboratories, Albuquerque, New Mexico.

SNL (2010): *Shale Disposal of U.S. High-Level Radioactive Waste*, Report SAND2010-2843, Sandia National Laboratories, Albuquerque, New Mexico.

SNL (2011): *Shale Disposal of U.S. High-Level Radioactive Waste*, Report SAND 2011-6203, Sandia National Laboratories, Albuquerque, New Mexico.

SNL (2013): *Generic Deep Disposal Safety Case*, Report SAND2013-0974P, Sandia National Laboratories, Albuquerque, New Mexico.

SNL (2016): *Deep Borehole Field Test Conceptual Design Report*, Report SAND2016-10246R, Sandia National Laboratories, Albuquerque, New Mexico, doi:10.2172/1333702.

Sone, H. and M.D. Zoback (2013): Mechanical properties of shale-gas reservoir rocks—Part 2: Ductile creep, brittle strength, and their relation to the elastic modulus, *Geophysics*, *78*(5), D393–D402, doi: 10.1190/GEO2013-0051.1.

Swift, P., G. Barr, R. Barnard, R. Rechard, A. Schenker, G. Freeze, and P. Burck (1999): *Feature, Event, and Process Screening and Scenario Development for the Yucca Mountain Total System Performance Assessment*, Proceedings of the NEA Workshop on Scenario Development, Madrid, Spain, May 10–12, 1999.

Trauth, K.M., S.C. Hera, and R.V. Guzowski (1993): *Expert Judgment on Markers to Deter Inadvertent Human Intrusion into the Waste Isolation Pilot Plant*, Report SAND92–1382; Sandia National Laboratories: Albuquerque, New Mexico.

Vrålstada, T., A. Saasenb, E. Fjæra, T. Øiaa, J.D. Ytrehusa, and M. Khalifehb (2019): Plug & abandonment of offshore wells: Ensuring long-term well integrity and cost-efficiency, *J. Petroleum Sci. Eng., 173*, 478–491, doi: 10.1016/j.petrol.2018.10.049.

Wagner, W., and A. Pruß (2002): The IAPWS formulation 1995 for the thermodynamic properties of ordinary water substance for general and scientific use, *J. Phys. Chem. Ref. Data*, *31*, 387, doi:10.1063/1.1461829.

Wainwright, H.M., and S. Finsterle (2016): *Global Sensitivity and Data-Worth Analysis in iTOUGH2, User's Guide*, Report LBNL-1005838, Lawrence Berkeley National Laboratory, Berkeley, Calif.

Wainwright, H., S. Finsterle, Y. Jung, Q. Zhou, and J.T. Birkholzer (2014), Making sense of global sensitivity analyses, *Computers & Geosciences*, *65*, 84–94, doi:10.1016/j.cageo.2013.06.006.

Wang, C.Y., X. Liao, L.P. Wang, C.H. Wang, and M. Manga (2016): Large earthquakes create vertical permeability by breaching aquitards, *Water Resour. Res.*, *52*(8), 5923–5937, doi: 10.1002/2016WR018893.

Woodward-Clyde Consultants (1981): *Very Deep Hole Systems Engineering Studies,* Woodward-Clyde Consultants, San Francisco, Calif.

Wu, Y.S., C.F. Ahlers, P. Fraser, A. Simmons, and K. Pruess (1996): *Software Qualification of Selected TOUGH2 Modules*, Report LBNL-39490, Lawrence Berkeley National Laboratory, Berkeley, Calif.

Yalçıntaş, E., X. Gaona, M. Altmaier, K. Dardenne, R. Polly, and H. Geckeis (2016): Thermodynamic description of Tc(IV) solubility and hydrolysis in dilute to concentrated NaCl, $MgCl_2$ and $CaCl_2$ solutions, *Dalton Trans.*, *45*, 8916, doi: 10.1039/c6dt00973e.

Zhou, Q., and J.T. Birkholzer (2011): On the scale and magnitude of pressure buildup induced by large-scale geologic storage of CO_2, *Greenhouse Gas Sci. Technol.*, *1*, 11–20 doi: 10.1002/ghg3.001.

Appendix A: Acronyms

2D	two-dimensional
3D	three-dimnesional
DOE	United States Department of Energy
EBS	Engineered Barrier System
EDZ	Excavation Damaged/Disturbed Zone
ERB	Example Reference Biosphere (IAEA, 2003)
EGS	Enhanced/Engineered Geothermal System
FEPs	Features, Events, and Processes
HLW	High-Level Waste
IAEA	International Atomic Energy Agency
LHS	Latin Hypercube Sampling
MS	Monte Carlo (simulations)
MTHM	Metric Tons of Heavy Metals
n/a	not applicable
NBS	Natural Barrier System
SA	Safety Analysis / Sensitivity Analysis
SF	Spent Fuels
SNF	Spent Nuclear Fuel
URL	Underground Research/Rock Laboratory
U.S.	United States

PAGE INTENTIONALLY LEFT BLANK

Appendix B: Model Input Parameters

Parameter [a]	Ref. value, Mode [b]	Distrib. Type [c]	Range [d]		Std. Dev., Scaling Factor [e]	Comment
			Minimum	Maximum		
Hydrogeological Parameters [f] (see Section 4.5.4.2)						
Intrinsic Permeability, k [m²]						
k waste [g]	10^{-20}	fixed	n/a	n/a	n/a	
k canister	10^{-24}	fixed	n/a	n/a	n/a	Time-dependent, increases to 10^{-16} m^2 within 10,000 years
k buffer [h]	10^{-16}	log-tri	10^{-18}	10^{-14}	1.0	

---

[a] Key parameters of reference scenario, potentially adjusted during sensitivity or probabilistic uncertainty propagation analyses. Each parameter refers to or multiple model input parameters (e.g., the horizontal permeability, k_h, affects two model input parameters: the permeabilities in X and Y direction).

[b] Reference value, value for nominal scenario, mean or mode of probability distribution used for uncertainty propagation analysis.

[c] Probability distribution used for sampling-based uncertainty propagation analysis; (log)-normal, (log)-uniform, or (log)-triangular; n/a = not applicable, i.e., parameter is fixed.

[d] Probability distributions used for sampling-based uncertainty propagation analyses are truncated at the minimum and maximum values.

[e] Standard deviation of (log)-normally distributed parameters; if log-normally distributed, the standard deviation refers to the logarithm; for (log)-uniform and (log)-triangular distributions, a parameter-scaling factor is provided (used to scale composite sensitivity measures, see Finsterle (2015)) rather than the standard deviation that corresponds to the sampling distribution (which are, respectively, $\sigma_{uni} = \sqrt{(max - \min)^2/12}$ and $\sigma_{tri} = \sqrt{(min^2 + mode^2 + max^2 + min \cdot mode + min \cdot max + mode \cdot max)/18}$)

[f] The categorization of parameters is somewhat arbitrary. For example, porosity may be considered a hydrogeological parameter, but it may also be considered a thermal or transport parameter, as it affects the heat capacity and diffusivity and advective transport velocity.

[g] The waste within a canister is conceptualized as an amorphous porous medium that includes the ceramic UO_2 fuel pellets, the zircaloy cladding of the assemblies, and any material (such as quartz sand) that fills the spaces within the canisters.

[h] Buffer refers to material between canisters (unless replaced by a plug) and between canisters and the casing. Buffers may consist of slurry,

Parameter	**Ref. value, Mode**	**Distrib. Type**	**Range**		**Std. Dev., Scaling Factor**	**Comment**
			Minimum	**Maximum**		
k casing	10^{-24}	fixed	n/a	n/a	n/a	Time-dependent, increases to 10^{-16} m^2 within 100 years
k cement [i]	10^{-15}	log-triang	10^{-17}	10^{-13}	1.0	(Monlouis-Bonnaire et al., 2004)
k plug [j]	10^{-16}	log-triang	10^{-18}	10^{-14}	1.0	
k backfill [k]	10^{-15}	log-triang	10^{-17}	10^{-13}	1.0	
k_a EDZ [l] host rock k_r EDZ host rock	10^{-15} 10^{-16}	log-norm log-norm	10^{-16} 10^{-17}	10^{-14} 10^{-15}	0.5 0.5	Anisotropy [m] ratio fixed; no self-sealing assumed
k_a EDZ overburden k_r EDZ overburden	10^{-12} 10^{-13}	log-norm log-norm	10^{-13} 10^{-14}	10^{-11} 10^{-12}	0.5 0.5	Anisotropy ratio fixed
k_a EDZ aquifer k_r EDZ aquifer	10^{-11} 10^{-12}	log-norm log-norm	10^{-12} 10^{-13}	10^{-10} 10^{-11}	0.5 0.5	

cementitious materials, grout mixtures, bentonite, oil-based materials (such as tar, bitumen or asphalt), pellets, or other suitable materials.

[i] Cement or other suitable material injected in the annulus between the casing and the drillhole wall. Assumed to partly degrade with time.

[j] Plugs refer to engineered components installed at select locations along the vertical and/or curved access hole and/or horizontal disposal section of the drillhole. They are designed using suitable materials to limit axial fluid flow and radionuclide transport; they may also serve as abutments.

[k] Backfill refers to material filling the vertical and curved portions of the access hole after removal of the casing. Backfills may consist of cementitious materials, grout mixtures, bentonite, oil-based materials (such as tar, bitumen or asphalt), crushed rocks, sand, or other suitable materials.

[l] EDZ = excavation damaged zone or excavation disturbed zone, i.e., the zone around the drillhole affected by the drilling process (fracturing, deformations due to stress redistribution, erosion or plugging due to mud invasion).

[m] Ratio of radial over axial permeability (for EDZ) or vertical over horizontal permeability (for geosphere). Anisotropy may be caused by stress-dependent fracturing or depositional layering, bedding, lamination, or other directional features.

Parameter	Ref. value, Mode	Distrib. Type	Range		Std. Dev., Scaling Factor	Comment
			Minimum	Maximum		
k_h host rock k_v host rock	10^{-17} 10^{-18}	log-norm log-norm	10^{-19} 10^{-20}	10^{-15} 10^{-16}	1.0 1.0	Anisotropy ratio fixed (Neuzil, 2019)
k_h overburden k_v overburden	10^{-14} 10^{-15}	log-norm log-norm	10^{-16} 10^{-17}	10^{-12} 10^{-13}	1.0 1.0	Anisotropy ratio fixed (Babadagli and Al-Salmi, 2004)
k_h aquifer k_v aquifer	10^{-12} 10^{-13}	log-norm log-norm	10^{-13} 10^{-14}	10^{-11} 10^{-12}	0.5 0.5	Anisotropy ratio fixed (Heath, 1983)
k_h saline formation k_v saline formation	3.0×10^{-16} 3.0×10^{-17}	log-norm log-norm	3.0×10^{-18} 3.0×10^{-19}	3.0×10^{-14} 3.0×10^{-15}	1.0 1.0	Anisotropy ratio fixed (Babadagli and Al-Salmi, 2004)
k_h fault k_v fault	10^{-14} 10^{-13}	fixed	n/a	n/a	n/a	Anisotropy ratio fixed
Porosity [n]***, ϕ [m^3 m^{-3}]***						
ϕ waste	0.40	fixed	n/a	n/a	n/a	Degraded waste
ϕ canister	0.10	fixed	n/a	n/a	n/a	Represents corrosion product
ϕ buffer	0.35	triangular	0.20	0.50	0.05	Range accounts for representation of different materials and gaps
ϕ casing	0.10	fixed	n/a	n/a	n/a	Represents corrosion product
ϕ cement, plug	0.20	triangular	0.10	0.30	0.05	Range accounts for representation of different grouts and gaps
ϕ backfill	0.30	triangular	0.20	0.40	0.05	
ϕ EDZ host rock	0.20	normal	0.10	0.30	0.05	Includes fracture porosity
ϕ EDZ overburden	0.20	normal	0.10	0.30	0.05	Includes fracture porosity

[n] Porosity affects fluid storativity and flow velocity, but also total heat capacity, diffusivity, adsorption, and advective transport velocities of brine and radionuclides.

Parameter	Ref. value, Mode	Distrib. Type	Range		Std. Dev., Scaling Factor	Comment
			Minimum	Maximum		
ϕ EDZ aquifer	0.30	normal	0.15	0.45	0.05	Includes fracture porosity
ϕ host rock	0.10	normal	0.02	0.20	0.05	(Neuzil, 2919)
ϕ overburden	0.15	normal	0.05	0.25	0.05	(Babadagli and Al-Salmi, 2004)
ϕ aquifer	0.30	normal	0.20	0.40	0.05	(Heath, 1983)
ϕ saline formation	0.10	normal	0.02	0.20	0.05	(Babadagli and Al-Salmi, 2004)
ϕ fault	0.10	fixed	n/a	n/a	1.0	Fast flow path porosity
			***Geostatistical Parameters* [o]**			
a geosphere [p]	1000.0	uniform	50.0	2000.0	500.0	Correlation range
c geosphere	0.01	triangular	0.004	0.04	0.01	Sill value
α geosphere	0.01	log-triang	0.01	1.0	0.25	Anisotropy ratio
β geosphere	0.0	fixed	n/a	n/a	n/a	Bedding angle

[o] Random, spatially correlated, anisotropic fields of porosity modifiers are generated to include spatial variability into the geosphere model. Porosity is chosen as the heterogeneous parameter because of its impact on transport velocity and diffusivity, which affect the dominant impacts on radionuclide migration in the geosphere. The porosity modifiers are log-normally distributed and follow a spherical semi-variogram, $\gamma(h) = c \cdot \mathrm{sph}(h/a)$, where h [m] is the lag distance, a [m] is the range (also referred to as correlation length), and c is the sill value. The correlation length is different in a minor (subvertical) and principal (subhorizontal) direction, with an anisotropy ratio $\alpha = a_v/a_h$. The structures could be rotated by an angle β [°] between the horizontal and the principal directions. No nugget effect is included. A new seed number is used for each Monte Carlo realization as a way to introduce irreducible spatial variability into the uncertainty quantification analysis. The porosity modifier fields are generated using the sequential Gaussian simulation routines of the geostatistical software library GSLIB (Deutsch and Journel, 1992).

[p] The geostatistical parameters are identical throughout the geosphere. Layer-specific reference porosities are multiplied by the stochastic modifiers, generating local heterogeneity in porosity while at the same time preserving the layered structure of the geosphere.

Parameter	Ref. value, Mode	Distrib. Type	Range		Std. Dev., Scaling Factor	Comment
			Minimum	Maximum		
Fault Zone Geometry [q]						
X fault center [m]	800	fixed	n/a	n/a	n/a	
Y fault center [m]	0	fixed	n/a	n/a	n/a	
Z fault center [m]	-2000	fixed	n/a	n/a	n/a	
Fault thickness [m]	50	fixed	n/a	n/a	n/a	Includes fracture zone
Fault width [m]	1000	fixed	n/a	n/a	n/a	
Fault height [m]	5000	fixed	n/a	n/a	n/a	Fault reaches aquifer
Azimuth [°]	10	fixed	n/a	n/a	n/a	
Dip [°]	10	fixed	n/a	n/a	n/a	
Plunge [°]	0	fixed	n/a	n/a	n/a	
Pore Compressibility, c_ϕ [Pa^{-1}]						
c_ϕ all materials	10^{-9}	log-norm	10^{-10}	10^{-8}	0.5	

[q] The seismic scenario considers a subvertical fault zone interesting the repository. The fault zone is modeled as an ellipsoidal high-permeability structure with permeabilities highest along the principal axes (representing the fault), with permeabilities tapering off away from the axes using a spherical function (representing the fault-associated fracture zone) and approaching the background value of the undisturbed formation at the edge of the ellipsoid.

Parameter	Ref. value, Mode	Distrib. Type	Range		Std. Dev., Scaling Factor	Comment
			Minimum	Maximum		
Thermal Parameters (see Section 4.5.4.5)						
Pore Expansivity, $\varepsilon\phi$ [°C^{-1}]						
$\varepsilon\phi$ all materials	10^{-5}	log-norm	10^{-6}	10^{-4}	0.5	
Thermal Conductivity, λ [J m^{-1} °C^{-1}]						
λ waste, canister, casing	40.0	fixed	n/a	n/a	n/a	
λ buffer, cement, backfill, plug	1.0	uniform	0.75	2.0	0.5	Range accounts for representation of different materials and gaps
λ EDZ	1.5	normal	1.0	2.0	0.5	
λ host rock, overburden, aquifer, saline formation	2.0	normal	1.5	2.5	0.5	(Robertson, 1988)
λ fault	1.5	fixed	n/a	n/a	0.5	
Heat Capacity, c_s [J kg^{-1} °C^{-1}]						
c_s waste	700.0	fixed	n/a	n/a	n/a	Assembly and canister backfill
c_s canister, casing	500.0	fixed	n/a	n/a	n/a	
c_s buffer, cement, backfill, plug	900.0	uniform	800.0	1000.0	50.0	Range accounts for representation of different materials and gaps
c_s geosphere	900.0	normal	800.0	1000.0	50.0	

Parameter	Ref. value, Mode	Distrib. Type	Range		Std. Dev., Scaling Factor	Comment
			Minimum	Maximum		
Transport Parameters (see Section 4.5.4.3)						
Solid Density [r]***, ρ_s [kg m^{-3}]***						
ρ_s waste	3000.0	fixed	n/a	n/a	n/a	Assembly and canister backfill
ρ_s canister, casing	7000.0	fixed	n/a	n/a	n/a	
ρ_s buffer, cement, backfill, plug	2700.0	uniform	2400.0	2900.0	50.0	Range accounts for representation of different materials and gaps
ρ_s geosphere	2700.0	normal	2600.0	2800.0	50.0	
Distribution Coefficient [s]***, k_d [m^3 kg^{-1}]***						
k_d waste	0.0	fixed	n/a	n/a	n/a	Waste form assumed non-sorbing
k_d canister, casing	0.0	fixed	n/a	n/a	n/a	Corrosion products assumed non-sorbing
k_d buffer, cement, backfill, plug						Based on data for bentonite (McKinley and Scholtis, 1993)
^{129}I	0.00	triangular	0.00	0.01	0.005	
^{36}Cl	0.00	fixed	n/a	n/a	n/a	
^{79}Se	0.00	triangular	0.00	0.02	0.01	
^{99}Tc	0.00	triangular	0.00	0.25	0.10	

[r] Solid density affects adsorption, but also heat capacity of the porous medium.

[s] Distribution coefficients are radionuclide-specific and rock-specific. ^{36}Cl is assumed non-sorbing in all environments.

Parameter	Ref. value, Mode	Distrib. Type	Range		Std. Dev., Scaling Factor	Comment
			Minimum	Maximum		
k_d geosphere						
^{129}I	10^{-5}	log-normal	10^{-7}	10^{-3}	1.0	
^{36}Cl	0.00	fixed	n/a	n/a	n/a	
^{79}Se	0.00	fixed	n/a	n/a	n/a	
^{99}Tc	10^{-2}	log-normal	10^{-3}	1.0	0.5	
Diffusion Coefficient [t]***, d_w^κ [m^2 s^{-1}]***						
^{129}I	2.0×10^{-9}	log-normal	10^{-10}	10^{-8}	0.5	Range and standard deviation account for uncertainty in assumption about effective diffusion coefficient and diffusion-accessible porosity.
^{36}Cl	2.0×10^{-9}	log-normal	10^{-10}	10^{-8}	0.5	
^{79}Se	2.0×10^{-9}	log-normal	10^{-10}	10^{-8}	0.5	
^{99}Tc	2.0×10^{-9}	log-normal	10^{-10}	10^{-8}	0.5	

[t] Diffusion coefficient in bulk water at 25°C; adjusted for temperature according to Stokes-Einstein equation. The effective diffusion coefficient in a porous medium is related to porosity by a factor $\phi^{4/3}$ (Millington and Quirk, 1961). The porosity accessible for ionic diffusion is assumed identical to bulk porosity.

Parameter	Ref. value, Mode	Distrib. Type	Range		Std. Dev., Scaling Factor	Comment
			Minimum	Maximum		
Initial and Boundary Conditions (see Section 4.5.10)						
Initial Radionuclide Inventory, m^{κ}_{waste} [kg per canister] (see** Table 2**)						
^{129}I ^{36}Cl ^{79}Se ^{99}Tc	1.36×10^{-1} 2.18×10^{-4} 4.57×10^{-3} 5.56×10^{-1}	normal normal normal normal	10^{-1} 1.5×10^{-4} 4.0×10^{-3} 5.0×10^{-1}	1.8×10^{-1} 3.0×10^{-4} 5.0×10^{-3} 6.0×10^{-1}	2.0×10^{-2} 2.0×10^{-5} 2.0×10^{-4} 2.0×10^{-2}	Represents variability in spent fuel's initial enrichment, burn-up, and cooling time.
Boundary Conditions [u]						
P_{top} [bar]	1.0	fixed	n/a	n/a	n/a	Atmospheric pressure at surface
P_{bot} [bar]	202.0	uniform	200.0	210.0	2.0	Boundary pressure at rightmost quarter of bottom boundary, inducing regional groundwater flow
T_{top} [°C]	13.0	fixed	n/a	n/a	n/a	Long-term average at surface
T_{bot} [°C]	73.0	fixed	n/a	n/a	n/a	Geothermal gradient: 0.03 °C m^{-1}
Sink/Source Terms						
q_{well} [kg s^{-1}]	2.0	uniform	0.2	4.0	1.0	Pumping rate at drinking water well, see Section 4.5.9.
ω [yr^{-1}]	10^{-5}	log-triang	10^{-6}	10^{-4}	0.5	Fractional waste degradation rate (Clayton et al., 2011, Section 3.3.3.3.2.2)
IRF	20%	fixed	n/a	n/a	n/a	Instant Release Fraction (Nagra, 2002a; Table A2.2.1)

[u] Initial pressure, temperature, and brine-mass-fraction distributions specified based on steady-state calculation as described in Section 4.5.10.

PAGE INTENTIONALLY LEFT BLANK

Appendix C: Mesh Generation

Mesh generation is an essential step in model development, as it determines the level of geometrical details that can be represented, the accuracy with which gradients can be resolved, and computational efficiency. Specifically (as described in Section 4.5.2), the integration of the radial-axial near-field submodel (which follows the trajectory of the drillhole) into the three-dimensional Cartesian model of the geosphere yields a better reproduction of the geometry of the engineered barrier components, a more accurate resolution of radial and axial gradients, and higher computational efficiency; however, it requires building the mesh in multiple steps as follows:

(1) *Define Model Domain*: The model domain has the geometry of a cuboid. The origin of the Cartesian coordinate system is the location of the vertical access hole at the land surface. The model domain in *X* direction (which is defined parallel to the horizontal disposal section of the drillhole repository) extends from -2,200 m to 3,550 m. The *Y* direction (which is horizontal and perpendicular to the *X* axis) extends from 0 m at the drillhole axis to 50 m, which is the distance to the vertical symmetry plane. In *Z* direction, the model extends from the land surface to a depth of -2,000 m. Two special layers are attached to the top and bottom of the model domain to allow the specification of Dirichlet boundary conditions at the land surface and at depth (see Step (9)).

(2) *Generate Basic Radial-Axial Mesh*: A radial-axial mesh in a local *R-Z* coordinate system is constructed as the basis for the near-field submodel.* The discretization in axial (*Z*) direction is 25 m for the vertical and curved sections of the drillhole. After a short transition, a sequence of elements with thicknesses of 0.5, 4.5, 0.5, and 1.0 m is generated, representing the waste canister (consisting of sections for the end-caps and hooking mechanisms and the waste) and the spacing between canisters, which may be backfilled or otherwise plugged. This four-element sequence is repeated 153 times for the explicit representation of as many PWR canisters. The axial mesh is extended by another 100 m beyond the last canister for a total length of the basic *R-Z* model of 2,320 m. In the radial direction, the discretization generates cylindrical shells with variable thicknesses that represent the inner and outer diameters of the canister and casing, as well as the radii of the drillhole (which has various diameters, decreasing with depth) and the associated excavation disturbed zones (EDZs) with a thickness that is half of the corresponding drillhole radius. The host rock from the drillhole wall to a radial distance of 10 m is discretized with logarithmically increasing shell thicknesses. The radial-axial near-field submodel consists of 12,806 elements. The axis of this radial-axial mesh is straight; it will be modified in the Step (7) to follow the actual drillhole trajectory.

(3) *Create Near-Field Model Mesh*: The basic radial-axial mesh generated in Step (2) is modified† to create a mesh for the near-field submodel that follows the trajectory

* The grid was created with the internal mesh generator RZ2D of TOUGH2 (Pruess et al., 2012).

† A Unix shell script (*runMESHdrill.sh*) and a Fortran program (*drillhole.f*) were developed to

of the drillhole. For each sequential drillhole segment of the basic radial-axial mesh, element coordinates are recalculated to account for a given axis orientation or build angle. In particular, the gravity component is projected to the drillhole axis as its angle changes. At the same time, material names are assigned in a radial direction to create the specific cross-section for a given location along the drillhole, which is described by the radii of the drillhole and the engineered components within it, the thickness of the excavation disturbed zone, and the geologic formation in the near field. The drillhole is vertical from the land surface to a depth of -700 m, at which point it curves with a build angle of 0.197°/m,* until it becomes near-horizontal at a depth of -990 m. The approximately 1,000 m long disposal section has an upward tilt of 3°. The end of the drillhole is at a depth of -936 m. The near-field model continues horizontally for another 100 m. Geometric parameters of the near-field model segments and associated cross sections are summarized in Table 5.

(4) *Prepare Transition Zone between Radial-axial and Cartesian Meshes*: In comparison to the far-field model, the resolution of the near-field model in axial direction is relatively fine, requiring a transition zone between the two sub-models. Points are generated at distances of 25, 50, and 100 m from the drillhole axis. The points at a distance of 25 m have the same axial spacing as the near-field model so that approximately cuboidal grid blocks are created where the near-field model will be embedded in Step (7). Points at distances of 50 and 100 m are farther apart, especially along the disposal section, to facilitate a smooth transition from the scale with which individual waste canisters are discretized (see Step (2)) and the scale of geosphere elements (see Step (5)).

(5) *Generate Basic Cartesian Mesh*: The geosphere is discretized into a structured Cartesian mesh with variable grid spacing. The process starts with generating a vertical, two-dimensional cross-section† (to be extended to three dimensions in Step (6)). In the axial direction within the repository area (-250 m < X < 1,650 m), grid spacing is 50 m, with element sizes increasing towards the left and right model boundaries at X = -2,220 and of 3,550 m, respectively. In vertical direction, grid spacing is uniform at 50 m. After generation of this structured mesh, all grid points within 100 m of the drillhole trajectory are removed‡ and replaced by the transition points created in Step (4). Because the program used in Step (6) requires input

allow processing of the basic radial-axial mesh. These programs were verified by (a) comparison of results with hand-calculated coordinates and other geometrical variables, (b) visual inspection of the mesh, and (c) a steady-state simulation to confirm that a hydrostatic pressure distribution is obtained.

* A build angle of 0.197°/m corresponds to 6°/(100 ft) or a radius of curvature of 290 m (880 ft).

† The grid was created with the internal mesh generator *XYZ* of TOUGH2 (Pruess et al., 2012).

‡ A Fortran program (*DeleteElements.f*) was developed to remove elements within a region defined by a polygonal prism. The program was verified by inspection of the resulting mesh coordinates and visualization of the mesh.

coordinates for a horizontal surface mesh rather than a vertical cross-section, the basic Cartesian mesh is rotated by 90° around the *X*-axis.

(6) *Create Voronoi Mesh*: Program *AMESH** is used to generate a Voronoi surface grid with the coordinates assembled in Step (5) as the element center points. The resulting two-dimensional Voronoi grid is extended vertically, creating parallel layers, each consisting of three-dimensional prismatic Voronoi elements. The thickness of the first layer is 12.5 m, i.e., thick enough to accommodate the 10 m radial extent of the near-field model (see Step (7)). Subsequent layers are 2.5, 5.0, 10.0, and 20.0 m thick for a total thickness of 50 m (half the separation distance between two parallel drillholes). The resulting mesh is rotated back by -90° around the *X*-axis.

(7) *Insert Near-Field Model into Far-Field Model*: The near-field mesh developed in Step (3) is inserted into the far-field mesh developed in Step (6)†. The volumes of the Voronoi elements intersected by the drillhole are reduced by the volume of the corresponding radial-axial section of the near-field model. The outermost cylindrical element is connected to the Voronoi element with appropriate cross-sectional areas and nodal distances, effectively embedding the near-field model into the far-field model. Elements of the near-field model are renamed to avoid redundancies.

(8) *Assign Material Names*: Material names are assigned to all geosphere elements‡ to generate the desired stratigraphy. The drinking water aquifer is 200 m thick, followed by a 500 m thick overburden layer to a depth of -700 m, which is the top of the 500 thick host rock. The underlying saline formation extends from a depth of -1,200 m to the bottom of the model at -2,000 m.

(9) *Add Boundary Elements*: The top and bottom surfaces of the model are subdivided into four equal sections, and special boundary elements are attached to all elements comprising a segment§. This allows specification of constant or time-dependent pressure and temperature (Dirichlet) boundary conditions at the land surface and the base of the model. See Section 4.5.10 for a discussion of boundary conditions.

---

* *AMESH* (Haukwa, 1998) has been qualified for use by the Yucca Mountain Project (MOL.19990519.0191). A Unix shell script (*runAMESH.sh*) was developed to create the input files needed by *AMESH* and to post-process the output files.

† A Fortran program (*InsertDrillhole.f90*) was developed to execute the various sub-steps comprising Step (7). The program was verified by (a) comparison of results with hand-calculated coordinates and other geometrical variables, (b) visual inspection of the mesh, and (c) a steady-state simulation to confirm that a hydrostatic pressure distribution is achieved.

‡ A Fortran program (*AssignRock.f*) was developed to assign material names to all elements within a region defined by a polygonal prism. The program was verified by inspection of the resulting mesh file and visualization of the mesh.

§ A Fortran program (*AddBound.f*) was developed to add special boundary elements to all elements within a region defined by a polygonal prism. The program was verified by inspection of the resulting mesh file and visualization of the mesh.

Details about the near-field discretization can be found in Table 5 and Table 6. The computational mesh consists of 34,424 elements and 91,765 connections between them. The three-dimensional model represents a symmetry cell of the repository system (containing one drillhole) from the waste form to the receptor.

A second mesh with the waste disposal section located at a depth of 1.5 km is generated for the sensitivity analysis described in Section 4.7.3.4 (see also Figure 26). This mesh consists of 42,024 elements and 119,306 connections between them. Furthermore, a dual permeability mesh with 78,117 elements and 167,111 connections is constructed to simulate flow and transport through a fractured formation (to be described elsewhere). The axial-radial near-field submodel is fully embedded in each of these three-dimensional, Cartesian Voronoi geosphere models, as shown in Figure 37.

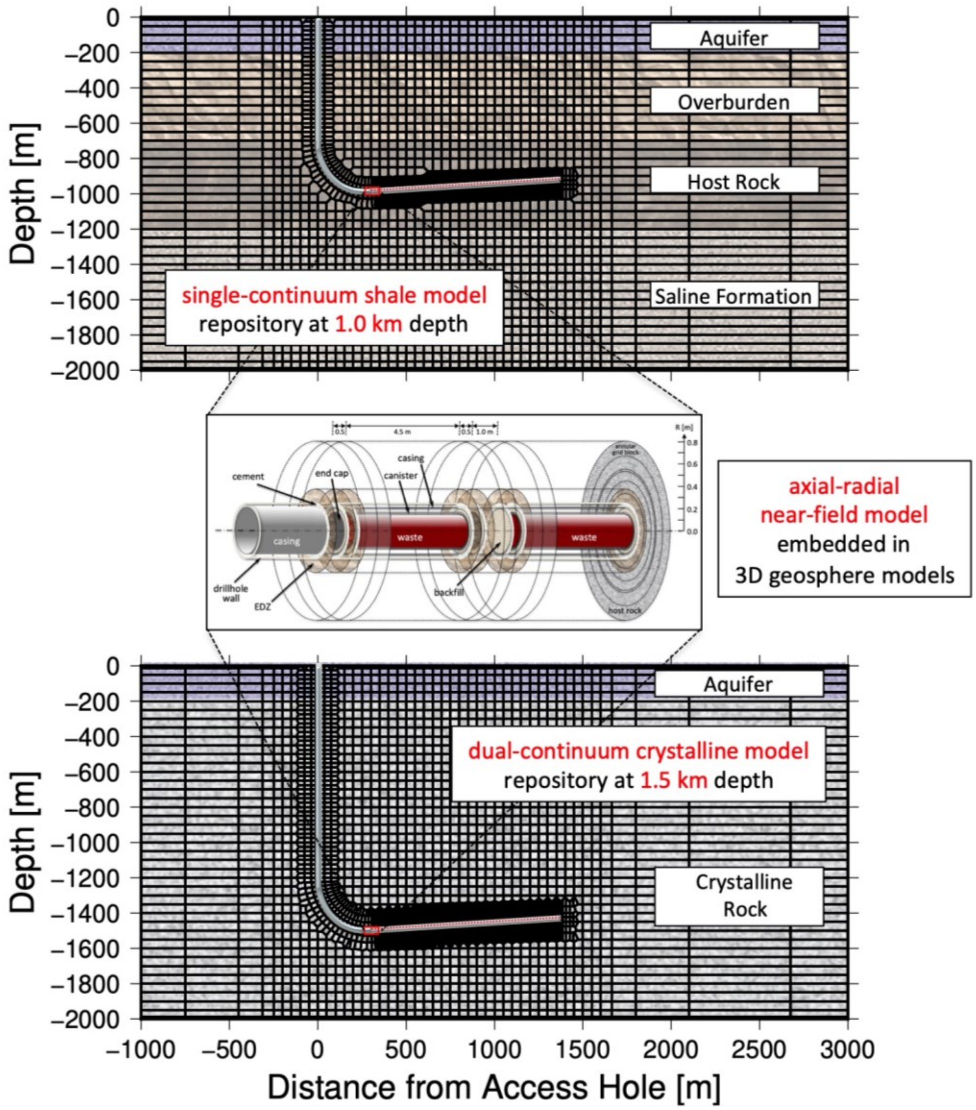

Figure 37. Illustration of axial-radial near-field model embedded in three-dimensional geosphere models for shale and crystalline host rocks with waste disposal sections at 1.0 km and 1.5 km depth, respectively.

Table 5: Radial discretization of near-field submodel material domains.

Component / Interface	Radius [m] Interface	Radius [m] Element	Thickness [m]
Drillhole axis	0.000		
Waste		0.070	0.140
Waste–Canister	0.140		
Canister		0.152	0.025 [a]
Canister–Buffer	0.165		
Buffer		0.178	0.025
Buffer–Casing	0.191		
Casing		0.197	0.013 [b]
Casing–Cement 4	0.203		
Cement 4 [c]		0.222	0.038
Cement 4–Disposal hole–EDZ 4	0.241		
Cement 3 [c]		0.286	0.089
Cement 3–Curved hole–EDZ 3	0.330		
Cement 2 [c]		0.346	0.032
Cement 2–Surface hole–EDZ 2	0.432		
Cement 1 [c]		0.397	0.089
Cement 1–Conductor hole–EDZ 1	0.533		
EDZ 4–Host rock	0.362		
EDZ 4 [d]		multiple	0.121
EDZ 3–Host rock	0.495		
EDZ 3 [d]		multiple	0.165
EDZ 2–Overburden	0.648		
EDZ 2 [d]		multiple	0.216
EDZ 1–Aquifer	0.800		
EDZ 1 [d]		multiple	0.267
Formation–Outer submodel boundary	10.000	multiple	logarithmically increasing

[a] Canister thickness is 1 inch = 0.0254 m

[b] Casing thickness is ½ inch = 0.0127 m

[c] Cements 1–4 refer to the cement in the annulus behind the conductor casing, surface casing, curved-hole casing, and disposal-section casing, respectively. They are installed in the numbered order. All casings are removed prior to drillhole sealing, with the exception of the casing in the disposal section.

[d] EDZ: Excavation Disturbed Zone; thickness is assumed ½ of drillhole radius. EDZs are numbered according to sequence with which corresponding drillhole section is completed.

Table 6: Near-field model cross-sections along the drillhole.

Drillhole Segment / Formation	Drillhole Length [m]	Depth [m]	Orientation	Cross-Section a)
Access Hole				
Conductor hole Aquifer	0 to 50	0 to -50	vertical	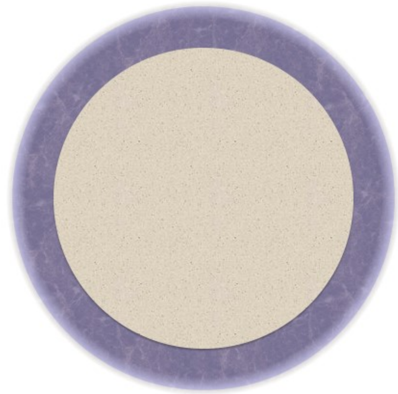
Vertical access hole Aquifer up to -200 m, Overburden from -200 to -700	50 to 700	-50 to -700	vertical	
Curved hole Host rock	700 to 1185	-700 to -990	curved, build angle 0.297°/m	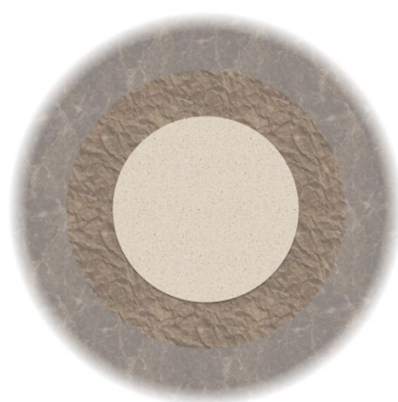

Drillhole Segment / Formation	**Drillhole Length [m]**	**Depth [m]**	**Orienta-tion**	**Cross-Section**
		Disposal Section		
Host rock Canister cross-section	1185 to 2218	-990 to -936	near-horizontal, inclination 3°	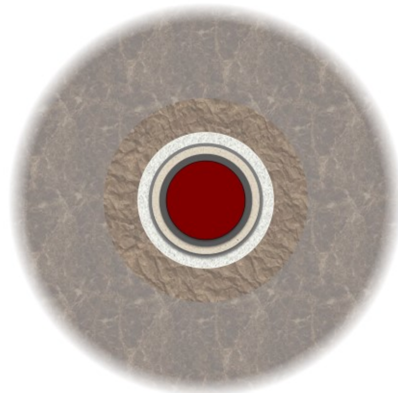
End-cap cross-section				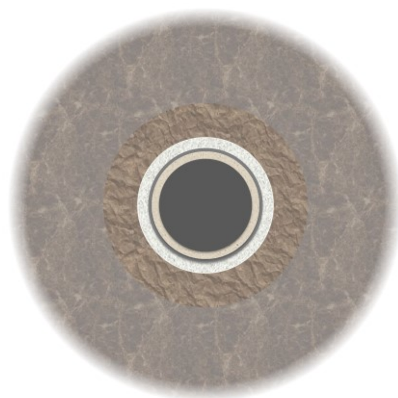
Canister-spacing cross-section				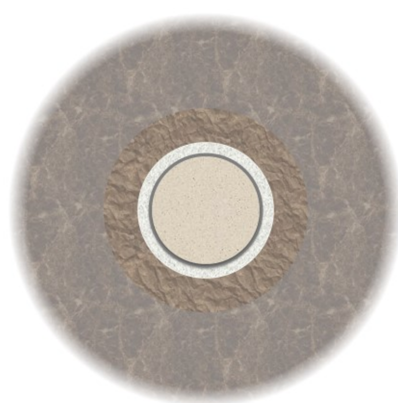

Drillhole Segment / Formation	Drillhole Length [m]	Depth [m]	Orienta-tion	Cross-Section
End drillhole	2218 to 2220	-936	horizontal	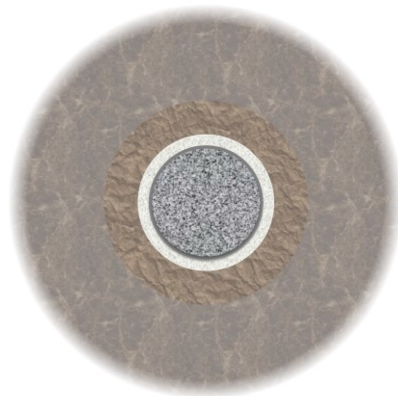
End model	2320	-936	horizontal	

[a] Cross-sections approximately to scale; see Table 5 for radii of each component. Outer model radius: 10 m.